Aus dem Muskuloskelettalen Universitätszentrum München

Orthopädie, Unfallchirurgie & Rehabilitative Medizin

Klinikum der Ludwig-Maximilians-Universität München

Regulatory effect of TGF-β3, BMP-2 and Noggin during the induction of endochondral bone formation: an *in vitro* study using rectus abdominis muscle from rat

Dissertation

zum Erwerb des Doktorgrades der Medizin

an der Medizinischen Fakultät der

Ludwig-Maximilians-Universität München

vorgelegt von

Heng Liu

aus

Tengzhou, China

Jahr

2022

Mit Genehmigung der Medizinischen Fakultät der

Ludwig-Maximilians-Universität zu München

Erster Gutachter:	Prof. Dr. med. Peter Ernst Müller
Zweiter Gutachter:	Priv. Doz. Dr. Thomas R. Niethammer
Dritter Gutachter:	Priv. Doz. Dr. Jörg Hausdorf
ggf. weitere Gutachter:	
Mitbetreuung durch den promovierten Mitarbeiter:	Dr. Roland Manfred Klar, PhD Dr. Tech. Yan Chevalier
Dekan:	Prof. Dr. med. Thomas Gudermann
Tag der mündlichen Prüfung:	19.09.2022

Table of content

Table of content

Zusammenfassung

Hintergrund: Die Regeneration von Knochen ist nach wie vor eine weltweite Herausforderung für das Tissue Engineering. Der biologische Wirkungsmechanismus der Wachstumsfaktoren, die beim Tissue Engineering von Knochen (BTE) eingesetzt werden, ist derzeit nicht geklärt. Muskelgewebe ist eine attraktive Quelle für Stammzellen und hat sich als hervorragendes Material für das Tissue Engineering von Knochen erwiesen. Transforming growth factor beta 3 (TGF-β3) und Bone morphogenetic protein-2 (BMP-2) spielen eine wichtige Rolle bei der endochondralen Knochenbildung, während Noggin, das als Antagonist von gewissen BMPs fungiert, normalerweise eine regulatorische Rolle spielt. In der vorliegenden Studie wurden diese drei Wachstumsfaktoren eingesetzt um die Wirkung auf die Knochenbildung in Muskelgewebe zu untersuchen. Ziel war es, das Potenzial von morphogen induziertem Muskelgewebe für die endochondrale Knochenbildung zu untersuchen und die räumlichen und zeitlichen molekularen Interaktionsmechanismen während des Differenzierungsprozesses zu entschlüsseln.

Methoden: Aus Ratten extrahiertes Muskelgewebe wurde mit verschiedenen Wachstumsfaktoren über längere Zeiträume stimuliert. Dafür wurden die rekombinantem Wachstumsfaktoren Ratten-(r) TGF-β3, rBMP-2 und rNoggin, entweder isoliert oder in verschiedenen Kombinationen, genutzt. Der Induktionseffekt wurde nach 7, 14 und 30 Tagen mittels Immunhistochemie (IHC), Histologie und quantitativer Reverse-Transkriptase-Polymerase-Kettenreaktion (RT-qPCR) nachgewiesen. Neben den Biomarkern für die Osteogenese (*Alp, Runx2, Bmp-2, Ocn, Col1a1*-Gene und OCN-Protein) wurden auch die mit der Chondrogenese (*Col2a1-, Acan-, und Sox9-Gene* und ACAN-Protein*),* artikulären Chondrogenese, *(Six1- und Abi3bp*-Gene) und der Angiogenese (*Vegfa- und Col4a1*-Gene) verbundenen Moleküle untersucht.

Ergebnisse: Alle nachgewiesenen Biomarker, die mit der Chondrogenese und Osteogenese zusammenhängen, erfuhren während des Differenzierungsprozesses eine signifikante Hochregulierung, sowohl auf Protein- als auch auf Genebene, was in fast allen stimulierten Gruppen geschah, mit Ausnahme der Gruppen, die nur mit rNoggin und der Kombination rBMP-2 + rNoggin stimuliert wurden. Außerdem wurden die Vegfa- und Col4a1-Gene in den meisten mit Morphogenen behandelten Gruppen hochreguliert. Die rBMP-2-Gruppe wies die höchste

und signifikante Genexpression an Tag 7 auf, aber die rBMP-2 + rTGF-β3-Gruppe war nicht signifikant. Danach zeigte die rBMP-2 + rTGF-β3-Kombination die höchste Genexpression an Tag 14 und blieb bis Tag 30 stabil. Die rTGF-β3 + rNoggin-Kombination zeigte die relativ hohe Genexpression an Tag 7 und 30, aber rNoggin stoppte den Aufwärtstrend von rTGF-β3 an Tag 14. rTGF-β3 + rBMP-2 + rNoggin-Dreifachstimulation zeigte die höchste Genexpression an Tag 30. Darüber hinaus hemmte die Anwendung von rBMP-2 die Bmp2-Genexpression, aber rNoggin und rTGF-β3 + rNoggin steigerten die Bmp2-Genexpression und die Kombination rTGF-β3 + rNoggin war die Einzige, die eine signifikante Bmp2-Genexpression an Tag 7 zeigte.

Schlussfolgerungen: Sowohl rBMP-2 als auch rTGF-β3 zeigten isoliert ihre Fähigkeit, die Differenzierung von Muskelgewebe in Richtung endochondraler Knochenbildung zu induzieren, und waren auch an der Chondrogenese beteiligt. rNoggin hemmte die rBMP-2-Wirkung zuverlässig und unterdrückte die rTGF-β3-Funktion während der 14-Tage Kultivierung, zeigte aber mit rTGF-β3 und in Kombination mit rTGF-β3 + rBMP-2 im späteren Zeitpunkt der Differenzierung eine positive oder zumindest keine hemmende Funktion. Dies beweist, dass TGF-b3 durchaus die Noggin-Funktion unterdrücken kann, was zeigt das TGF-b3 die Funktion des Noggins reguliert, um die Osteogenese im zeitlichen Verlauf zu modulieren. Darüber hinaus zeigte die Kombination von rTGF-β3 und rBMP-2 einen frühen Antagonismus, aber einen späten Synergismus. Die zelluläre Mikroumgebung kann ein Schlüsselfaktor bei der Bestimmung der komplexen Interaktionsmechanismen zwischen diesen Signalmolekülen sein. Außerdem wurden in diesem Differenzierungssystem negative Rückkopplungsschleifen zwischen Protein/Gen und Protein/Antagonist festgestellt. Die Daten dieser Studie liefern einige wichtige Beweise für die Entschlüsselung des molekularen Interaktionsmechanismus während der endochondralen Knochenbildung und bestätigten, dass nur durch variable Wachstumsfaktorapplikationen das gewünschte Gewebe mit der Zeit gebildet werden kann und nicht durch einzelne Signale.

Abstract

Background: The regeneration of bone remains a worldwide dilemma for tissue engineering, with the biological mechanism regarding proper growth factor/s application in bone tissue engineering (BTE) still require more extensive elucidation. Muscle tissue is an appealing source for studying the effect of morphogenesis as it consists of multiple cell types and is one of the key tissues to assess the induction of bone formation *in vivo*. Transforming growth factor-beta 3 (TGF-β3) and bone morphogenetic protein-2 (BMP-2) are suggested to play vital roles in endochondral bone formation, while Noggin, acts as an antagonist of certain BMPs, usually plays a regulatory role for osteogenesis. Therefore, the present study applied these three growth factors to induce endochondral bone formation in muscle tissue, with the aim directed towards to confirm the potential of morphogen-induced muscle tissue for BTE and try to unravel the underlining molecular interaction mechanisms during the differentiation process.

Methods: A series of recombinant rat (r) BMP-2, rTGF-β3, and rNoggin were applied continuously to the rat collected rectus abdominis muscle tissue over the designated culturing period. The bone induction effect was assessed at 7, 14, and 30 days by immunohistochemistry (IHC), histology, and RT-qPCR. Apart from ultimately aimed osteogenesis biomarkers (*Alp, Runx2, Bmp-2, Ocn, Col1a1* genes and OCN protein), the chondrogenesis (*Col2a1, Acan, Sox9 genes* and ACAN protein*),* the articular chondrogenesis *(Six1 and Abi3bp* genes,) and the angiogenesis (*Vegfa and Col4a1* genes) related molecules were also assessed.

Results: All the detected chondrogenesis and osteogenesis related biomarkers underwent significant upregulation during the differentiation, both at protein and gene level, which happened in nearly all of the stimulated groups but excepted the rNoggin alone and rBMP-2 + rNoggin combination stimulated groups. Besides, the *Vegfa* and *Col4a1* genes were also upregulated in most morphogen/s treated groups. At 7 days, the rBMP-2 single group displayed a peaked and significant gene expression, but rBMP-2 + rTGF-β3 group was non-significant. After that, the rBMP-2 + rTGF-β3 combination showed the highest gene expression on day 14 and kept stable until day 30. rTGF-β3 + rNoggin combination displayed relatively high gene expression on days 7 and 30, but rNoggin stopped the upward trend of rTGF-β3 on day 14. rTGF-β3 + rBMP-2 + rNoggin triple stimulation showed the highest gene expression on day 30. In addition, rBMP-2 application

inhibited *Bmp-2* gene expression, but rNoggin and rTGF-β3 + rNoggin upregulated *Bmp-2* gene expression, and rTGF-β3 + rNoggin combination became the only one that showed significant *Bmp-2* gene expression on day 7.

Conclusions:

Both rBMP-2 and rTGF-β3 showed their capability of inducing muscle tissue towards endochondral bone formation alone and stimulating the involved chondrogenesis as well. rNoggin inhibited rBMP-2 activities reliably and repressed rTGF-β3 function in the middle 14-day stage, but showed positive or at least no inhibitory function when used with rTGF-β3 in the initial and late stages of osteo-chondrogenesis and in combination with rTGF-β3 + rBMP-2 in the late stage of differentiation. This strongly suggests that TGF-b3 seems to regulate the Noggins molecule antagonistic effect possibly showing how bone formation is internally modulated by the expression of specific growth factors with time. Additionally, rTGF-β3 + rBMP-2 combination presented an early antagonistic action but later a synergistic interaction. The cellular microenvironment may be a key factor in determining the complex interaction mechanisms among these signaling molecules. Moreover, the negative feedback loops between protein/gene and protein/antagonist were detected in this differentiation system. The data of this study provided some key evidence in how endochondral bone formation is regulated and shows that only through a temporal specific application of multiple growth factors and other modulatory factors can proper osteogenesis be achieved.

List of figures

List of tables

List of appendixes

List of abbreviations

3D	3-dimension
Abi3bp	ABI family member 3 binding protein
ACAN	Aggrecan
Actb	Actin beta
ActRII	Activin type II receptor
Alp	Alkaline phosphatase
ALK	Activin receptor like kinases
AMHRII	anti-Mullerian hormone receptor type II
BMP	Bone morphogenetic protein
BMPR	Bone morphogenetic protein receptor
BMSCs	Bone marrow-derived mesenchymal stem cells
BTE	Bone tissue engineering
Col4a1	Collagen type IV alpha 1
Col2a1	Collagen type II alpha 1
Col1a1	Collagen type I alpha 1
cDNA	Complementary DNA
CDS	Coding sequences
cKO	Conditional knockout
CNRQs	Calibrated normalized relative quantities
Cq	Quantification cycle
Dlx5	Distal-Less Homeobox 5
ECM	Extracellular matrix

List of abbreviations

Erk1/2	Extracellular signal regulated kinase1/2
FGF	Fibroblast growth factors
FBS	Fetal bovine serum
Gapdh	Glyceraldehyde-3-phosphate dehydrogenase
GAGs	Glycosaminoglycans
GS	Glycine/serine
GDFs	Growth & differentiation factors
HA	Hydroxyapatite
IOD	Integrated optical density value
IHC	Immunohistochemistry
LAP	Latency-associated protein
LMU	Ludwig-Maximillian's-University
JNK	c-Jun N-terminal kinase
MAPK	Mitogen-activated protein kinase
MIQE	Minimum information for publication of quantitative real-time PCR experiments
MSCs	Mesenchymal stem cells
OCN	Osteocalcin
One-way ANOVA	One-way analysis of variance
Polr2e	RNA polymerase II subunit e
P/S	Penicillin and streptomycin
PTH	Pituitary hormone
rTGF-β3	Rat transforming growth factor-beta3
rBMP-2	Rat bone morphogenetic protein-2

List of abbreviations

rNoggin	Rat Noggin
RNA28S4	RNA 28S ribosomal 4
Runx2	Runx family transcription factor 2
R-Smads	Receptor-activated Smads
Rplp0	Ribosomal protein lateral stalk subunit p0
Rpl13a	Ribosomal protein L13a
SEM	Standard error of the mean
Smad	Mothers against decapentaplegic
Sdha	Succinate dehydrogenase complex flavoprotein subunit a
Six1	Sineoculis homeobox homolog 1
Sox9	Sex determining region Y (SRY)-box transcription factor 9
Tbp	TATA-binding protein
TGF-βRII	Transforming growth factor-beta receptor II
TGF-β	Transforming growth factor-beta
Vegfa	Vascular endothelial growth factor a
RT	Room temperature
RT-qPCR	Quantitative reverse transcription-polymerase chain reaction

1. Introduction

Bone regeneration, as an imperative category of tissue engineering, is still challenging to achieve, as the spatial and temporal chronological order of biological growth factors applied for bone tissue engineering (BTE) is still a mystery[1,2]. The following introduction sections provide a review of the basics of bone tissue, the current challenges faced in bone regeneration, as well as the role of some important growth factors in bone formation, in the hope of elucidating in detail some of the current problems within BTE and possible solutions.

1.1 The basics of bone tissue

Bone is a mineralized connective tissue with heterogeneous, hierarchical, composite structures that combined make up foundation of the human musculoseletal system[3,4]. The skeleton mainly consists of 4 components: bone cells, extracellular organic matrix, extracellular minerals and water[5,6]. The various bone cells usually make up 5% of the bone volume with the bone extracellular matrix (ECM) making up the remainder[7].

Five types of bone cells have been characterized: osteogenic cells, osteoblasts, osteocytes, bone lining cells, and osteoclasts. (1) Osteogenic cells are locally undifferentiated mesenchymal cells that can differentiate into osteoblasts[8,9]. (2) Osteoblasts are usually found in areas where new bone is being formed actively; they are in charge of bone deposition, by synthesizing and secreting osteoid and releasing calcium salts that then help mineralize the soft osteoid tissue[10,11]. (3) Osteocytes are derived from entrapped osteoblasts and are susceptible to mechanical and certain chemical changes in the bone matrix either where these cells then adjust their activity and assist thus processes such as in bone remodeling and/or homeostasis. Osteocytes can also control the matrix mineral concentration by regulating enzyme secretion[12,13]. (4) Bone lining cells are essential for the formation of the bone surface; they generally exist in the internal layer of the bone surface, where they function through matrix metalloproteases[14,15]. (5) Osteoclasts are multinucleate bone cells originating from white blood cells (monocytes

and macrophages). Inversely to osteoblasts, osteoclasts are active during bone resorption. They break down bone tissue in an acid milieu by secreting hydrogen ions and specialized proteinases. Regulated by and cooperated with other bone cells, osteoclasts play a crucial role in maintaining bone homeostasis[16,17].

Organic material (or osteoid) is made up of collagen fibers (~90% type I collagen) and a small number of other substances, such as glycoprotein, osteocalcin (OCN), and proteoglycans[18]. Collagen is a triple-helical fibrous protein and has a particular advantage of a highly repetitive insoluble property within bone tissue[19,20]. It forms the framework for bones and confers the bone with high elasticity and considerable intrinsic tensile strength so that bone is not brittle[21]. In addition, some non-collagenous proteins, although in a small number but with unignored functions, could also be found in the bone matrix, such as OCN, a relatively bone-specific protein, which has a high affinity for bone minerals, and also binds to collagen[22]. Fibronectin, is involved in mediating the attachment of bone cells to the matrix[23,24]. Notably, the inside secreted growth factors also belong to the category of non-collagenous proteins, which play an irreplaceable role in the biological function of bone cells[19]. Hydroxyapatite (HA), with the chemical formula of [Ca10 (PO4)6 (OH2)], is the principal inorganic component of bone tissue[25]. HA forms from calcium phosphate and calcium carbonate combined, with a needle-like or thin plate shape[26]. It crystallizes or calcifies with other inorganic salts like magnesium hydroxide, fluoride, and sulfate, laying down the collagen fibers, thus giving the bone mechanical rigidity and compressive strength[27].

1.1.1 Bone formation

Skeletogenesis arises through a series of spatiotemporal events involving epithelial-mesenchymal interaction, condensation, and differentiation[28]. The generation of the skeleton derives from three distinct derivatives[29,30]: (1) the long bones are formed from the lateral plate mesoderm; (2) the craniofacial bones, clavicles, and cartilages arise from the cranial neural crest; (3) the somite forms the axial skeleton. Bone formation is the production of new bone, also termed osteogenesis or ossification scientifically. This process starts in about the sixth to seventh week of embryogenesis in humans and continues until approximately late puberty[19,31]. The healthy normal bone formation in the embryo is mainly through two different but mutually intersecting processes, namely intramembranous and/or endochondral ossification[32]. Although both processes initiate from the mesenchymal cells condensation and differentiation, their osteogenesis formation pathways are distinctive [33]. In addition, heterotopic ossification is a pathological or induced bone formation that can provide some clues for the implementation of BTE[34].

1.1.1.1 Intramembranous ossification

Few bones, such as the lateral clavicles, mandible, maxilla, and the flat bones of the skull form through intramembranous ossification[35,36]. During this process, the undifferentiated mesenchyme (fibrous membranes) converts into the bone directly[37]. Firstly, in the place where bone formation is required, the neural crest-derived mesenchymal cells condense to form a framework for future bone. The condensed mesenchymal cells then differentiate into osteoblasts, which then cluster together into an ossification center. The osteoblasts then begin secreting osteoid, that binds calcium in the meantime. Along with the calcium deposition, the matrix slowly hardens, entrapping some of the osteoblasts at the zone of osteoid to bone mineralization, which later become osteocytes. The continually secreted osteoid from osteoblasts, and part of bone not yet mineralized settles around blood vessels forming later the cancellous or trabecular bone. The matrix contained connective tissue along with these blood vessels will differentiate into red bone marrow eventually. On the peripheral layer of the spongy bone, the secreted osteoid is arranged in a parallel direction with the existing matrix, thus

forming the cortical (or the compact) bone. Subsequently, the periosteum, differentiated from mesenchymal cells, is finally formed on the surface of the cortical bone[38].

1.1.1.2 Endochondral ossification

The majority of the bones such as long bones, vertebrae, and ribs form through endochondral ossification, which is responsible for more than 80% of the bone volume[39,40]. This indirect bone formation process begins with a hyaline cartilage intermediate that is then invaded by vascular tissue and finally replaced by mineralized bone tissue[41]. Similarly, to the intramembranous ossification, endochondral bone formation also starts from mesenchymal cells condensation that, however, then differentiate into chondrocytes, proliferating rapidly and secreting cartilaginous matrix, thereby forming a cartilage anlage (or mold) of the future long bone. Subsequently, with the cartilage matrix calcification and blood vessels invasion, the cartilage is resorbed simultaneously, whereby the medullary was formed. Cofunction with osteoclasts, the activity of osteoblasts permits bone deposition and compact bone formation eventually[42].

The actual process however of cartilage tissue transformation towards the mineralized state is still unclear. It has been proposed over many decades that the chondrocytes undergo hypertrophy and then undergo apoptosis due to a nutrient loss when the cartilage ECM mineralizes [36,43]. However, recent studies, using genetic tracing technology, suggest that the mature chondrocytes trans-differentiation [44-46], either directly, or indirectly[31,43,47]. The direct chondrocyte-to-osteoblast trans-differentiation process involves the hypertrophic chondrocytes differentiating into osteoblasts without a step of pluripotency or progenitor-like cell stage. In contrast, indirect trans-differentiation suggests that chondrocytes dedifferentiate first into immature chondrocytes and then re-differentiated into osteoblasts[43,47]. In addition, several researchers pointed out that the final designation of these mature chondrocytes depends on their location. Cells closer to the mid-

diaphysis would more readily transdifferentiate into osteoblasts, while those further away are more prone to undergo apoptosis. The two different processes function mutually to promote bone development and skeletal homeostasis[48,49].

1.1.1.3 Heterotopic bone formation

Heterotopic bone formation is generally a pathological state that is known to spontaneously form bone in tissue where it is not normally found [50-52]. The predominantly endochondral-mediated formation process of heterotopic ossification is akin to but not strictly in accordance with normal bone development[53,54], which involves stages of inflammation, destruction, chondrogenesis, osteogenesis, and maturation[50,55]. In the early stages of heterotopic bone formation, often caused by severe injury, a large number of lymphocytes accumulate in the surrounding muscle or other connective tissues of the injury site due to blood vessel leakage. This accumulation results in an inflammatory response accompanied by the structural disruption of the tissue. With the lymphocytic invagination and the tissue breakdown, fibrosis and angiogenesis occur, which cause the release of osteogenic factors, such as bone morphogenetic proteins (BMPs)[53,56]. These factors stimulate the local differentiation of the microenvironment and promote chondrogenesis and osteogenesis of mesenchymal precursor cells eventually leading to the formation of endochondral bone formation[55,57]. Indeed, heterotopic bone development necessitates (1) cells that can differentiate or transform into the lineage of cartilage and/or bone, (2) osteogenic-inducing factors to trigger the cellular and molecular events, (3) a special conducive microenvironment[58,59].

1.2 Current state of bone tissue defect regeneration clinically

The regeneration of critical sized bone tissue defects is still a current worldwide problem in clinical treatment that affects the health and living quality of millions of people[60,61]. Critical size bone defects mainly result from huge traumatic injuries, congenital malformations, bone tumor resections, failed joint replacements, fracture non-unions, or infections, which cause a great challenge in reconstructive surgeries[62-64].

Bone tissue is capable of excellent natural regeneration, which involves two simultaneous and interlinked processes, osteoinduction and osteoconduction, that restore the original function and framework[64]. The autogenous bone graft procedure is still the golden standard of bone defect healing. It involves harvesting bone from a site, usually rib or hip bones, of a patient's own bone that is then transplanted within different musculoskeletal sites[60,65]. The transplant of autologous bone is totally biocompatible and virtually non-immunoreactive; it possesses enough viable osteogenic cells, all the osteoinductive necessary growth factors, and functional non-collagenous proteins[62]. Furthermore, the transplanted bones collagen and mineral matrix structure provide a scaffold for proper osteoconduction[62]. However, the technique does suffer from various limitations especially donor site chronic pain, additional surgeries and expenses, increased risk of infection/complications, and associated donor site morbidity[64,66,67]. Therefore, there is an urgent clinical need for a feasible and effective alternative procedure that can quickly and efficiently ensure proper bone defect reconstruction of critical sized defects[68].

1.3 Bone tissue engineering

As an attractive branch of regenerative medicine, bone tissue engineering (BTE) aims to synthesize new biological bone tissue like native one[69,70]. There are four basic parameters included in the typical BTE paradigm[66,71]: (1) cells which can differentiate to osteogenic cells that ultimately secrete bone matrix and deposit new bone tissue (2) a biocompatible substratum which allows cell migration and growth possessing similar ECM-like capabilities such as bone (3) soluble signals such as growth factors which can stimulate the cells towards osteogenesis phenotypes, and (4) vascularization which provide support for metabolism (nutrient supply and waste removal). During the past decades, many scholars have researched BTE to create ideal biomimetic constructs that replicate bone tissue, both in structural and functional terms[72-74]. Although some successes have been reached, there are still numerous difficulties and challenges that need to be investigated and elucidated properly to realize a reliable clinical application.

1.4 Muscle tissue bone regeneration

According to previous studies, the growth factors loaded, muscle tissue-based, biomaterial induction system is a promising novel technology for BTE[75-78]. Muscle is a relatively easy obtained tissue with a firm and durable self-repair capability; thus, muscle tissue harvesting will not cause severe morbidity of donor area[79]. It is well known that muscle tissue is an attractive pool of cell sources for tissue engineering since it contains a large amount of stem cells, which possess the potential to differentiate into an osteogenic lineage [80,81]. Compared to the traditional cell culturing-based BTE approaches, the tissue culture system does not need extraction and proliferation of autologous-derived osteoprogenitor cells, thus making it easier to operate and much cheaper[82-84]. Additionally, the muscle tissue fragment itself is a one hundred percent biocompatible scaffold with a complex 3-dimension (3D) structure[81,84]. Its intrinsic ECM contains the necessary amino acids and the essential signaling molecules, providing an *in vivo*-like culturing milieu, which supports the cells' growths and activities[85-87]. Moreover, as a natural soft tissue scaffold, its easy deformability facilitates the matching of bone

defect sites. Furthermore, the muscle tissue normally contains small blood vessels and numerous capillaries, which are critical for nutrient flow and anabolic activities[88-90].

Experimentally, several investigations have demonstrated the feasibility of muscle tissue osteogenic induction when combined with relevant signals, both *in vivo* and *in vitro*[91-94]. For example, Betz et al. (2009, 2010) confirmed that critical size osseous defects could be repaired by implantation of gene-activated muscle tissue fragments in rats[79,95]. Interestingly, one preclinical experiment of Betz et al. (2013) also found that muscle tissue transplanting could be as effective as autologous bone grafting[88]. In addition, using the agonist empowered coral-derived carriers, Klar et al. (2014) induced ectopic bone formation of the rectus abdominis muscle tissue within adult non-human primates[96]. In general, these clues provide solid evidence that muscle tissue is an appealing biomaterial for BTE.

1.5 TGF-β superfamily growth factors

Growth factors are secreted proteins that have a critical impact on the biological activities of organisms[97]. They are crucial in tissue engineering for inducing cellular differentiation or transformation into desired cell lineages[98,99]. Most of them are grouped as signaling protein families according to their related structures, exemplified by the transforming growth factor-beta (TGF-β) superfamily, the large cluster of secretion polypeptides[100], where all members within this family possess a characteristic quaternary dimer structure[101,102]. The TGF-β superfamily comprises over 35 proteins[103,104], they can be divided into the TGF-β subfamily and the BMP subfamily. The former comprises TGF-β isoforms, Nodals and activin A/B, while the latter is made up of BMPs and the growth & differentiation factors (GDFs)[105,106].

1.5.1 TGF-β superfamily pathway

Proteins of the TGF-β superfamily evoke signal transduction via a heteromeric tetrameric multi-complex containing dual type-I and dual type-II threonine/serine kinase receptors[107,108]. There are 7 type-I receptors, named activin receptor-like kinases (ALK) 1–7, and 5 type-II receptors, activin type II receptor (ActRII) A/B, transforming growth factor-beta receptor II (TGF-βRII), anti-Mullerian hormone receptor type II (AMHRII), and bone morphogenetic protein receptor (BMPR) type II have been identified[109]. Different ligands can bind to multiple receptors and vice versa, but the affinity between ligands and receptors varies greatly[110-112]. TGF-βs preferentially bind to ALK4, -5, and -7, whereas BMPs normally bind to ALK1, -2, -3, and -6[113,114]. Upon ligand binding, activated type II receptors are brought close to the type I receptors glycine/serine (GS) domains to phosphorylate and active them; thus, the mothers against decapentaplegic (Smad)-dependent and Smad-independent signaling reactions are triggered[115,116]. In the canonical Smad-dependent signaling pathway, the activated receptors phosphorylate the C-terminal of receptor-activated Smads (R-Smads)[117,118]. Conventionally, TGF-βs activated ALK5 induce R-Smad2/3 phosphorylation, whilst BMPs activated ALK1, -2, -3, and −6 stimulate the phosphorylation of R-Smad1/5/8[107,119]. Subsequently, the phosphorylated R-Smads form a heteromeric complex with a whole TGF-β superfamily shared mediator, Smad4, which is then transported into the nucleus and functions via binding gene promoter sites, thereby initiating the expression of target gene[54,93,120].

This process also stimulates the Smad6 or 7 (two inhibitory Smads) activity, modulating the signaling pathway by suppressing the activity of the transcription factor complex via a negative feedback loop[121,122]. Furthermore, TGF-βs ligands also trigger Smad independent pathways, like extracellular signal regulated kinase1/2 (Erk1/2), c‐Jun N‐terminal kinase (JNK), and mitogen-activated protein kinase (MAPK) mediated -p38 signaling cascades[123-125]. These intricate signaling pathways are collectively and finely regulated, act synergistically or antagonistically, to promote the development or maintain the homeostasis[126]. However, dysregulation may lead to pathological diseases[127,128].

The TGF-β superfamily members perform a variety of pleiotropic functions during both the antenatal and postnatal development process[129]. By precisely regulating fundamental cellular activities (cell proliferation, differentiation, and gene expression, which controls phenotypes), the TGF-β superfamily signaling is linked to tissue/organ formation and maintenance, immune surveillance, including inflammation response[130,131]. Between themselves, TGF-βs and BMPs play crucial functions in skeletogenesis, including regulating mesenchymal stem cell condensations, chondrocyte differentiation, osteoblast differentiation, growth plate expansion, and skeletal morphogenesis[121,132].

1.5.2 TGF-β isoforms

The TGF-β isoforms are cytokines that belong to one category of the TGF-β supergene family of proteins that have a diverse and pleiotropic function in both embryonic development and adult tissue homeostasis[133,134]. There are three different TGF-β isoforms in mammals, including TGF- beta 1 (TGF-β1), TGF-β2, and TGF-β3[135]. All of these isoforms are synthesized and expressed from the perichondrium, periosteum, and epiphysial growth plate, while TGF-β receptors are expressed in the perichondrium and chondrocytes[136,137]. The precursor of the TGF-β isoform molecule comprises mature TGF-β and non-covalently combined latency-associated protein (LAP), that upon cleavage of the latter allows these signaling molecules to activate and perform multiple biological functions[138].

The active TGF-β initiates and stimulates chondrogenesis, including mesenchymal stem cells (MSCs) proliferation, differentiation into chondrocytes, and deposition of the collagen II including other cartilage-specific ECM[139,140]. Interestingly, the TGF-β isoforms have a bi-functional impact on the cartilage metabolic homeostasis maintenance[141]. On the one hand, TGF-β isoform favors early-stage chondrocyte proliferation but arrests downstream chondrocyte hypertrophy[142,143]; this special property makes it crucial for hyaline cartilage integrity preservation. Loss of TGF-β isoform function in chondrocytes leads to hypertrophic differentiation and eventually cartilage degeneration; thus, the pharmacological active TGF-β signaling could be detected in osteoarthritis models to rescue the pathological

process[144,145] However, on the other hand, TGF-β isoform is known to also induce osteogenesis and accelerate osteoarthritis through a Smad2/3 independent signaling pathway[107,146].

The osteogenic potential of TGF-β isoforms has been demonstrated in many different models. For instance, several studies demonstrated that TGF-β1 promotes osteogenesis via increasing osteoprogenitors chemotaxis and proliferation[147,148], and mutation of the *TGF-β*1 gene will cause abnormal bone capacity, both in human[145,149] and mice models[150]. Similarly, the abnormal endochondral and intramembranous ossification were investigated in TGF-β2-null mice[151]. In addition, Klar et al. (2014)[96] and Ripamonti et al. (2015)[152] identified in an *in vivo* experiment that the TGF-β3 isoform functions as the crucial signaling regulating osteogenic relative mRNA expression and thus inducing ectopic bone formation within adult baboons.

1.5.3 BMPs

The BMPs contain a series of critical signals that are considered potent osteogenic growth factors[153,154]. BMP signaling is necessary for the osteoblastic lineage fate decision of mesenchymal stromal cells during bone formation[155]. BMPs are prerogative molecules during bone formation; they play roles in nearly the whole endochondral bone development process[156,157]. They are also involved in subsequent bone remodeling, maintenance, and reconstruction[158,159]. There are 20 types of BMPs that have been identified inside the grouped subfamily until now; each member has a homologous core structure in which the active binding site is the only unique variation by which BMPs can be differentiated and which confer exclusive activities and expression patterns[160,161]. Among them, BMP-2, -4, -5, -6, -7 and -9 have been identified as strong promoters of osteogenic activity[162-164]. Evidence has shown that BMP-2 is one of the most powerful inducers for osteogenic differentiation[165], in which Neol et al. certified that even a short duration of BMP-2 expression is sufficient enough to induce irreversible endochondral bone *in vivo* [166]. In addition, studies showed that BMP-2 knockout (cKO) mice had impaired fracture healing[167], while BMP-7 null mice embryos undergo

fetal death because of deficient skeletal architecture[168], which indicates the crucial function of BMPs in mammalian skeletal genesis. Moreover, amongst their other tissue inductive capabilities, BMPs also possess the capability to promote chondrogenesis[100,140]. The first evidence was given by Urist (1965), who discovered that BMP-2 could induce both ectopic cartilage and bone formation within the rectus abdominis muscle of adult rabbits[169]. After that, several other studies further confirmed the BMP-2 involved in chondrogenic activity both *in vivo*[170,171] and *in vitro*[172].

1.5.4 Noggin

A growing body of evidence suggests that the opposite activities of specific ligands and their antagonists have a key role in regulating many aspects of cell behavior during the vertebrate development process; they exert the function mutually to regulate spatial domains activation securely[173,174]. Research studies have discovered that BMP actions are negatively fine-tuned by a group of antagonists at different cellular levels[175,176]. For example, Noggin, Sclerostin, Gremlin, and Chordin are all specific TGF-β/BMP antagonists[114,177]. Among them, Noggin is an extracellular secreted glycoprotein, which was initially characterized as a neural inducer in *Xenopus* by Smith and Harland (1992)[178]. This 64-kDa molecular mass homo-dimeric protein is a member of the Spemann organizer and expressed conspicuously in the central nervous system and was also discovered in lung, skin, skeletal muscle, cartilage, and bone[155,179]. Noggin performs pleiotropic roles in the various physiological and pathological developmental processes, such as being involved in the induction of neural and skeletal muscle tissue in early embryogenesis[178], and being crucial for chondrogenic and osteogenic differentiation as well[180,181].

In the ectopic Noggin expression model, the osteoblastic lineage recruitment and differentiation were impaired, which caused decreased bone mineral density and weakened osteoblastic function[182,183] and fractures as well[184]. Nevertheless, downregulation of Noggin in cells of the bone environment increases the osteo-

genic differentiation markers expression and thus enhances the bone defects regeneration[185,186]. Additionally, transgenic mice with cKO Noggin led to severe malformed axial skeletons and embryonic decease, sequesters the analysis of skeletal phenotype in adult Noggin null mice[187,188]. Furthermore, the proximal symphalangism and multiple synostoses syndrome in human beings can also be attributed to Noggin mutations[189].

1.5.5 Growth factors combination

Previous experimental studies have reported that a combination of more than single morphogens could reach a superior morphogenesis result synergistically or modulatory[190,191]. For example, Fei et al. (2019) demonstrated that the combined treatment of BMP-2, -7 and TGF-β3 could promote a chondrogenic inductive effect more efficiently than either morphogen applied on its own or as various duplicate combinations when administered to muscle tissue as a temporary or permanent application *in vitro*[75]. Similar synergistic studies in osteogenic differentiation have also been investigated by other scientists, where an improved bone formation was observed when BMP-2 was applied with TGF-β3, in which both growth factors synergized with each other[192-194]. However, the antagonistic effect between different TGF-β isoforms and BMPs has also been discussed by other researchers [113,195,196]. In addition, the mutual impact between BMPs and Noggin has been intensively explored in the last decades[197-199]. Recent studies have also shown the association between TGF-β3 and Noggin during the endochondral bone formation process within muscle tissue[96]. But the detailed complex interaction mechanisms among these growth factors, in terms of temporal and spatial behavior, are still not thoroughly explained. Nevertheless, the detailed complex interaction mechanisms in a spatial and temporal context by which these factors interact with one another remain not thoroughly explained.

2. Aims and Hypotheses

2.1 Aims

- To assess the osteogenic induction potential of the muscle tissue after one month of continuous application of BMP-2, TGF-β3, and Noggin, applied alone or in diverse duplicate and a triplicate combination.

- To investigate the so far unclear interaction mechanisms between the three growth factors during the endochondral bone induction process and if there are unique interactions in respect to tissue morphogenesis between the various growth factor combinations.

- To expand on the possibility of using this muscle tissue model to generate specific tissue types for clinical transplantations.

2.2 Hypotheses

- The muscle tissue would differentiate toward an endochondral bone formation direction following a chronological signaling pattern indicative of first chondrogenesis and subsequent osteogenesis.

- Both BMP-2 and TGF-β3 could facilitate osteogenic induction alone, also a better trend would be stimulated by BMP-2 and TGF-β3 synergistically.

- In addition to BMP-2, Noggin would also antagonize TGF-β3 induced morphogenetic activity.

- The multiple growth factors loaded *in vitro* muscle tissue model would be a good candidate for BTE.

3. Materials and Methods

3.1 Experiment design

The detailed mechanisms and the associations between the BMP-2, TGF-β_3 and Noggin, in terms of temporal and spatial behavior, in a muscle tissue model *in vitro*, are still unclear. Therefore, the present study attempted to detect the osteogenic effects, if any, under a temporal signaling cascade of these 3 growth factors, which are applied to this specialized muscle tissue model platform in 7 different patterns **(Figure 1)**. The differentiated cultured muscle tissue was analyzed after 7, 14, and 30 days using three parts: (1) quantitative reverse transcription-polymerase chain reaction (RT-qPCR), (2) immunohistochemistry (IHC), and (3) histology **(Figure 1)**.

3.2 Collection of muscle tissue samples

The rectus abdominis muscle tissue was collected from two Fischer-344 adult Rattus norvegicus (Charles River Wiga, Sulzbach, Germany), pre-killed with an excess of isoflurane (Abbot, Chicago, USA) and disinfected with 10% povidone-iodine (Betadine, Bonn, Germany) and 75% alcohol (Apotheke Großhadern, Munich, Germany). Under a sterile environment, the harvested muscle was incubated in graded concentrations of penicillin and streptomycin (2% and 1%) (P/S, Biochrom GmbH, Berlin, Germany) contained Alpha medium 20min, respectively. Then 288 fragments of tissue in diameter of 4mm were cleanly separated with a specific biopsy punch (PFM medical, Cologne, Germany).

The rules and regulations of the Animal Protection Laboratory Animal Regulations (2013) of European Directive 2010/63/EU Act was strictly complied with during the upper procedures, which was also approved by the Animal ethics research committee of the Ludwig Maximillian's University of Munich (LMU), Bavaria, Germany Tierschutzgesetz §1/§4/§17 (https://www.gesetze-im-internet.de/tierschg/TierSchG.pdf) with regard to animal usage for pure tissue or organ harvest only.

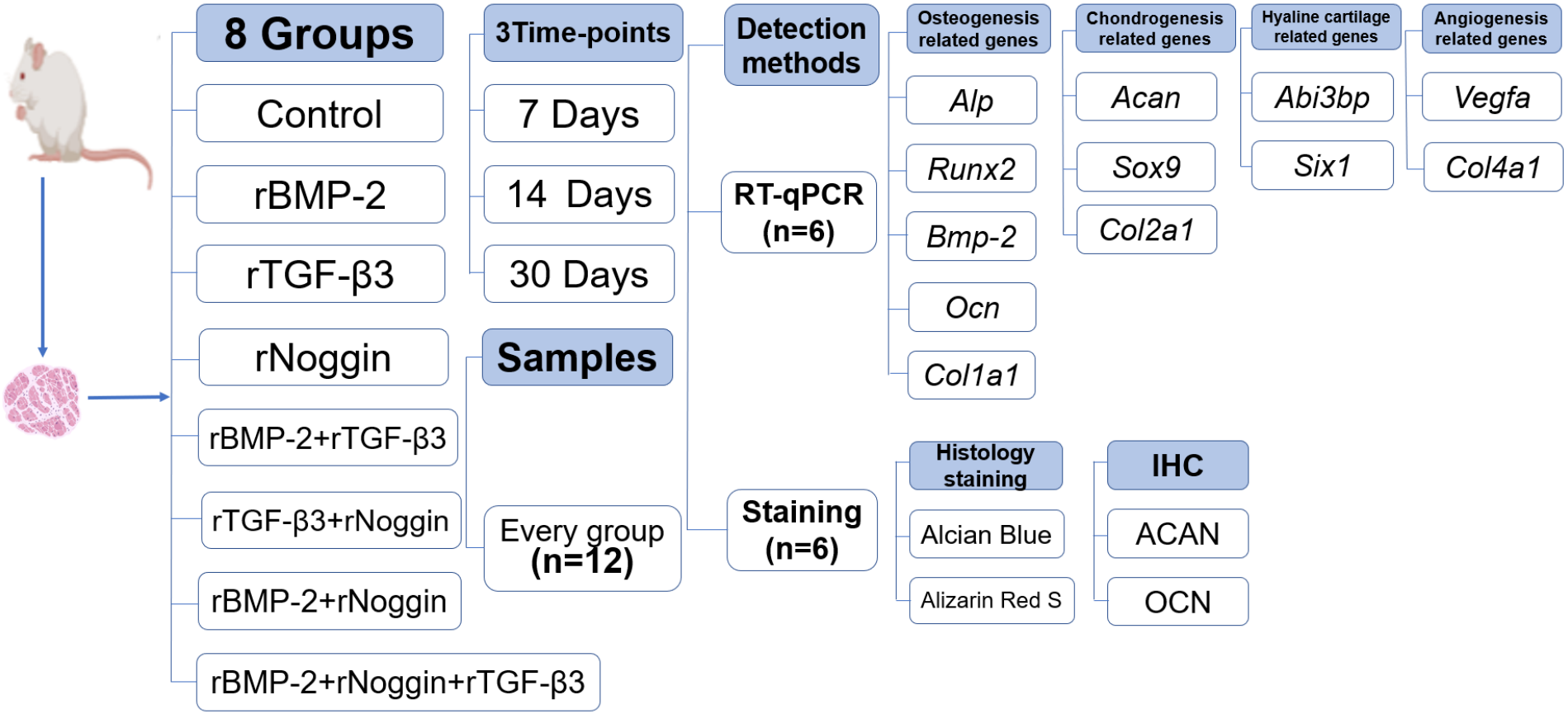

Figure 1. The framework for the induction of endochondral bone formation *in vitro* using muscle tissue.Three growth factors were applied in seven different patterns. The detection methods included RT-qPCR, IHC and histological staining, which were performed at 7, 14, and 30 days.

3.3 Tissue culture

The extracted muscle tissue biopsies (n=288) were put into 96-well plates (Thermo Fisher Scientific, Waltham, MA, USA) with the normal culture medium for 48h, to allow for the cells in the tissue to recover. The muscle tissue fragments were then divided into eight groups according to the below-mentioned different culture or differentiation medium. Each group contained a total number of 36 tissue samples, which were harvested on day 7(n=12), day 14(n=12), and day 30 (n=12), respectively, and then collected for subsequent RT-qPCR (n=6) and tissue staining (n=6) analyses. All samples were incubated at 37°C with 5% CO2 in a humidified incubator.

The growth factor treatment groups were set up as follows:

(1) **Con** represented the control group. The culture medium in this group contained Alpha medium (Biochrom GmbH, Berlin, Germany), 1% P/S, 15% fetal bovine serum (FBS; Biochrom GmbH, Berlin, Germany) and 0.02 mM/mL L-glutamine (Biochrom GmbH, Berlin, Germany) (= **normal culture medium**).

(2) **B** represented the recombinant rat (r) BMP-2 group, containing the normal culture medium and 50 ng/mL rBMP-2 (CusaBio, USA).

(3) **T** represented the recombinant rat (r) TGF-β3 group, containing the normal culture medium and 50 ng/mL rTGF-β3 (Cloud-Clone Corp, USA).

(4) **N** group represented the recombinant rat (r) Noggin group, containing the normal culture medium and 50 ng/mL rNoggin (Cloud-Clone Corp, USA).

(5) **T + B** represented the rTGF-β3 + rBMP-2 group, containing the normal culture medium and 50 ng/mL rTGFb3 + 50 ng/mL rBMP-2.

(6) **T + N** represented the rTGF-β3 + rNoggin group, containing the normal culture medium and 50 ng/mL rTGF-β3 + 50 ng/mL rNoggin.

(7) **B + N** represented the rBMP-2 + rNoggin group, containing the normal culture medium and 50 ng/mL rBMP-2 + 50 ng/mL rNoggin.

(8) **T+ B + N** represented the rTGF-β3 + rBMP-2 + rNoggin group, containing the normal culture medium and 50 ng/mL rTGF-β3 + 50 ng/mL rBMP-2 + 50 ng/mL rNoggin.

3.4 Quantitative reverse transcription PCR (RT–qPCR)

The minimum information for publication of quantitative real-time PCR experiments (MIQE) principles[200] was strictly applied to guide the entire RT–qPCR procedure.

3.4.1 Total RNA isolation and reverse transcription

After flash freezing in liquid nitrogen, the harvested muscle tissue samples were homogenized by a mortar and pestle under an RNase-free work hood. Then at room temperature (RT), added TRIzol™ reagent (Thermo Fisher Scientific, Waltham, MA, USA) -- (1000μL, incubated 5min), Chloroform (Sigma-Aldrich Corp, St. Louis, MO, USA) --(200μL, vortexed 15sec, then incubated 3min). Subsequently, in a preset 4 °C centrifuge, the mixture was centrifuged at 12,000x g for 15min. The total RNA existed in the upper aqueous phase, which was then mixed with 75% Ethanol (Merck, Billerica MA, USA). After that, the RNA was purified by aRNeasy® Fibrous Tissue Mini Kit (Qiagen, Hilden, Germany) and resuspended in 35 μL RNase-free H_2O (Gibco, Invitrogen, Merelbeke, Belgium). The A260/A280 ratio of the obtained RNA was 1.86–2.07, and the concentration was 76.7–123.7 ng/μL, which were measured by a NanoDrop™Lite (Thermo Fisher Scientific, Waltham, MA, USA). Finally, a QuantiTect complementary DNA (cDNA) Synthesis Kit (Qiagen, Hilden, Germany) was applied according to their specialized protocol to conduct reverse transcription. The resulting cDNA was deposited at -20 °C for subsequent qPCR analysis.

3.4.2 Primer design

1. The relevant gene coding sequence (CDS) for relevant genes to be analyzed was found in PubMed (https://www.ncbi.nlm.nih.gov/pubmed/).

2. Primer design and validation were conducted on the website of Integrated DNA Technologies (https://eu.idtdna.com/site).

(1) Input the CDS into the PrimerQuest Tool, according to customized design parameters, the preliminary potential primer sequences could be obtained.

(2) According to the Gibbs standard free energy change (ΔG) scores and heterodimers nonspecific amplification, the best available forward and reverse primers were selected from primers generated in the previous step through OligoAnalyzer Tool.

(3) The practicality of selected primers was validated by a temperature gradient RT-qPCR optimization process, the PCR amplification products were collected and purified by the Mini Elute PCR Purification Kit (Qiagen, Hilden, Germany). After that, the Nucleotide mega blast analysis (https://blast.ncbi.nlm.nih.gov/Blast.cgi?PAGE_TYPE=BlastSearch) and Sanger sequencing (GATC Biotech, Cologne, Germany) were used to validate the feasibility[201,202].

3, According to the above-mentioned method, the primers of eight reference genes and twelve interest target genes were designed **(Table 1)**.

(1) Eight reference genes included: *Actin beta (Actb)*, *Glyceraldehyde-3-phosphate dehydrogenase (Gapdh)*, *Ribosomal protein l13a (Rpl13a)*, *Ribosomal protein lateral stalk subunit p0 (Rplp0)*, *RNA 28S ribosomal 4 (RNA28S4), Succinate dehydrogenase complex flavoprotein subunit A (Sdha)*, *TATA-binding protein (Tbp)*, *RNA polymerase II subunit e (Polr2e)*.

(2) Twelve interest target genes included: *Aggrecan (Acan), Collagen type II alpha 1 (Col2a1), Sex determining region Y (SRY)-box transcription factor 9 (Sox9), Sineoculis homeobox homolog 1 (Six1), Abi family member 3 binding protein (Abi3bp), Osteocalcin (Ocn), Collagen type I alpha 1 (Col1a1), Runx family transcription factor 2 (Runx2), Alkaline phosphatase (Alp), Bmp-2, Collagen type IV alpha 1 (Col4a1) and Vascular endothelial growth factor a (Vegfa).*

Col2a1, *Acan* and *Sox9* were chosen to evaluate the general chondrogenesis, and *Six1* and *Abi3bp* were chosen to evaluate the articular chondrogenesis. *Alp, Runx2, Bmp-2, Ocn and Col1a1* were selected to assess the ultimately aimed osteogenesis. *Vegfa* and *Col4a1* were selected to assess the biological vitality of the muscle tissue after incubation.

Table 1. The target and reference genes information.

	Gene name	Accession Nr.	Fwd. (5´-3´)	Rev. (5´-3´)
Reference genes	*Actb*	NM_031144.3	AGCTATGAGCTGCCTGA	GGCAGTAATCTCCTTCTGC
	Gapdh	BC083511.1	CATGGGTGTGAACCATGA	TGTCATGGATGACCTTGG
	Rplp0	BC001834.2	CAACCCAGCTCTGGAGA	CAGCTGGCACCTTATTGG
	Rpl13α	NM_173340.2	TTTCTCCGAAAGCGGATG	AGGGATCCCATCCAACA
	RNA28S4	NR_145822.1	GCGGCCAAGCGTTCATA	CCTGTCTCACGACGGTCTAA
	Polr2e	BC158787.1	GACCATCAAGGTGTACTGC	CAGCTCCTGCTGTAGAAAC
	Tbp	BC081939.1	TAACCCAGAAAGTCGAAGAC	CCGTAAGGCATCATTGGA
	Sdha	NM_130428.1	GCGGTATGAGACCAGTTATT	CCTGGCAAGGTAAACCAG
Target genes	*Col2a1*	NM_012929.1	ATCCAGGGCTCCAATGA	TCTTCTGGAGTGCGGAA
	Acan	NM_022190.1	CAAGTGGAGCCGTGTTT	TTTAGGTCTTGGAAGCGAG
	Sox9	NM_080403.1	CCAGAGAACGCACATCAAG	ATACTGATGTGGCTGGTGG
	Six1	NM_053759.1	CAGGTTCTTGTGGTCGTT	TTTGGGATGGTTGTGAGG
	Abi3bp	XM_017598145.1	ACGGGACATTCCTCTCATA	GGTGCCTGAGTTGTCTTT

	Alp	NM_013059.2	CGACAGCAAGCCCAAG	AGACGCCCATACCATCT
	Runx2	NM_001278484.2	CCCAAGTGGCCACTTAC	CTGAGGCGGTCAGAGA
	Ocn	NM_013414.2	GCGACTCTGAGTCTGACA	GGCAACACATGCCCTAAA
Target genes	*Col1a1*	NM_053304.1	GGTGACAGAGGCATAAAGG	AGACCGTTGAGTCCATCT
	Bmp-2	NM_017178.1	GGAAGTGGCCCACTTAGA	TCACTAGCAGTGGTCTTACC
	Vegfa	NM_001317043.1	CTACCAGCGCAGCTATTG	GATCCGCATGATCTGCATAG
	Col4a1	NM_001135009.1	CTGGGAATCCCGGACTT	GGGATCTCCCTTCATTCCT

Actb = Actin beta, Rplp0 = Ribosomal protein lateral stalk subunit p0, Gapdh = Glyceraldehyde-3-phosphate dehydrogenase, Rpl13a = Ribosomal protein l13a, Polr2e = RNA polymerase II subunit e, RNA28S4 = RNA 28S ribosomal 4, Sdha = Succinate dehydrogenase complex flavoprotein subunit A, Tbp = TATA-binding protein; Acan = Aggrecan, Col2a1= Collagen type II alpha 1, Sox9 = Sex determining region Y (SRY)-box transcription factor 9, Six1= Six homeobox 1, Abi3bp = Abi family member 3 binding protein, Runx2 = Runx family transcription factor 2, Alp= Alkaline phosphatase, Bmp-2 = Bone morphogenetic protein-2, Ocn = Osteocalcin, Col1a1 = Collagen type I alpha 1 chain, Col4a1 = Collagen type IV alpha 1 chain, Vegfa = Vascular endothelial growth factor a.

3.4.3 Quantitative real time-polymerase chain reaction (qPCR) process

The qPCR process was subsequently executed on the LightCycler® 96 Instrument (Roche, Switzerland), utilizing the FastStart Essential DNA Green Master and SYBR Green I Kit (Roche, Switzerland). Thermal cycling parameters are shown in **(Table 2)**. The final reaction components are shown in **(Table 3)**, with a volume of 10 µL. Quantification cycle (Cq) represented relative gene expression level, which was generated by the LightCycler® software (Roche, Switzerland).

Table 2. The process of qPCR thermal cycling.

Initialization	95° C	3min	
Denaturation	95° C	10s	40 cycles
Annealing	60° C	15s	
Extension/elongation	72° C	30s	
Final extension	72° C	5min	

Table 3. The qPCR reaction components.

Components	**Volumes (µL)**
Fwd. primer	0.6
Rev. primer	0.6
cDNA(5ng/µL)	2
RNase-free H2O	1.8
Green Master	5
Total	**10**

3.4.4 Reference gene selection (GeNorm)

To get more precise relative gene expression levels, the GeNorm(https://www.researchgate.net/publication/343548360_GeNorm_v35_xl) was applied to assess and select the optimal number of reference genes needed from the eight previously designed reference genes[203], that are stabily expressed between all samples and are necessary for the internal normalization/calibration of the relevant test genes.

The eight candidate reference genes were first applied to the RT-qPCR procedure to obtain the corresponding Cq values for each sample. After the conversion calculation by the following formula:

$$\Delta Cq = 2^{(Cq\ mean - Cq\ sample)}$$

The delta (Δ)- Cq values of all the samples were obtained, which were then imported into GeNorm software to generate the following two charts (**Figure 2 - A/B**), which could be used to filter the most reliable reference genes.

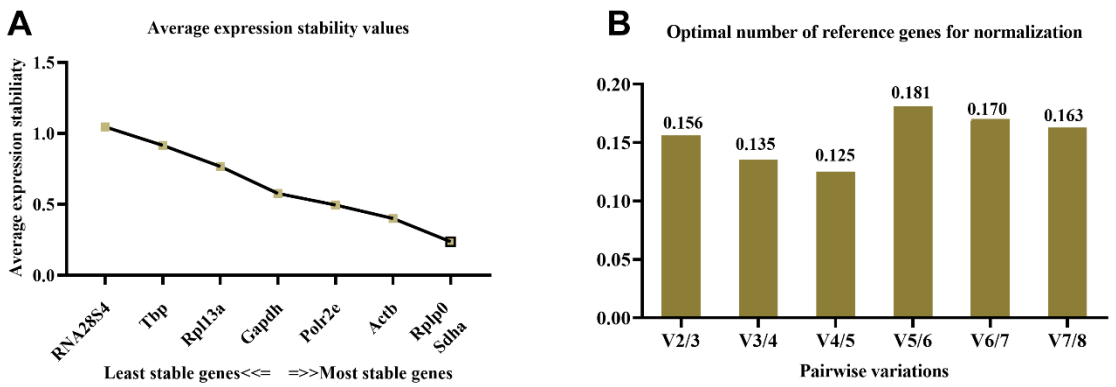

Figure 2. Filtering the most reliable reference genes by GeNorm.**A.** The genes expression stability, which increased from left to right on the x-axis, with the ***Sdha*** **and** ***Rplp0*** repented the most stable genes. **B.** The result of the matched variation (V) between 2 sequence normalization factors, predicted the number of optimal reference genes. The lowest column (V4/5) means the suitable reference gene quantity.

After the comprehensive analysis of the two graphs, five reference genes were finally identified: *Sdha, Rplp0, Actb*, *Polr2e, and Gapdh*, which would be used for subsequent gene relative expression calibration.

3.4.5 Calibrated normalized relative quantities (CNRQs)

The final gene relative expression levels were characterized as the calibrated normalized relative quantities (CNRQs), which were obtained in the qBase+ software (https://www.qbaseplus.com/) by standardization with the pre-determined five reference genes, including the relevant endogenous control (fresh muscle tissue 0-day)

3.5 Histological staining

Harvested samples for histological analysis were first placed in 4% paraformaldehyde (Microcos GmbH, Garching, Germany) for overnight fixation, followed by dehydration in Spin Tissue Processor-120 (Especialidades Médicas Myr, S.L., Tarragona, Spain), then embedded in paraffin blocks. Afterwards, 3μm-thick sections were cut for subsequent staining.

3.5.1 Alcian Blue staining

In the present project, acidic polysaccharides were evaluated using an Alcian Blue staining kit (Morphisto, Frankfurt, Germany). By observing the content of acidic polysaccharides, the efficiency of chondrogenic induction in each group was evaluated. In terms of the staining steps, briefly, sections were deparaffinized in xylene (GmbH, Germany; 2x 5min), then hydrated through graded alcohols (100% 1x 5min, 96% 1x 5min, 70% 1x 5min, ending in distilled water 1x 2min). After the hydration, slides were incubated in Acetic Acid Solution (Morphisto, Frankfurt, Germany) for 3min, followed by Alcian Blue (pH 2.5, 30min, RT). Subsequently, slides were immersed in Acetic Acid Solution (3min, RT). After being washed in distilled water for 5min, slides were put into Fast Red solution (Morphisto, Frankfurt, Germany) for 5min. Finally, after the dehydration via graded alcohols, slides were mounted in synthetic resin (O. Kindler GmbH, Bobingen, Germany). After staining, a PreciPoint M8 Digital Microscope & Scanner (PreciPoint GmbH, Freising, Germany) was used to acquire stained images, which were then analyzed for semi-quantitative histomorphometrical analysis using Image-Pro plus 6.0 software (Media Cybernetics, Inc. Silver Spring, MD USA). The ratio of the positive range-optical density value (IOD) to the whole range of the sample was the raw staining result.

3.5.2 Alizarin Red S staining

In the present project, calcium deposits were evaluated using the Alizarin Red S staining kit (Morphisto, Frankfurt, Germany). By observing the content of calcium deposits, the efficiency of osteogenesis induction in each group was evaluated. In terms of the staining steps, after deparaffinized and hydration (same as above), slides were incubated in Alizarin Red S solution (pH 9, Morphisto, Frankfurt, Germany; 60min, RT), followed by Alizarin Red S solution (pH 7, Morphisto, Frankfurt, Germany; 5min, RT). After being washed in buffer solution (pH 7, Morphisto, Frankfurt, Germany;10 sec), slides were dehydrated via graded alcohols, and then mounted in synthetic resin (O. Kindler GmbH, Bobingen, Germany). The semi-quantitative analysis was conducted in the same way as mentioned above.

3.6 Immunohistochamistry (IHC) staining

To observe the chondrogenic or osteogenic response within the muscle tissue samples, ACAN (1:150) and OCN (1:100) antibodies (Biorbyt, Eching, Germany) were utilized for IHC staining. Rabbit-on-Rodent HRP-Polymer (ZYTOMED SYSTEMS GmbH) was applied as second antibody. Negative control was also set up using Antibody Diluent (ZYTOMED SYSTEMS GmbH, Berlin, Germany) instead of the ACAN or OCN. Finally, a Vina-Green™ chromogenic kit (Biocare-Medical, Concord, CA, USA) was used to show positive interactions between antigen and antibody. The images acquisition and semi-quantitative analysis were conducted in the same way as mentioned above (shown in **3.5**).

3.7 Statistical analysis

GraphPad Prism software 8 (La Jolla, CA, USA, http://www.graphpad.com) was used for statistical assessment. The comparison between different experimental and corresponding control groups was performed by One-way analysis of variance (One-way ANOVA) with Dunnet's multiple comparisons test. The comparison between each group at different time periods was performed by One-way ANOVA with Tukey's multiple comparisons test. $p<0.05$ was considered statistically significant, and the statistical outcomes were finally expressed as mean ± standard error of the mean (SEM). Rstudio (R-Studio, Boston, MA, USA; http://www.rstudio.com) was utilized to create the final heat maps. Depending on the culture conditions, the heat map was grouped into 8 clusters.

4. Results

4.1 RT-qPCR analysis

4.1.1 *Col2a1*

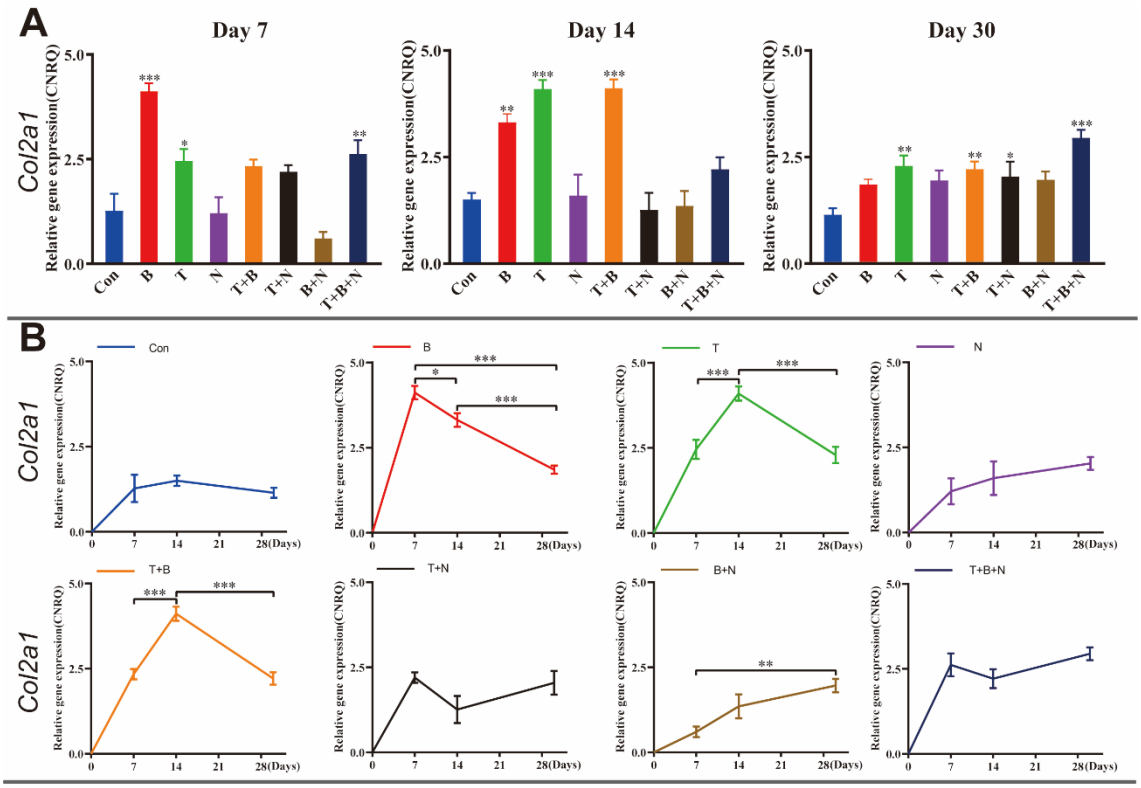

Figure 3. The relative gene expression of *Col2a1* was shown as CNRQ.**A.** Control group vs. stimulated groups at 7, 14, and 30 days. **B.** The relative gene expression change trend of *Col2a1* over time in each group. The asterisks in **(A)** indicate that the stimulated group is statistically significant compared to the control group, whereas in **(B)** they indicate a statistically significant comparison between different periods in the same group. The baseline number 0 indicates non-cultured fresh tissue was used as the normalization parameter. (n= 6; *p < 0.05; **p < 0.01; ***p < 0.001)

For *Col2a1*, rBMP-2 stimulated group showed the highest relative gene expression on day 7 and, like rTGF-β3 stimulated group, underwent a significant upregulation. However, the rTGF-β3 + rBMP-2 stimulated group presented a non-significant expression at the same time. More interestingly, this rTGF-β3 + rBMP-2 combined stimulation increased the *Col2a1* expression significantly after both day 14 and day 30. Besides, the rTGF-β3 + rBMP-2 and rTGF-β3 + rBMP-2 + rNoggin stimulated group showed the highest relative gene expression on day 14 and 30, respectively. Except for 30-day rTGF-β3 + rNoggin and rTGF-β3 + rBMP-

2 + rNoggin stimulated groups, *Col2a1* gene expression in all other rNoggin involved groups was not significant **(Figure 3-A, Appendix A)**. Regarding the trend of *Col2a1* gene expression over time, the rBMP-2 group reached the peak on day 7 but significantly decreased after that. The rTGF-β3 and rTGF-β3 + rBMP-2 groups have the same changing trend; they both rose sharply from 7 to 14 days, peaked at 14 days, and then fell sharply. Another point to be mentioned is that, although no significant changes were shown in this *Col2a1* gene expression, the rTGF-β3 + rNoggin combined group did display a 14-day depression, which was in stark contrast to the rTGF-β3 induced 14-day expression peak. In addition, the rTGF-β3 + rBMP-2 + rNoggin stimulated group seemed to always maintain an overall upward trend from the beginning to 30 days **(Figure 3-B, Appendix A)**.

4.1.2 *Sox9*

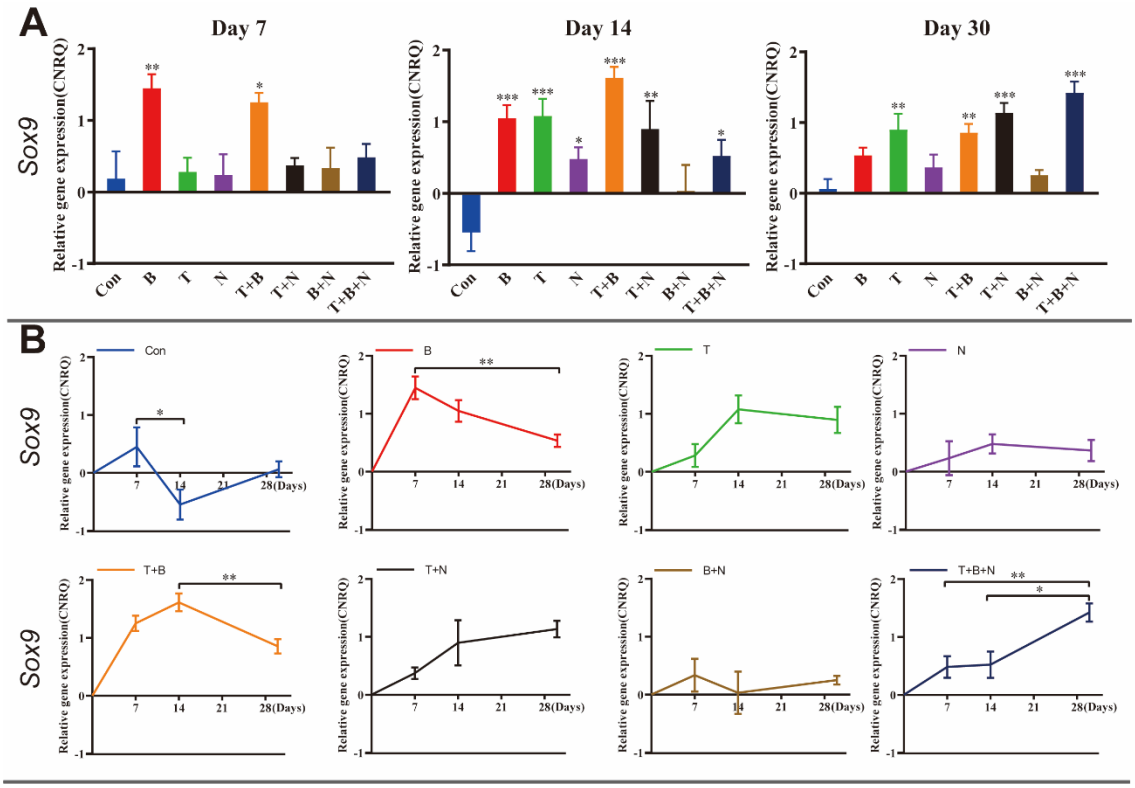

Figure 4. The relative gene expression of *Sox9* was shown as CNRQ.**A.** Control group vs. stimulated groups at 7, 14, and 30 days. **B.** The relative gene expression change trend of *Sox9* over time in each group. The asterisks in **(A)** indicate that the stimulated group is statistically significant compared to the control group, whereas in **(B)** they indicate a statistically significant comparison between different periods in the same group. The baseline number 0 indicates non-cultured fresh tissue was used as the normalization parameter. (n= 6; *p < 0.05; **p < 0.01; ***p < 0.001)

For *Sox9*, the highest relative gene expression appeared in rBMP-2, rTGF-β3 + rBMP-2, and the rTGF-β3 + rBMP-2 + rNoggin stimulated groups on days 7, 14, and 30, respectively, and all these three groups had a significant difference. Moreover, the *Sox9* gene expression in almost all rNoggin involved treatment groups showed no significant difference but except for the rNoggin alone group on day 14, plus rTGF-β3 + rBMP-2 + rNoggin and rTGF-β3 + rNoggin stimulated groups at 30 days **(Figure 4-A, Appendix A)**. Regarding the trend of *Sox9* gene expression over time, the rBMP-2 group peaked on day 7 but severely decreased after that, which was similar to *Col2a1* gene expression data. While the rTGF-β3 + rBMP-2 treated group peaked on 14 days, and then fell severely until day 30. In addition, the *Sox9* gene expression in the rTGF-β3 + rBMP-2 + rNoggin stimulated group went through a clear upward course from the beginning to 30 days **(Figure 4-B, Appendix A)**.

4.1.3 *Acan*

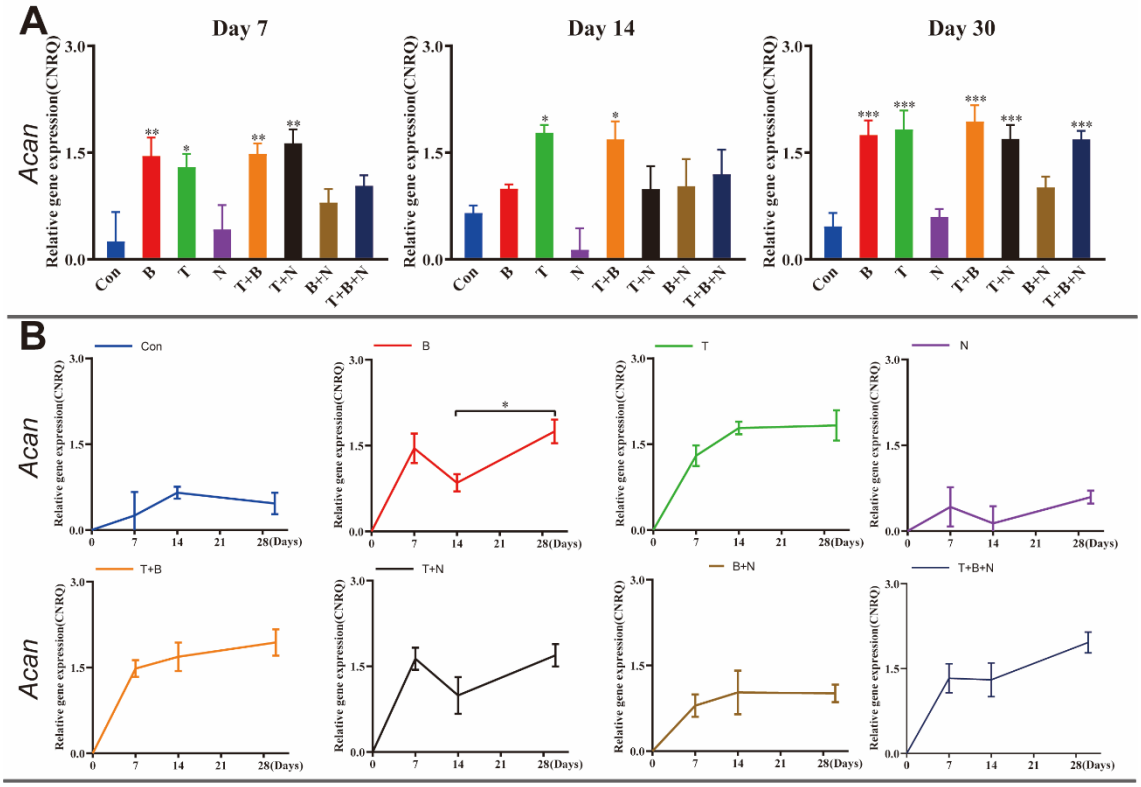

Figure 5. The relative gene expression of *Acan* was shown as CNRQ.**A.** Control group vs. stimulated groups at 7, 14, and 30 days. **B.** The relative gene expression change trend of *Acan* over time in each group. The asterisks in **(A)** indicate that the stimulated group is statistically significant compared to the control group, whereas in **(B)** they indicate a statistically significant comparison between different periods in the same group. The baseline number 0 indicates non-cultured fresh tissue was used as the normalization parameter. (n= 6; *p < 0.05; **p < 0.01; ***p < 0.001)

For *Acan*, the significantly upregulated gene expression was found in the rBMP-2, rTGF-β3, rTGF-β3 + rBMP-2, and rTGF-β3 + rNoggin stimulated groups on day 7, but only found in the rTGF-β3 and rTGF-β3 + rBMP-2 treated groups on day 14. Besides, only the rNoggin and rBMP-2 + rNoggin treated groups presented no significant difference across all stimulated groups by 30 days **(Figure 5-A, Appendix A)**. Regarding the trend of *Acan* gene expression over time, the rBMP-2 group showed a peaking trend on day 7, then declined but increased significantly between 14 and 30 days. Similar to *Col2a1* gene expression, although no significant difference was found, the rTGF-β3 + rNoggin combined group displayed a low *Acan* gene expression on day 14, and the rTGF-β3 + rBMP-2 + rNoggin stimulated group seemed to keep an overall upward trend from the beginning to 30 days **(Figure 5-B, Appendix A)**.

4.1.4 *Six1*

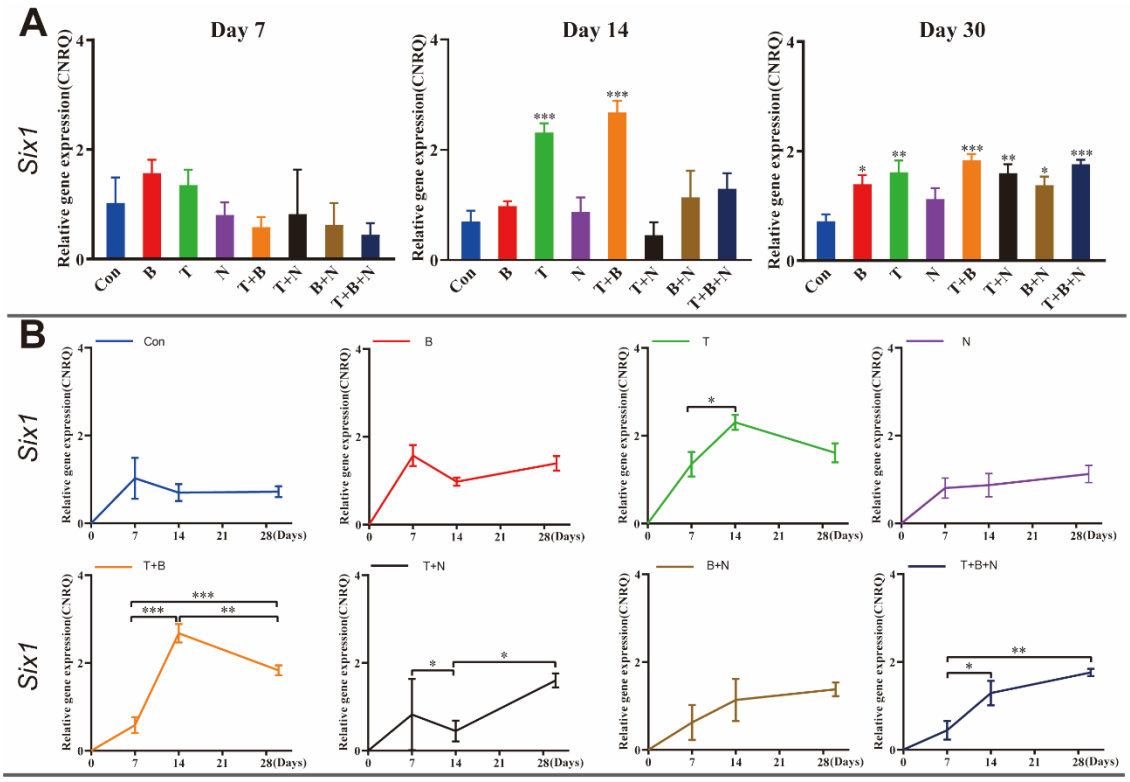

Figure 6. The relative gene expression of *Six1* was shown as CNRQ.**A.** Control group vs. stimulated groups at 7, 14, and 30 days. **B.** The relative gene expression change trend of *Six1* over time in each group. The asterisks in **(A)** indicate that the stimulated group is statistically significant compared to the control group, whereas in **(B)** they indicate a statistically significant comparison between different periods in the same group. The baseline number 0 indicates non-cultured fresh tissue was used as the normalization parameter. (n= 6; *p < 0.05; **p < 0.01; ***p < 0.001)

For relative *Six1* gene expression, no significant gene increase was found in all stimulated groups at 7 days, while the rTGF-β3 + rBMP-2 and rTGF-β3 stimulated groups displayed significant upregulation of *Six1* gene on day 14, and the latter exhibited higher levels of gene expression. By day 30, all the treatment groups showed the ability to upregulate the *Six1* gene expression significantly, except the rNoggin group **(Figure 6-A, Appendix A)**. Regarding the trend of *Six1* gene expression over time, the rBMP-2 treated group showed a peaking trend at 7 days, while the rTGF-β3 + rBMP-2 and rTGF-β3 treated groups presented the peak tendency at 14 days. The *Six1* gene expression was significantly upregulated in the rTGF-β3 and rTGF-β3 + rBMP-2 stimulated groups but significantly downregulated in the rTGF-β3 + rNoggin collaborative group from day 7 to day 14. And the rTGF-β3 + rNoggin collaborative group increased the *Six1* gene expression after 14 days. Besides, the rTGF-β3 + rBMP-2 + rNoggin stimulated

group maintained a general upward trend from the beginning to 30 days **(Figure 6-B, Appendix A)**.

4.1.5 *Abi3bp*

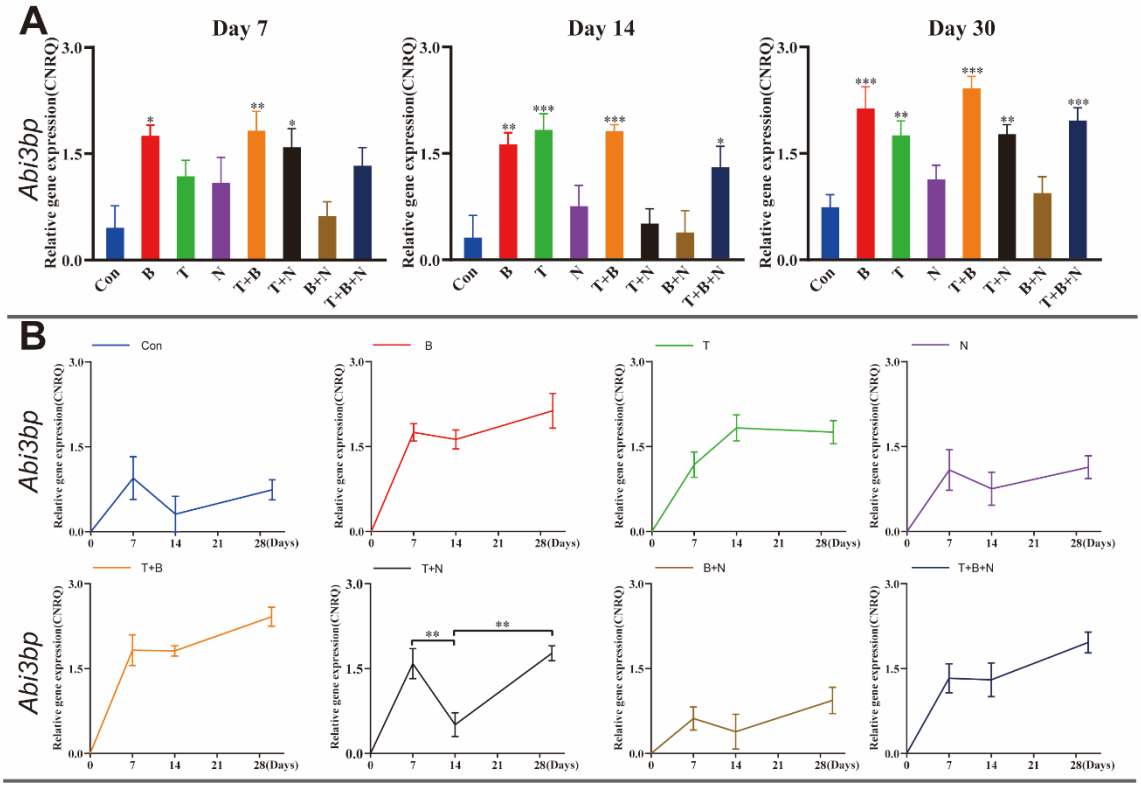

Figure 7. The relative gene expression of *Abi3bp* was shown as CNRQ.**A.** Control group vs. stimulated groups at 7, 14, and 30 days. **B.** The relative gene expression change trend of *Abi3bp* over time in each group. The asterisks in **(A)** indicate that the stimulated group is statistically significant compared to the control group, whereas in **(B)** they indicate a statistically significant comparison between different periods in the same group. The baseline number 0 indicates non-cultured fresh tissue was used as the normalization parameter. (n= 6; *p < 0.05; **p < 0.01; ***p < 0.001)

For relative *Abi3bp* gene expression, the significantly upregulated gene expression was found in the rBMP-2, rBMP-2 + rTGF-β3, and rTGF-β3 + rNoggin stimulated groups at 7 days. Besides, the rBMP-2 + rTGF-β3 and rTGF-β3 + rBMP-2 + rNoggin stimulated groups displayed a significant difference compared with control group at both 14 and 30 days. Moreover, the *Abi3bp* gene expression in all rNoggin and rNoggin + rBMP-2 treated groups showed no significant difference at all three-time points **(Figure 7-A, Appendix B)**. Regarding the trend of *Abi3bp* gene expression over time, the rTGF-β3 + rNoggin combined group exhibited a significant downregulation of *Abi3bp* gene expression from 7 to 14 days, however, it subsequently displayed a significant upregulation from 14 to 30 days. Additionally, the rTGF-β3 + rBMP-2 + rNoggin stimulated group seemed to maintain a general upward trend from day 0 to day 30 **(Figure 7-B, Appendix B)**.

4.1.6 *Alp*

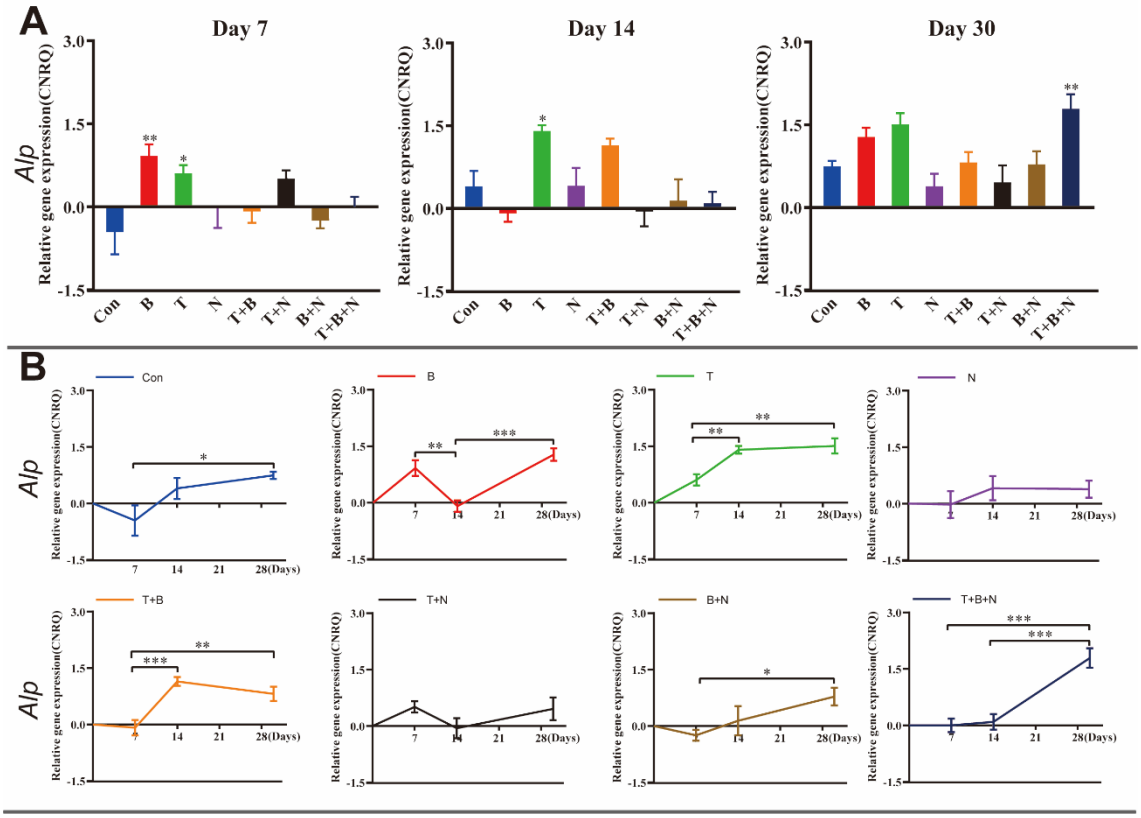

Figure 8. The relative gene expression of *Alp* was shown as CNRQ.**A.** Control group vs. stimulated groups at 7, 14, and 30 days. **B.** The relative gene expression change trend of *Alp* over time in each group. The asterisks in **(A)** indicate that the stimulated group is statistically significant compared to the control group, whereas in **(B)** they indicate a statistically significant comparison between different periods in the same group. The baseline number 0 indicates non-cultured fresh tissue was used as the normalization parameter. (n= 6; *p < 0.05; **p < 0.01; ***p < 0.001)

For *Alp*, the rBMP-2 stimulated group showed the highest relative gene expression on day 7, which was significantly upregulated along with the rTGF-β3 and rBMP-2 + rTGF-β3 + rNoggin stimulated groups. Additionally, the rTGF-β3 induced group was the only one that presented a significant *Alp* expression on day 14, and only the rTGF-β3 + rNoggin and rTGF-β3 + rBMP-2 + rNoggin stimulated group demonstrated a significant *Alp* expression upregulation. On the other hand, *Alp* expression in all rNoggin involved groups showed no significant difference compared with corresponding control groups **(Figure 8-A, Appendix B)**. Regarding the trend of *Alp* gene expression over time, the rBMP-2 group reached the peak on day 7 sharply but severely decreased after that and severely increased again until 30 days. The rTGF-β3 group rose quickly from 7 to 14 days before gradually remaining stable, while the rBMP-2 + rTGF-β3 group peaked at 14

days, then declined gradually. Besides, the rTGF-β3 + rBMP-2 + rNoggin stimulated group displayed an upregulation from 7 to 14 days significantly. Additionally, the rBMP-2 + rNoggin combined group and even the control group both showed upregulated expression from day 7 to 30 **(Figure 8-B, Appendix B)**.

4.1.7 *Runx2*

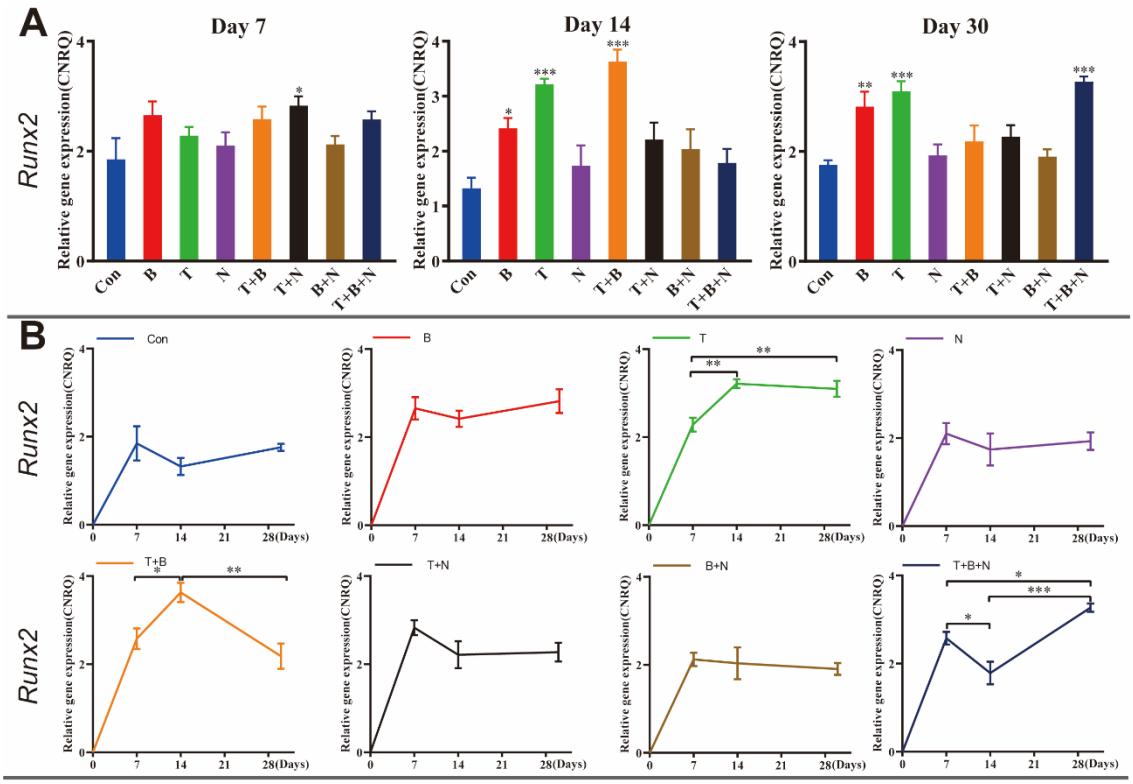

Figure 9. The relative gene expression of *Runx2* was shown as CNRQ.**A.** Control group vs. stimulated groups at 7, 14, and 30 days. **B.** The relative gene expression change trend of *Runx2* over time in each group. The asterisks in **(A)** indicate that the stimulated group is statistically significant compared to the control group, whereas in **(B)** they indicate a statistically significant comparison between different periods in the same group. The baseline number 0 indicates non-cultured fresh tissue was used as the normalization parameter. (n= 6; *p < 0.05; **p < 0.01; ***p < 0.001)

For the relative *Runx2* gene expression, the rTGF-β3 + rNoggin stimulated group became the only group that showed a significant difference at 7 days, while at 14 days, the significantly upregulated *Runx2* gene expression was found in the rBMP-2, rTGF-β3, and rBMP-2 + rTGF-β3 stimulated groups. By 30 days, the rBMP-2, rTGF-β3, and rBMP-2 + rTGF-β3+ rNoggin treated groups showed high and significant gene expression. In addition, except for the 7-day rTGF-β3 + rNoggin and 30-day rTGF-β3 + rBMP-2 + rNoggin stimulated groups, *Runx2* gene expression in all other rNoggin involved groups was not significant **(Figure 9-A, Appendix B)**. Regarding the trend of *Runx2* gene expression over time, the rTGF-β3 treated group rose significantly from 7 to 14 days, then kept stable. While the rTGF-β3 + rBMP-2 stimulated group peaked on day 14, then declined severely. Furthermore, the rTGF-β3 + rBMP-2 + rNoggin treated group presented

a decreased expression trend on day 14 but subsequently continued to rise forcefully **(Figure 9-B, Appendix B)**.

4.1.8 *Bmp-2*

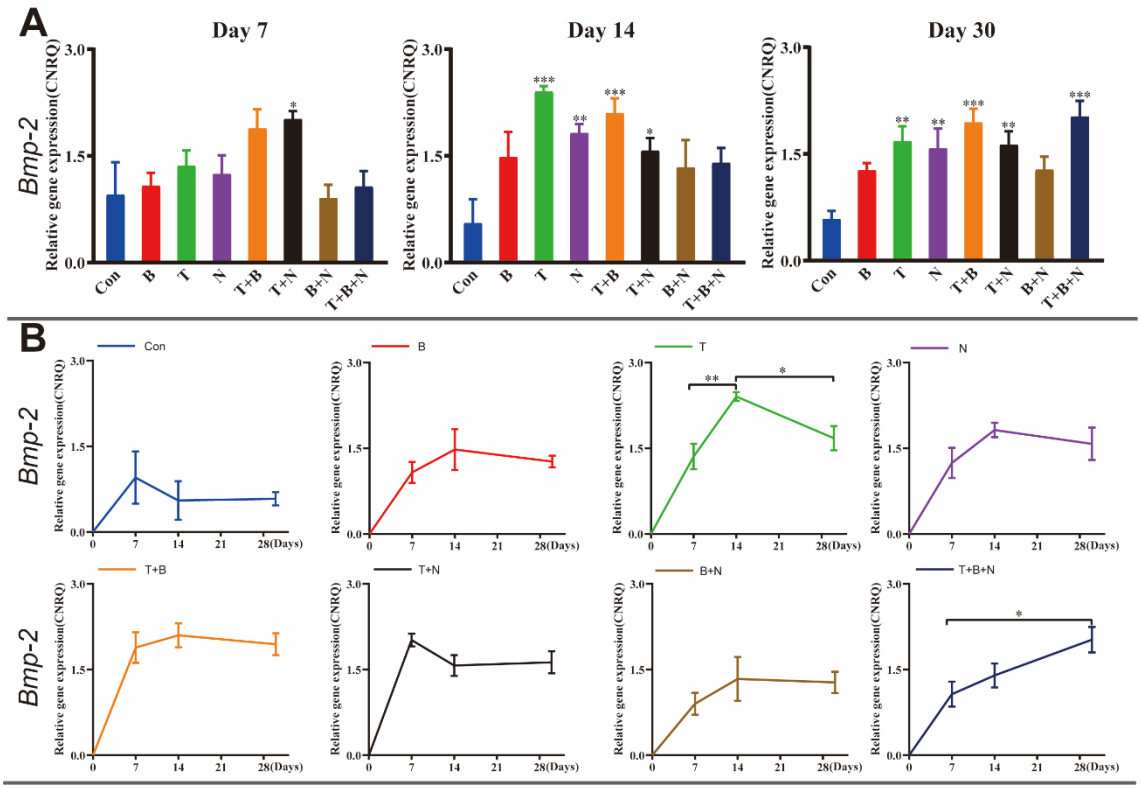

Figure 10. The relative gene expression of *Bmp-2* was shown as CNRQ.**A.** Control group vs. stimulated groups at 7, 14, and 30 days. **B.** The relative gene expression change trend of *Bmp-2* over time in each group. The asterisks in **(A)** indicate that the stimulated group is statistically significant compared to the control group, whereas in **(B)** they indicate a statistically significant comparison between different periods in the same group. The baseline number 0 indicates non-cultured fresh tissue was used as the normalization parameter. (n= 6; *p < 0.05; **p < 0.01; ***p < 0.001)

For the relative *Bmp-2* gene expression, the rTGF-β3 + rNoggin stimulated group showed a significant difference across all three-time points, plus rTGF-β3, rNoggin, and rBMP-2 + rTGF-β3 treated groups presented significant upregulated *Bmp-2* gene expression at both day 14 and 30. Besides, the rTGF-β3+ rBMP-2+ rNoggin treated groups showed the highest and significant gene expression on day 30. In addition, all the rBMP-2+ rNoggin treated groups showed non-significant *Bmp-2* gene expression **(Figure 10-A, Appendix B)**. Regarding the trend of *Bmp-2* gene expression over time, the rTGF-β3 stimulated group rose significantly from day 7 to 14 and peaked there but dropped harshly until 30 days. Moreover, the rTGF-β3 + rBMP-2 + rNoggin stimulated group always maintained an overall upward trend from the beginning to 30 days but more significantly from day 7 to 30 **(Figure 10-B, Appendix B)**.

4.1.9 *Ocn*

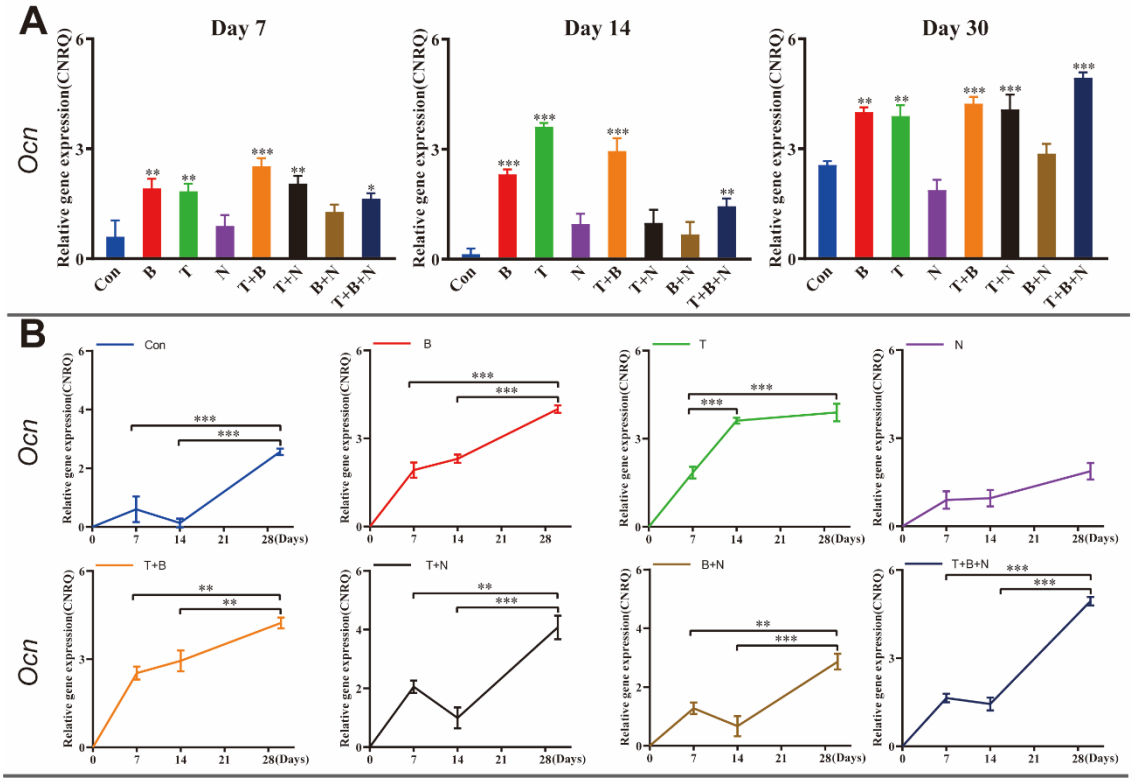

Figure 11. The relative gene expression of *Ocn* was shown as CNRQ.**A.** Control group vs. stimulated groups at 7, 14, and 30 days. **B.** The relative gene expression change trend of *Ocn* over time in each group. The asterisks in **(A)** indicate that the stimulated group is statistically significant compared to the control group, whereas in **(B)** they indicate a statistically significant comparison between different periods in the same group. The baseline number 0 indicates non-cultured fresh tissue was used as the normalization parameter. (n= 6; *p < 0.05; **p < 0.01; ***p < 0.001)

For the relative *Ocn* gene expression, the rBMP-2, rTGF-β3, rBMP-2 + rTGF-β3, and rBMP-2 + rTGF-β3 + rNoggin stimulated groups all presented significant up-regulation among the three-time points. Additionally, the rTGF-β3 + rNoggin stimulated group also showed significant *Ocn* gene expression on days 7 and 30, but a non-significant difference was found on day 14. Furthermore, the rNoggin and rBMP-2 + rNoggin treated groups exhibited non-significant *Ocn* gene expression all the time **(Figure 11-A, Appendix C)**. Regarding the trend of *Ocn* gene expression over time, the rBMP-2, rTGF-β3 + rBMP-2 and rTGF-β3 + rBMP-2 + rNoggin stimulated groups showed a significant upward trend from day 7 or 14 until day 30, while the rTGF-β3 and rBMP-2 + rNoggin treated groups, and even non-treated control group showed the significant rising trend from day 7 until day 14 or 30. On the other hand, the rTGF-β3 + rNoggin stimulated group displayed a severely *Ocn* gene expression decline trend from day 7 to 14, but subsequent a significant upward trend from day 14 to 30 **(Figure 11-B, Appendix C)**.

4.1.10 *Col1a1*

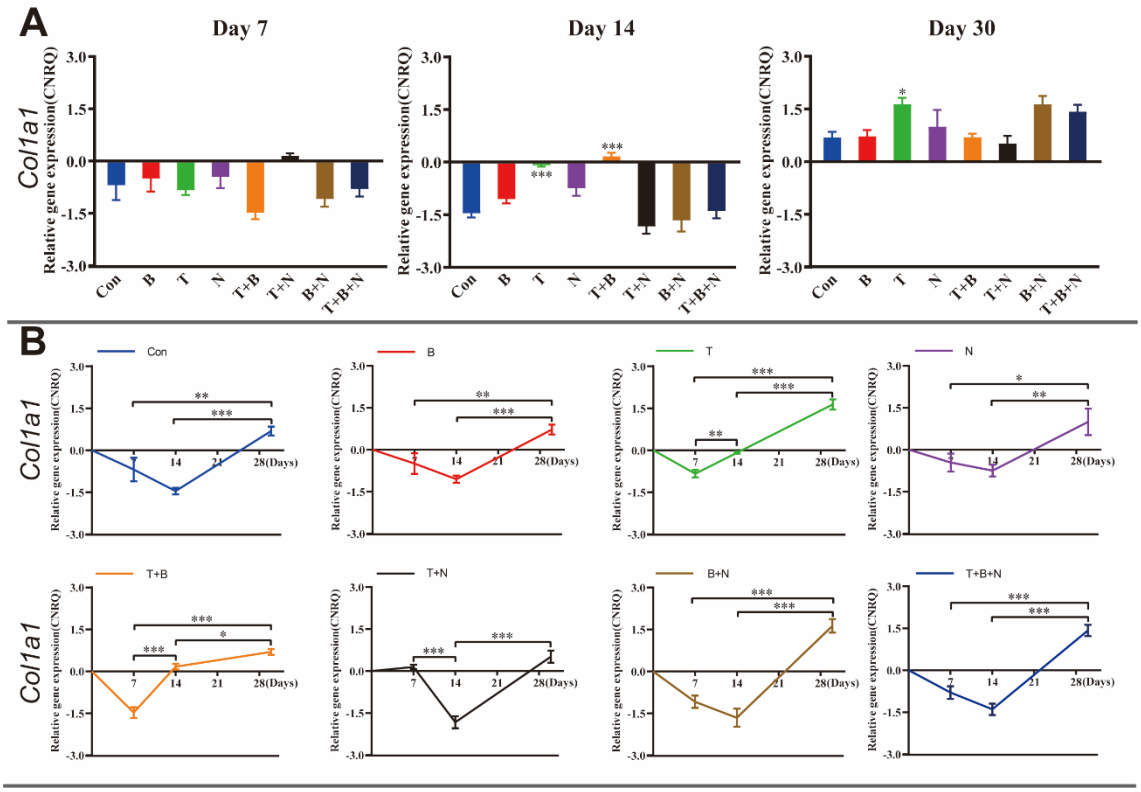

Figure 12. The relative gene expression of *Col1a1* was shown as CNRQ.**A.** Control group vs. stimulated groups at 7, 14, and 30 days. **B.** The relative gene expression change trend of *Col1a1* over time in each group. The asterisks in **(A)** indicate that the stimulated group is statistically significant compared to the control group, whereas in **(B)** they indicate a statistically significant comparison between different periods in the same group. The baseline number 0 indicates non-cultured fresh tissue was used as the normalization parameter. (n= 6; *p < 0.05; **p < 0.01; ***p < 0.001)

For *Col1a1*, no treatment group showed upregulated relative gene expression at 7 days, while the rTGF-β3 and rBMP-2 + rTGF-β3 stimulated groups were significantly upregulated at 14 days. By 30 days, although most stimulated groups showed upregulation of *Col1a1* gene expression, only the rTGF-β3 stimulated group exhibited a significant difference **(Figure 12-A, Appendix C)**. Regarding the trend of *Col1a1* gene expression over time, from 7 to 14 days, the rTGF-β3 + rNoggin treated group presented a significant downregulation, while the rTGF-β3 and rBMP-2 + rTGF-β3 stimulated groups exhibited a significant upregulation. From day 14 to 30, all the stimulated groups and even the non-treated control group displayed a significant *Col1a1* gene upregulation trend. When analyzing the data from day 7 to 30, an overall rising tendency of *Col1a1* gene expression could be found in involved groups except for the rTGF-β3 + rNoggin stimulated group **(Figure 12-B, Appendix C)**.

4.1.11 *Vegfa*

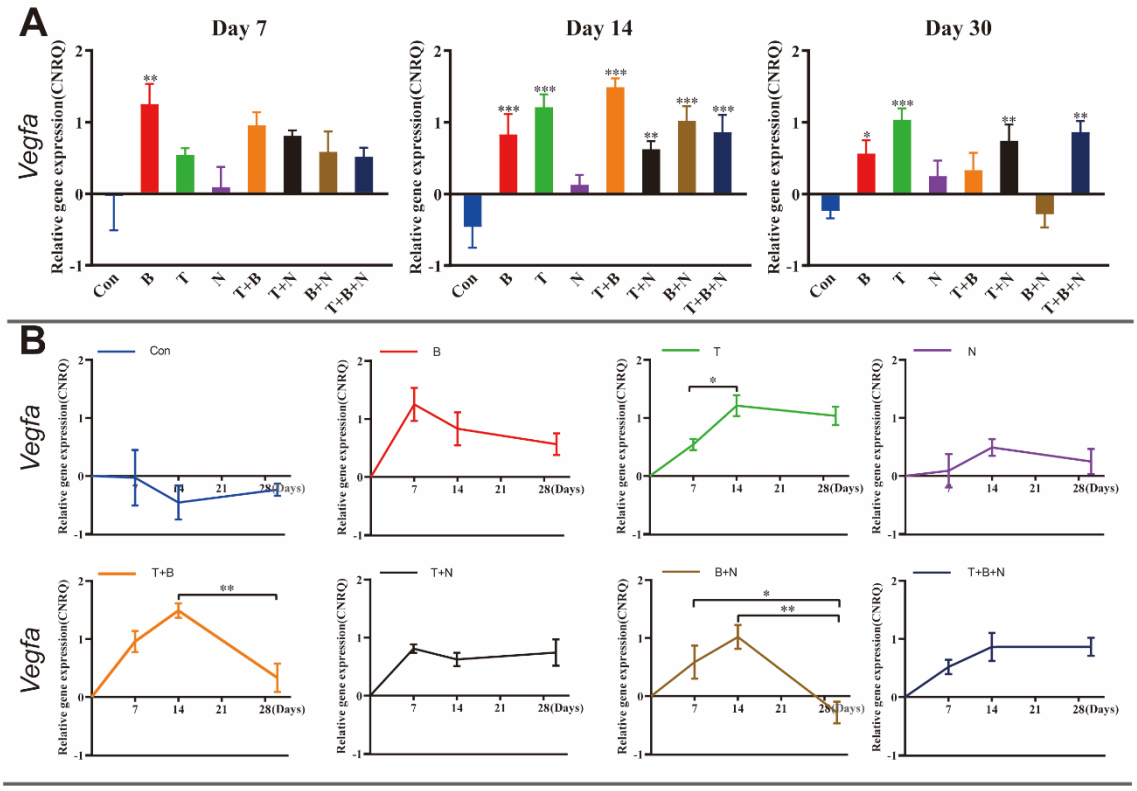

Figure 13. The relative gene expression of *Vegfa* was shown as CNRQ.**A.** Control group vs. stimulated groups at 7, 14, and 30 days. **B.** The relative gene expression change trend of *Vegfa* over time in each group. The asterisks in **(A)** indicate that the stimulated group is statistically significant compared to the control group, whereas in **(B)** they indicate a statistically significant comparison between different periods in the same group. The baseline number 0 indicates non-cultured fresh tissue was used as the normalization parameter. (n= 6; *p < 0.05; **p < 0.01; ***p < 0.001)

For *Vegfa*, the rBMP-2 stimulated group showed the highest relative gene expression on day 7, which was also the only significant expression group on 7 days, while the rTGF-β3 + rBMP-2 combined group showed no significant difference at the same time. By day 14, almost all treated groups displayed a significant difference, only except for the rNoggin treated group. In addition, the rTGF-β3, rBMP-2, rTGF-β3 + rNoggin, rBMP-2 + rTGF-β3 + rNoggin stimulated groups exhibited significant *Vegfa* gene expression on day 30 **(Figure 13-A, Appendix C)**. Regarding the trend of *Vegfa* gene expression over time, the rTGF-β3 stimulated group showed a significant upregulation trend from day 7 to 14, and the rTGF-β3 + rNoggin treated groups presented the *Vegfa* gene expression downregulation trend from day 14 to 30. While the rBMP-2 + rNoggin treated group displayed both upregulation and downregulation trends, as gene expression rose from day 7 to 14, and reduced from day 14 to 30 **(Figure 13-B, Appendix C)**.

4.1.12 *Col4a1*

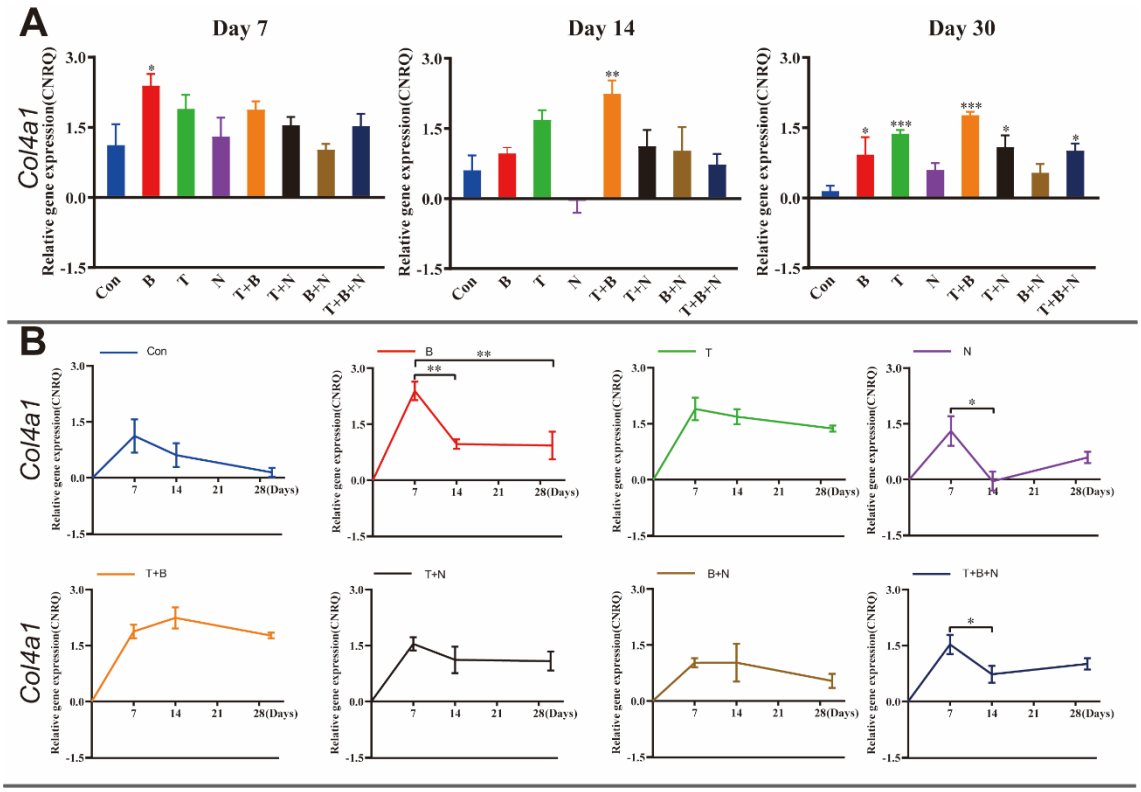

Figure 14. The relative gene expression of *Col4a1* was shown as CNRQ.**A.** Control group vs. stimulated groups at 7, 14, and 30 days. **B.** The relative gene expression change trend of *Col4a1* over time in each group. The asterisks in **(A)** indicate that the stimulated group is statistically significant compared to the control group, whereas in **(B)** they indicate a statistically significant comparison between different periods in the same group. The baseline number 0 indicates non-cultured fresh tissue was used as the normalization parameter. (n= 6; *p < 0.05; **p < 0.01; ***p < 0.001)

For *Col4a1*, the rBMP-2 stimulated group showed the highest relative gene expression on day 7, which was also the only significant expression group on 7 days, while the rTGF-β3 + rBMP-2 combined group showed no significant difference at the same time. By day 14, only the rTGF-β3 + rBMP-2 combined group presented significant difference. However, nearly all stimulated groups exhibited significant *Col4a1* gene expression except for the rNoggin and rBMP-2 + rNoggin treated groups on day 30 **(Figure 14-A, Appendix C)**. Regarding the trend of *Col4a1* gene expression over time, the rBMP-2 group reached the peak on day 7 but severely decreased after that and kept stable from 14 to 30 days. Additionally, the rNoggin and rTGF-β3 + rBMP-2 + rNoggin treated group showed a significant downregulation tendency from day 7 to 14 **(Figure 14-B, Appendix C)**.

4.2 Heat map of gene expression analysis

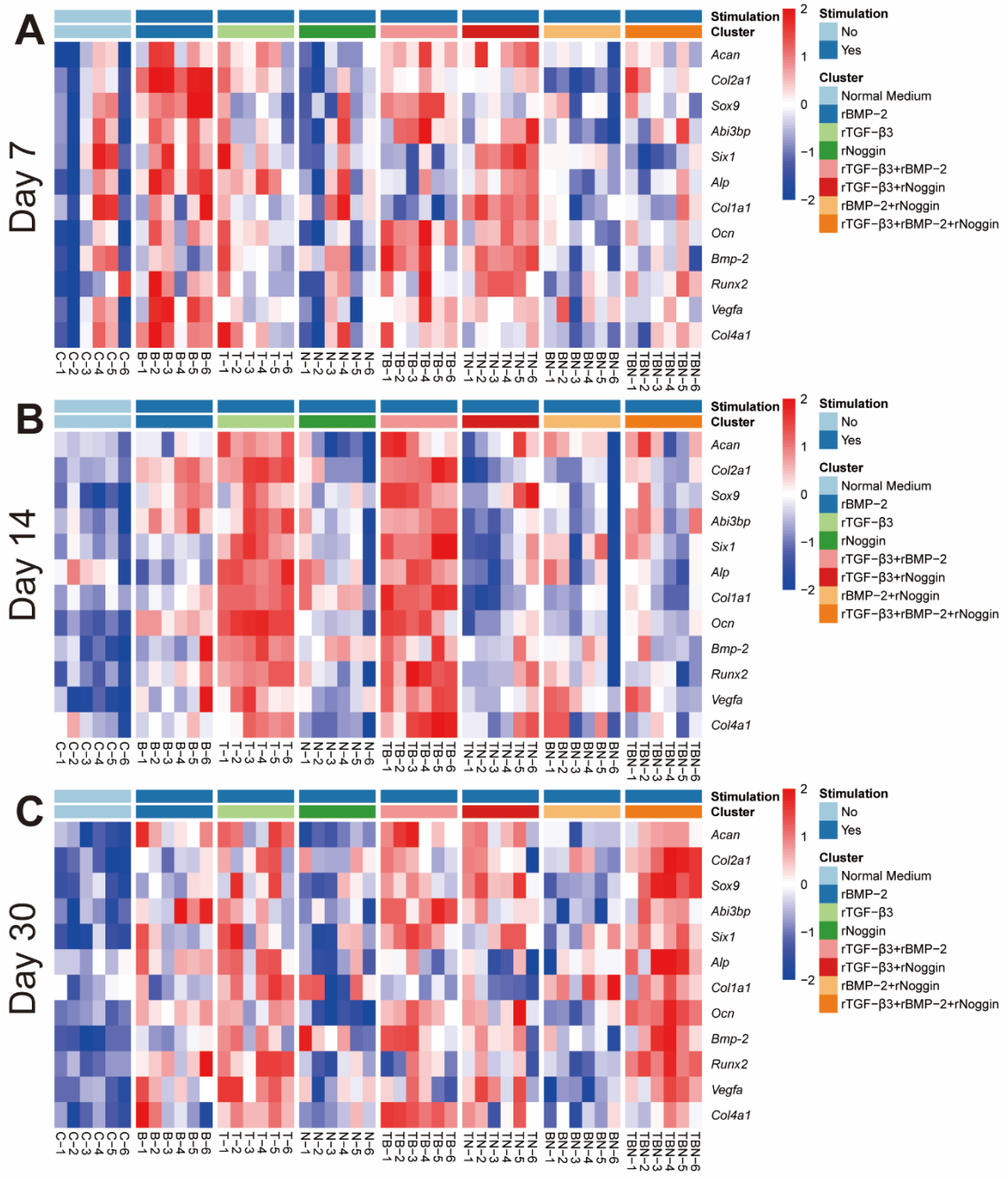

Figure 15. Heat map of gene expression.**A.** All relative gene expression at 7 days. **B.** All relative gene expression at 14 days. **C.** All relative gene expression at 30 days. *Acan* = Aggrecan, *Col2a1*= Collagen type II alpha 1, *Sox9* = Sex determining region Y (SRY)-box transcription factor 9, *Six1*= Six homeobox 1, *Abi3bp* = Abi family member 3 binding protein, *Runx2* = Runx family transcription factor 2, *Alp*= Alkaline phosphatase, *Bmp-2* = Bone morphogenetic protein-2, *Ocn* = Osteocalcin, *Col1a1* = Collagen type I alpha 1 chain, *Col4a1* = Collagen type IV alpha 1 chain, *Vegfa* = Vascular endothelial growth factor a; (n = 6).

Heat map of gene expression showed that the rBMP-2 and rTGF-β3 + rNoggin stimulated groups promoted relatively high gene expression at 7 days **(Figure 15-A)**; the rTGF-β3 and rTGF-β3 + rBMP-2 stimulated groups displayed relatively high gene expression at 14 days **(Figure 15-B)**; while the stimulation of rTGF-β3, rTGF-β3 + rNoggin, rTGF-β3 + rBMP-2 and rTGF-β3 + rBMP-2 + rNoggin exhibited high gene expression at 30 days **(Figure 15-C)**. Compare to 7 and 30 days, the stimulation of rTGF-β3 + rNoggin resulted in less gene expression at 14 days. Additionally, rNoggin and rBMP-2 + rNoggin treated groups did not show high gene expression at all time periods.

4.3 Histological analysis

4.3.1 Alcian Blue

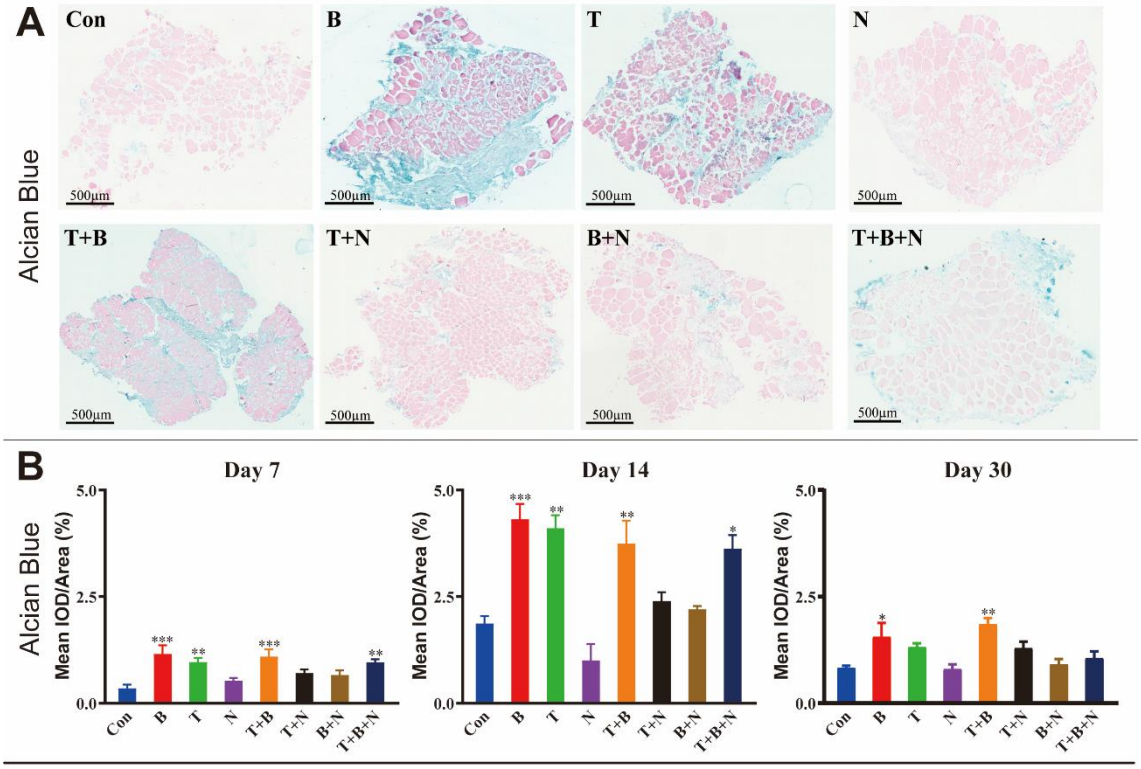

Figure 16. The staining results of Alcian Blue in each group.**A.** Staining results on day 30, the positive staining color was blue. **B.** Histomorphometrical assessment, the result was shown as Mean IOD/Area. Control group vs. stimulated groups at 7, 14, and 30 days, the asterisks indicate that the stimulated group is statistically significant compared to the control group. (Magnification: 40x; n = 6; *p < 0.05; **p < 0.01; ***p < 0.001)

Alcian Blue staining was used to confirm possible chondrogenic-like morphogenesis in the cultured samples. The positive staining area, stained in blue, was observed near the fascia or in the intercellular region of the muscle when stimulated by rTGF-β3, rBMP-2, rBMP-2 + rTGF-β3, and rBMP-2 + rTGF-β3 + rNoggin at all detection time points **(Figure 16-A)**. Histomorphometrical assessment showed that the rBMP-2, rTGF-β3 + rBMP-2 stimulated groups presented a positive reaction during all three time points, while rTGF-β3 and rTGF-β3 + rBMP-2 + rNoggin stimulated groups displayed a positive reaction on day 7 and 14. On the other hand, all groups showed the strongest positive Alcian Blue staining results at 14 days, while rNoggin and rBMP-2 + rNoggin combined groups consistently showed no significant differences **(Figure 16-B, Appendix D)**.

4.3.2 Alizarin Red S

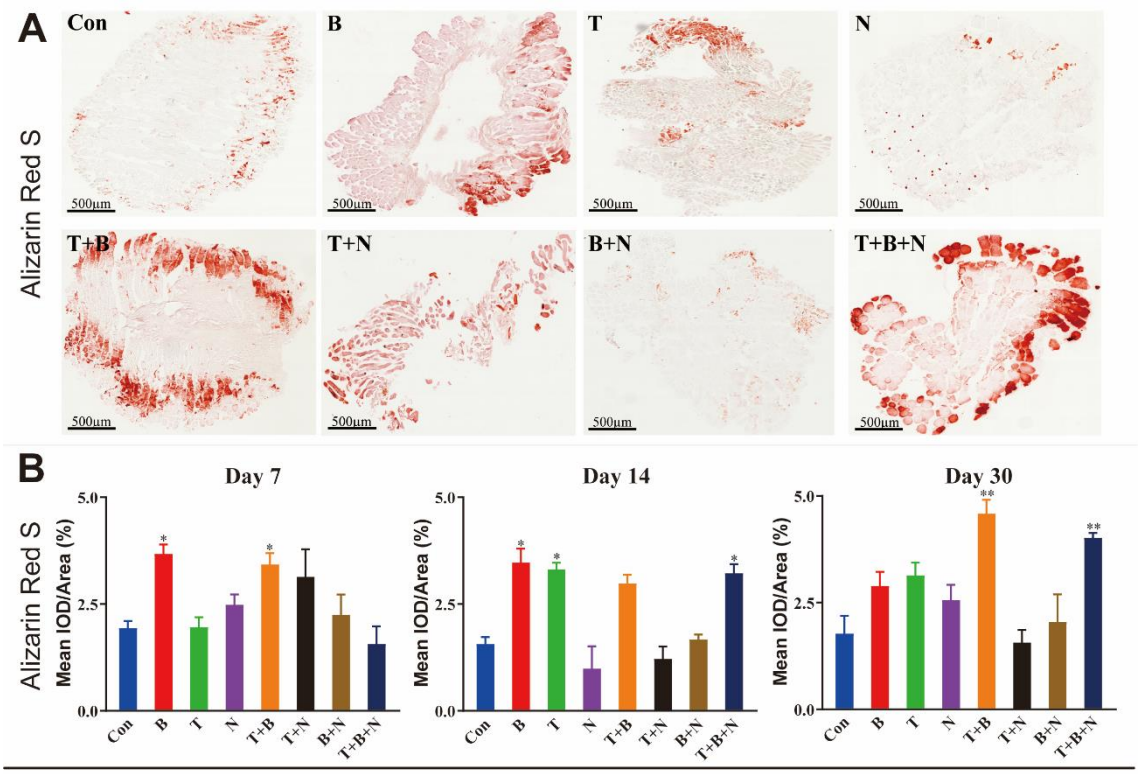

Figure 17. The staining results of Alizarin Red S in each group. **A.** Staining results on day 30, the positive staining color was red. **B.** Histomorphometrical assessment, the result was shown as Mean IOD/Area. Control group vs. stimulated groups at 7, 14, and 30 days, the asterisks indicate that the stimulated group is statistically significant compared to the control group. (Magnification: 40x; n = 6; *p < 0.05; **p < 0.01; ***p < 0.001)

Alizarin Red S staining shows the depositions of calcium ions in tissues. It was used to assess the spatial and relative quantity of new or developing osteogenic morphogenesis. Under stimulation of rBMP-2, rTGF-β3, rTGF-β3 + rBMP-2, rTGF-β3 + rNoggin, and rTGF-β3 + rBMP-2 + rNoggin, areas of positive staining were observed in close proximity to the fascia or intercellular regions of the muscle with red color at all detection time points **(Figure 17-A)**. Histomorphometrical assessment of Alizarin Red S staining showed that the rBMP-2 stimulated group presented a positive reaction on days 7 and 14, while rTGF-β3 stimulated group only displayed a positive reaction on day 14. In addition, rTGF-β3 + rBMP-2 stimulated group displayed a positive reaction on day 7 and 30. Moreover, rTGF-β3 + rBMP-2 + rNoggin treated group started showing significant stimulation from day 14, until day 30. Additionally, rNoggin and rBMP-2 + rNoggin combined group consistently showed no significant difference **(Figure 17-B, Appendix D)**.

4.4 Immunohistochemistry (IHC) analysis

4.4.1 IHC- ACAN

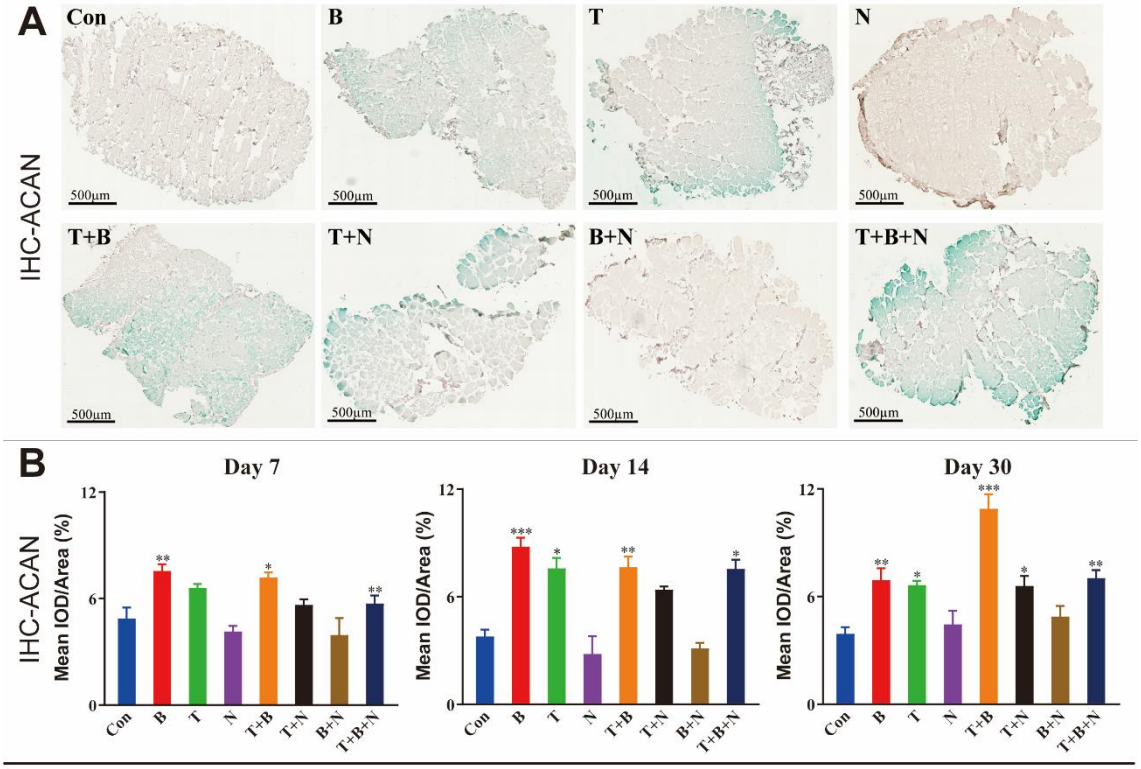

Figure 18. The staining results of ACAN antigen in IHC in each group.**A.** Staining results on day 30, the positive staining color was green. **B.** Histomorphometrical assessment, the result was shown as Mean IOD/Area. Control group vs. stimulated groups at 7, 14, and 30 days, the asterisks indicate that the stimulated group is statistically significant compared to the control group. (Magnification: 40x; n = 6; *p < 0.05; **p < 0.01; ***p < 0.001)

IHC-ACAN staining was done to show the existence of ACAN antigen. A positive antigen-antibody interaction would be stained in a green color, which could be observed in close proximity to the fascia or in the intercellular region of the muscle when stimulated by rBMP-2, rTGF-β3, rTGF-β3 + rBMP-2, rTGF-β3 + rNoggin, and rTGF-β3 + rBMP-2 + rNoggin at all detection time points **(Figure 18-A)**. Histomorphometrical assessment of IHC-ACAN staining showed that the rBMP-2, rTGF-β3 + rBMP-2 stimulated groups presented a positive reaction during all three time points, while rTGF-β3 and rTGF-β3 + rBMP-2 + rNoggin stimulated groups displayed a positive reaction on day 14 and 30. In addition, the rTGF-β3 + rNoggin stimulated group also exhibited a significant difference on day 30. Additionally, no rBMP-2 + rNoggin combined group showed a significant difference **(Figure 18-B, Appendix D)**.

4.4.2 IHC-OCN

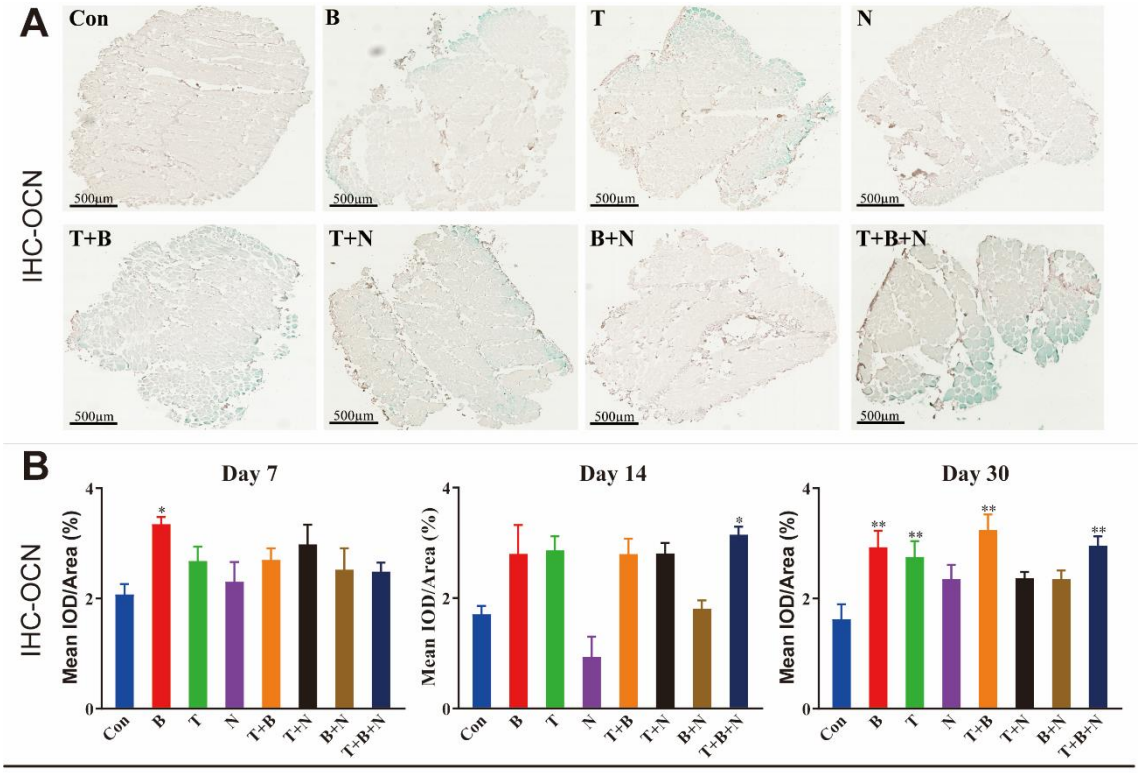

Figure 19. The staining results of OCN antigen in IHC in each group.**A.** Staining results on day 30, the positive staining color was green. **B.** Histomorphometrical assessment, the result was shown as Mean IOD/Area. Control group vs. stimulated groups at 7, 14, and 30 days, the asterisks indicate that the stimulated group is statistically significant compared to the control group. (Magnification: 40x; n = 6; *p < 0.05; **p < 0.01; ***p < 0.001)

IHC-OCN staining was done to show the existence of OCN antigen. Under stimulation of rBMP-2, rTGF-β3, rTGF-β3 + rBMP-2, rTGF-β3 + rNoggin, and rTGF-β3 + rBMP-2 + rNoggin, areas of positive staining were observed in close proximity to the fascia or intercellular regions of the muscle with green color at all detection time points **(Figure 19-A)**. Histomorphometrical assessment of IHC-OCN staining showed that, although with a general high positive reaction on day 7, the rBMP-2 stimulated group was the only one that had a significant difference. Besides, the rTGF-β3 + rBMP-2 + rNoggin stimulated group became the only significant positive stimulation group at 14 days, while rTGF-β3, rBMP-2, rTGF-β3 + rBMP-2 and rTGF-β3 + rBMP-2 + rNoggin treated groups all showed significant difference by day 30. Additionally, no rBMP-2 + rNoggin combined group showed a significant difference **(Figure 19-B, Appendix D)**.

4.5 Heat map of histomorphometrical analysis

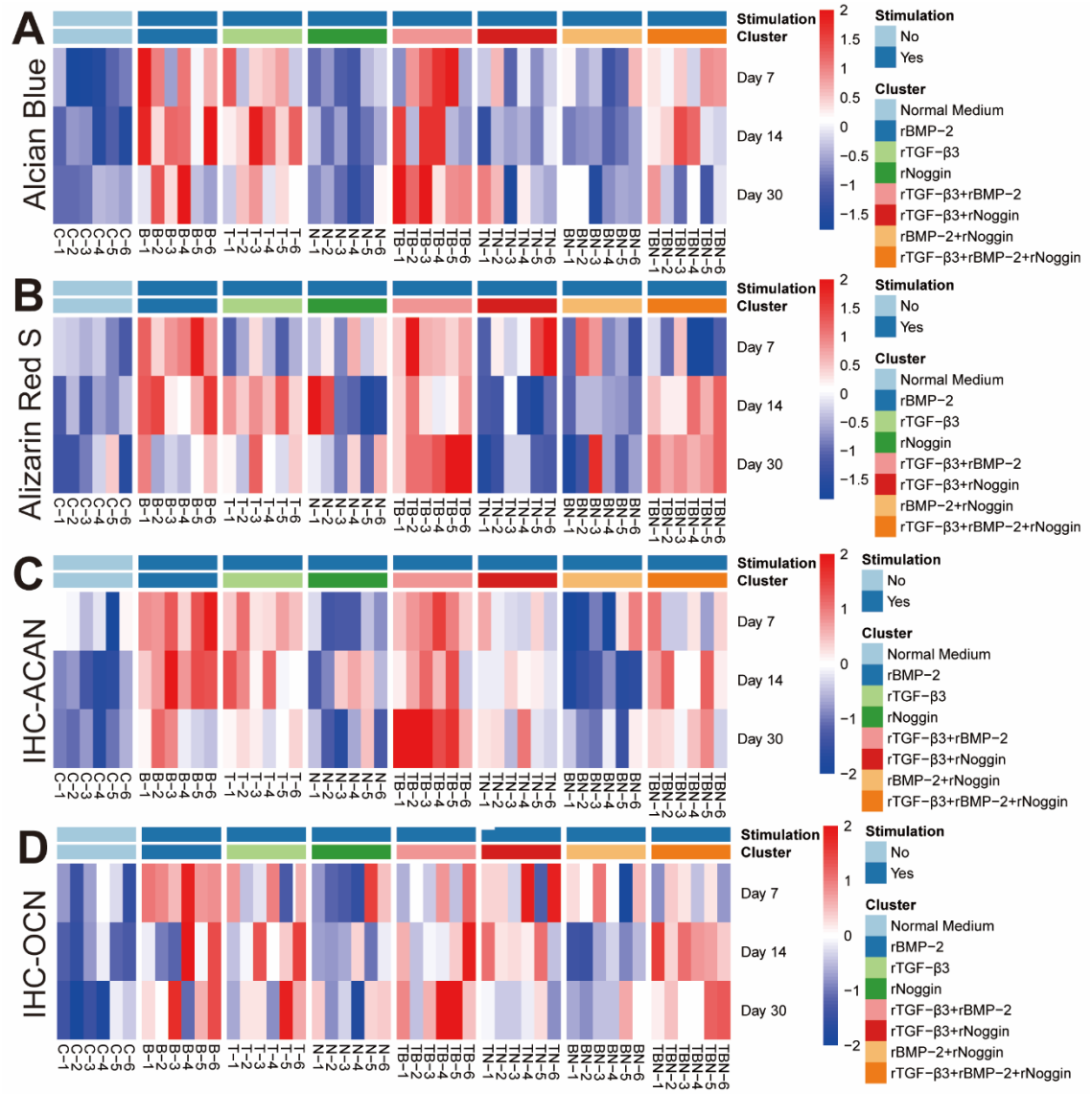

Figure 20. Heat map of histomorphometrical analysis.**A.** Alcian Blue staining. **B.** Alizarin Red S staining. **C.** IHC-ACAN staining. **D.** IHC-OCN staining. IHC = Immunohistochemistry, ACAN = Aggrecan, OCN = Osteocalcin; (n = 6).

As seen in all the histomorphometrical analyses of the heat map, the rBMP-2 and rBMP-2 + rTGF-β3 stimulated groups presented the most robust positive response results compared to the other participating groups. However, the rBMP-2 single group performed better in the early phase (7 and 14 days), while the rBMP-2 + rTGF-β3 combined group was more dominant in the late phase (30 days). In addition, rTGF-β3 stimulation alone also displayed positive results, although slightly weaker than the rBMP-2 + rTGF-β3 combination. Furthermore, the

rTGF-β3 + rBMP-2 + rNoggin stimulated group resulted in relatively higher positive reactions in all staining at late stages (at 14 and 30 days), except for the 30-day Alcian Blue staining **(Figure 20)**.

5. Discussion

All kinds of tissue morphogenesis need a precise temporal and spatial regulation by numerous growth factors, cytokines and modulators, which drive multiple complex cellular activities, including antagonism and/or synergy, positive and/or negative feedback[132,204]. The TGF-β/BMP signaling is a vital thread that cannot be bypassed in the osteogenic induction system[205-207]. A large number of gene products are involved in this inherent signaling pathway, resulting in the extensive interaction between diverse signaling pathways[208]. Therefore, analyzing the changes in related gene expression provides us with an excellent way to unlock the potential interaction mechanisms of involved molecules. As such, some skeletal differentiation related key genes were analyzed in the present study, along with IHC and histological staining outcomes, to evaluate the promoted induction effect of the 3 applied growth factors (rTGF-β3, rBMP-2, and rNoggin) on a muscle tissue-based *in vitro* model, and try to explain the possible mechanisms. As far as we know, this study remains uniquely novel, attempting to explore the osteogenic-inducing effects of multiple morphogens and their antagonist in an *in vitro* muscle tissue system.

5.1 *Ex vivo* osteogenesis using muscle tissue

Skeletal muscle and bone tissue have the same origin during the embryonic differentiation, as both are derived from mesodermal mesenchymal cell precursors, while the differentiated fate is determined by extracellular secreted signals[209-211]. As muscle-resident stem cells, satellite cells play a key role in postnatal muscle growth and tissue regeneration during injury repair[210,212,213]. Developmental biology has long established that the committed satellite stem cell population is actually heterogeneous, for their different stemness, gene expression characteristics, propensity for myogenic differentiation, and non-myogenic differentiation potential[214]. Remarkably, it has been generally accepted that satellite cells could be divided into two distinct subpopulations according to their regenerative potential [215]. One is myogenic progenitor cells, which possess an intrinsic potential to assume myogenic lineage fate[212,213,216]. The other one is mesenchymal progenitor cells, which act as multipotent stem cells, and retain the capability to differentiate into various non-myogenic lineages[214,217], such as osteocytes and adipocytes[209,218,219].

Due to this functional similarity to bone marrow-derived mesenchymal stem cells (BMSCs), many investigations proved that muscle-derived satellite cells could differentiate towards an osteochondrogenic direction in diverse animal models[220-222]. For example, Tajbakhsh et al.[223] and Asakura et al.[217] demonstrated that mouse-muscle satellite cells had the potential to undergo osteogenic differentiation *in vivo* and *in vitro*, respectively. In another study, Paolo et al.[224] found that human satellite cells could also differentiate into osteocytes through molecular and morphological analyses. Similarly, Lee et al.[225] established that human muscle-derived stem cells could enhance skull defect healing in mice with BMP-2 morphogen overexpress. On the other hand, other experiments even discovered that usually intended myogenetic muscle satellite cells could also be transformed to express cartilage or bone related transcripts or translational molecules when cultured in a differentiation medium containing TGF-βs or BMPs[217,226]. In addition, Ripamonti et al. suggested that many mesenchymal cells within baboon rectus abdominis muscle tissue, including myoblastic, myoendothelial, and even perivascular stem cells, could be converted into osteoblast-like cells with growth factor induction[132,152,227].

Accordingly, the muscle tissue-based *in vitro* differentiation model system was utilized in this study to assess its prior chondrogenesis and subsequent endochondral ossification potential in response to 3 different morphogens (rTGF-β3, rBMP-2, and rNoggin) and their diverse combinations. Since the vitality of the samples could not be observed directly under the microscope as in normal cell culture, we selected two angiogenesis-related genes, *Vegfa* and *Col4a1*, which can also be used for tissue vitality demonstration[90,113]. Expression of these two genes was upregulated in all intervention groups throughout the *in vitro* differentiation process, combined with positive histological staining and IHC result, the tissue model showed us its excellent *in vitro* activity and reliability of the results similar to the *in vivo* culture. Though not yet perfected these indications for an *ex vivo* tissue responding in such a manner provides new possibilities towards solving how tissue morphogenesis, especially that of osteogenesis or chondrogenesis function.

5.2 Chondrogenesis vs. endochondral ossification

During endochondral bone development, articular chondrogenesis and endochondral osteogenesis are closely coupled and fine-coordinated by diverse crucial growth factors[228-230]. The results of this study showed that both chondrogenic and osteogenic-related genes underwent significant upregulated changes on 30 days, in most rTGF-β3 and/or rBMP-2 involved groups, and even in almost all the rTGF-β3 + rBMP-2 + rNoggin triple combined groups, combined with morphogenesis results, suggesting that our muscle tissue may be undergoing a chondrogenesis/ chondro-osteogenesis transdifferentiation/ endochondral ossification process.

5.2.1 Chondrogenesis

Articular cartilage is a highly specialized connective tissue, which is comprised of a dense ECM and chondrocytes but has no blood vessels, no nerves, nor a lymphatic system. Such a unique structure results in its limited self-recovery properties[231-233]. Due to its important function in the lubrication of diarthrodial joints and physical stress transmission with a low coefficient of friction, the formation and maintenance of articular cartilage phenotypes in cartilage tissue engineering is of paramount importance[234,235]. The positive IHC-ACAN and the strong Alcian Blue staining results revealed that proteoglycans and polysaccharides such as glycosaminoglycans (GAGs) contained special ECM was induced by these growth factors[236-238], at the same time, the significant upregulation of *Sox9, Acan,* and *Col2α1* genes further confirmed the occurrence of cartilage formation throughout the differentiation culture process[239,240]. In addition, the upregulated *Abi3bp* and *Six1* gene expression indicated a form of articular chondrogenesis was being induced[75], which complied with the principle that the process of endochondral bone formation is always accompanied by the appearance of hyaline cartilage[241,242].

5.2.2 Endochondral ossification

On the other hand, the positive results of IHC-OCN and Alizarin Red S staining showed the presence of abundant OCN protein and calcium, indicating a bone-related ECM was being formed[237,243,244]. Likewise, the transduction also caused significant increases in *Runx2, Alp, Ocn, Bmp-2,* and *Col1α1* genes expression. As such, a trend of osteogenic morphogenesis was also confirmed at both protein and gene levels in the same system[245,246].

In a previous study, Tomas et al.[247] described that cell-mediated *TGF-β3* and *BMP-2* gene delivery resulted in both chondrogenesis and osteogenesis, either acting alone or in combination. This result was consistent with our present study, as we all demonstrated that BMP-2 and TGF-β3 had the capability to induce both chondrogenic and osteogenic differentiation. However, since the transduced muscle tissue obtained both bone and cartilage phenotypes, could it be used for endochondral BTE, or even used for articular cartilage tissue engineering? Actually, many investigations have discussed this challenging issue. For instance, Betz et al.[83] repaired chondral and osteochondral defects in rabbits with BMP-2 transdifferentiated muscle tissue grafts and achieved respective phenotypic differentiation of cartilage and bone. At about the same time, Aijuan et al.[248] also verified the regeneration of both articular cartilage and subchondral bone within an autologous BMSCs and bio-scaffold mediated swine model. Indeed, the key point for the final *in vivo* tissue lineage fate is principally determined by specific implantation microenvironment[249-251]. Under a cartilage-specific hypoxia microenvironment, stimulated by abundant endogenous molecules and proper *in vivo* mechanical pressure, the induced tissue was favorably driving towards a chondrogenic differentiation direction, forming and keeping an articular cartilage-like state[252-254]. Similarly, in a bone defect normoxia microenvironment, endogenous osteogenic growth factors, and mechanical stimulation were all prevailing conditions for inducing bone formation through an endochondral ossification pathway[79,255,256]. Therefore, the transduced muscle tissue in the present experiment may be a promising candidate for both bone and cartilage tissue engineering, a fate that will ultimately depend on discerning the correct endogenously applied signals that drive the tissue morphogenesis to the desired phenotypic tissue type. If this can be achieved, the possibilities for future clinical application would be limitless.

5.3 Molecular functions and mechanisms of interactions

5.3.1 The role of BMP-2 and TGF-β3 during endochondral bone formation

The present research experiment verified that both BMP-2 and TGF-β3 could initiate the endochondral chondrogenesis and subsequent concomitant osteogenesis. Many cartilage and bone-specific markers involved in this cooperative osteo-chondroprogenitors differentiation activity were examined at the mRNA level, among these, *Sox9* and *Runx2* are two master transcription factors for chondrogenesis and osteogenesis, respectively[257,258]. Their overlapped and significantly increased expression in this study was regulated by both intrinsic secreted molecules and these exogenous recombinant growth factors temporally, which was a realization of the involved signaling network mechanisms[259].

On day 7, *Sox9* mRNA was positively expressed in the rBMP-2 single group, while no significant result was detected of *Runx2* gene expression. This result was consistent with many previous studies that *Sox9* and *Runx2* play a reciprocal inhibition during osteo-chondrogenesis to influence mesenchymal cell fate[259,260]. During the early chondrogenic differentiation stage, BMP-2 induced *Runx2* expression was suppressed by *Sox9* to inhibit the subsequent endochondral ossification and maintain hyaline cartilage phenotype[229,261]. However, *Sox9* also contributed to BMP-2 induced osteogenic differentiation since *Sox9* silencing even caused reduced osteogenesis of BMSCs[262,263]. In addition, TGF-β3 induced *Bmp-2* and *Runx2* gene expression on days 14 and 30 singly, which confirmed the BMP signaling involvement and the regulatory role of TGF-β3 in osteogenesis. That means TGF-β3 provoked bone formation through upregulating of endogenous *Bmp-2* levels and followed by increased *Runx2* expression, a result supported by several other studies[96,193].

5.3.2 The interaction between BMP-2 and TGF-β3

Interestingly, in the BMP-2 and TGF-β3 concomitant applied groups, both positive and negative effects, namely synergistic and antagonistic activities, were found but occurred at different differentiation stages.

From day 0 to day 7 and 14, compared to the rBMP-2 singly applied group, the addition of rTGF-β3 blocked rBMP-2 induced gene upregulation and protein increase, indicating an antagonistic effect was involved in the early stage of differentiation. One possible explanation for the mechanism might be competitive inhibition, because TGF-βs and BMPs have overlapping signaling pathways during the canonical signal pathway. They all need to trans-phosphorylate Smad4 to complete the transmission. However, only the total quantity of Smad4 is stable, therefore TGF-βs and BMPs need to bind the downstream effector molecule competitively[100]. Another relevant mechanism could be that TGF-βs blocked BMP signaling transduction by forming a mix-linked Smad1/5-Smad3 inhibitory complexes[107,264,265]. Furthermore, it could also be possible that TGF-β3 induced inhibitory Smad6 or Smad7 that then blocked the BMP signaling pathway[100].

Many other scientists have described/observed a similar negative regulatory effect between the TGF-β signaling superfamily in different models[266,267]. For instance, Sabrina et al.[268,269] showed that Smad1/5/8-mediated BMP-2 and -7 signaling could be blocked completely by adding recombinant human TGF-β in primary human osteoblasts. Similarly, Mehlhorn et al.[195] presented that BMP-2 induced chondrogenesis and osteogenesis in adipocyte-derived stem cells and could be inhibited by simultaneous applying any of the three TGF-β isoforms. Moreover, Lee et al.[270] displayed BMP-2 induced osteogenic transdifferentiation was opposed by TGF-β1 treatment via suppressing Distal-Less Homeobox 5 (Dlx5) in a C2C12 cells model.

In marked contrast, however, the synergistic activities between BMP and TGF-β signaling were also found in the same system but during the late stages of culture. From 7-14 days to 30 days, most detected genes and proteins were significantly upregulated in rTGF-β3 + rBMP-2 combined group and higher than the single group. In particular, in the heat map of gene expression on day 14, the rTGF-β3 + rBMP-2 combined group showed the highest gene expression level among all the participating groups **(Figure 15-B)**. The possible underlying mechanisms of their synergistic effect could be that TGF-βs can utilize BMPs pathways to stimulate cell activities, it means that apart from binding ALK5 to stimulate the canonical Smad2/3 signaling pathway, TGF-βs can also exert function via activating BMP signaling pathway, which binds ALK1 and ALK2 directly and then triggers Smad1/5/8 for signal transmission[100,271]. Another possible explanation might be

TGF- β could increase the activity of bone BMPR type I-B and thus lead to enhanced BMP-2 induced ossification[272]. Besides, the up-mentioned TGF-β3 elicited endogenous *Bmp-2* gene upregulation was also evidence of synergistic activities between BMPs and TGF-βs signaling[96].

This synergistic effect between TGF-βs and BMPs has also been observed by many other investigators, both in osteogenesis[273] and chondrogenesis[274,275]. Daniel et al.[194] and other scientists[192,193] demonstrated that more markedly *in vitro* osteogenic differentiation could be promoted by TGF-β3 and BMP-2 combination. Further studies have also shown that BMP-2 induced ectopic bone formation could be significantly enhanced by the presence of TGF-β1[276,277]. Besides, Shen et al. also testified that BMP-2 could potentiate the TGF-β3 mediated chondrogenic effects and keep with better chondrocyte phenotype in a human BMSCs *in vitro* model, and the evidence was supported by the upregulated gene markers of type-II collagen and ACAN[278]. In addition, by showing the significantly increased chondrogenic *Sox9* and *Col2a1* gene expression and augmented proteoglycans & collagens quantity, the data from Kim et al. demonstrated a triple morphogens combination of TGF-β3, BMP-2, and -7 resulted in the most effective chondrogenesis[191].

Apparently, the BMP-2 and TGF-β3 interaction in this study indicated a phase separation of short-term and long-term combination effects during the endochondral osteogenesis process within the same culture system. Interestingly, it's not the only case, in the induced ectopic osteogenesis *in vivo* baboon model, Klar et al. described that TGF- β3 downregulated *Bmp-2* gene expression in the early stages but restored it later[96]. But why did the early antagonism but late synergism phenomenon happen? It has been well established by now that tissue develop over time occurs over various molecules that become, necessary or later obsolete and only through the presence of new signals or specific combinations can a further developmental process occur. Actually, on day 7, the highest gene expressions of *Col2a1, Sox9,* and *Alp* were found in the rBMP-2 singly applied group, which was consistent with the heat map of gene expression analysis result **(Figure 15-A)**. However, these highly expressed signals dropped quickly and did not last long. These data suggest that BMP-2 activated the osteo-chondrogenic differentiation rapidly and potently, but only for a short duration[75,279]. Thus, in the early stage of the endochondral bone formation, BMP-2 may work as a promoter, which creates a proper cellular differentiation milieu conducive to the activity of

TGF-β3. After that, i.e., in the late stage of differentiation, BMP-2 may function only as an enhancer, act synergistically with TGF-β3[100,280]. Consequently, BMPs and TGF-βs may serve sequentially and programmatically during induced endochondral bone formation process, the antagonistic or synergistic interaction was adapted to the development stage and corresponding cellular environment[281,282].

5.3.3 The interaction between BMP-2 and Noggin

Ectopic application of Noggin in our experiment has confirmed the role of Noggin as an effective BMP-2 antagonist negatively manipulated BMP-2 induced bone differentiation, since nearly all rBMP-2 + rNoggin combined application groups presented non-significant expression, both at the RT-qPCR reflected gene level and the staining results indicated protein level, at all three time points. As a key natural BMPs antagonist polypeptide, Noggin can specifically bind BMP-2, -4, -5, -6, and -7 with several degrees of affinity, and GDF-5/-6 as well, but no more other TGF family peptides members[93,178,283,284]. Unlike Smurf and inhibitory Smads function at the intracellular level, Noggin performs extracellular antagonist regulation[187,198]. In the context of this experiment, Noggin bound to BMP-2 epitopes with eager affinity and competitively blocked the contact with two types of BMPRs**,** therefore inhibiting BMP-2-induced nuclear translocation in turn effectively inactivated Smad1/5/8 signaling actions[199,285]. Similar research studies conducted by other investigators have also demonstrated that, as an effective antagonist of BMPs, Noggin suppressed BMP-2 mediated osteogenic differentiation reliably[186,286,287].

5.3.4 The interaction between TGF-β3/Noggin and BMP-2/TGF-β3/ Noggin

It is worthy of mentioning that, from day 7 to day 14, almost all detected genes expression increased significantly in the rTGF-β3 single application group, but rNoggin prevented this upward trend, with 14-day gene expression heat map data can also provide evidence **(Figure 15-B)**. Indeed, the inhibitory effect of Noggin on TGF-β3 has been discovered and reported by many scholars. E.g., Klar et al.[96] described that bone formation induced by TGF-β3 alone was significantly decreased using the same dosage of Noggin and TGF-β3 in the baboon *in vivo* model. Moreover, Naoki et al.[288] proved that the Noggin could be a stumbling block to TGF-β3 induced cartilage genesis and suggested a BMP-associated pathway was involved. Besides, Andrey et al.[181] put forward a novel inhibitory

function of Noggin, they demonstrated that in addition to BMPs, a number of non-BMP ligands, like Activin B, Xnr2, and Xnr4, can also be antagonized by Noggin in a less efficient way. Interestingly, these blocked non-BMP ligands regulate specific genes transcription through cytoplasmic Smad2/3. This point may indicate another link between TGF-β3 and Noggin regarding non-BMP ligands and downstream effectors Smad2/3. Therefore, the application of Noggin inhibited both the differentiation function of BMP-2 and TGF-β3 signaling in this study.

However, the inhibition of rNoggin to rTGF-β3 did not happen at the other two time points. On day 7 and day 30, in rTGF-β3 + rNoggin binary applied groups, most detected parameters increased significantly, both at protein and gene levels. This may suggest a positive function of rNoggin in osteo-chondrogenesis at the initial and late stages, or at least an inactivation of the inhibitory effect. Interestingly, a similarly positive result could also be analyzed from the data of rTGF-β3 + rBMP-2 + rNoggin triple application groups in the final stage, which was also supported by heat map analyses **(Figure 15-A/C, Figure 20-B/C/D)**. Although it is overturning the traditional concept that Noggin, as an antagonist of BMPs, a kind of growth factor with osteogenic function, is capable of promoting osteogenesis, this osteogenesis ability of Noggin, actually, has been reported in many studies. For instance, Chen et al.[289] proposed that Noggin is provocatory to human MSCs osteogenesis, for Noggin suppression significantly inhibited BMP-2-induced ALP activity and other osteoblastic genes expression. Besides, Rifas et al.[290] made a similar observation in a former study, it was shown that Noggin could induce ALP action and upregulate *Bmp-2* and *Ocn* gene expression. Unusually, besides these ordinary osteogenic markers, they also found increased ActRII expression[290]. Furthermore, in a recent study, Saeed M. Hashimi presented a novel signaling mechanism for Noggin-induced osteogenesis that needs further confirmation. Through fluorescent labeling techniques, the author found that exogenous Noggin treatment could induce osteogenesis by binding and stimulating the BMP-2 receptor[291].

As such, in combination with previous findings, our discoveries would suggest that Noggin may perform as a stimulatory or at least no inhibition when used with TGF-β3 in the initial and late stages of osteo-chondrogenesis and conjunction with TGF-β3 + BMP-2 in the late stage. Nevertheless, Noggin alone could not show a facilitative effect, and its inhibitory effect was still reliable when used together with TGF-β3 in the intermediate stage of differentiation.

5.4 Negative Feedback Mechanism

When we focused on the *Bmp-2* gene expression graphs, a universal negative feedback principle associated with BMP signaling within biological development was discovered: (1) The negative feedback between *Bmp-2* gene expression and rBMP-2 protein, as in *Bmp-2* gene expression in rBMP-2 alone group, no significant difference was found, at all three time points. This may mean that the treatment of rBMP-2 protein suppressed the expression of *Bmp-2* gene. (2) The negative feedback between *Bmp-2* gene expression and Noggin protein, as in *Bmp-2* gene expression in rNoggin alone group, a significant difference was found on day 14 and day 30. This may mean that the treatment of Noggin protein promoted the expression of *Bmp-2* gene. (3) The negative feedback between *Bmp-2* gene expression and rNoggin + rTGF-β3 proteins combination, as the significant difference was only found in *Bmp-2* gene expression in rNoggin + rTGF-β3 combination group, but not rNoggin or rTGF-β3 alone group on day 7. This may happen because of the dual antagonistic effect of Noggin and TGF-β3 proteins in the early differentiation stage, which resulted in *Bmp-2* gene expression upregulation, which may also explain why the rNoggin + rTGF-β3 combination could increase the expression of many genes on 7 days, which may be related to the upregulation of BMP signaling.

BMP signaling is organized by both initiators and antagonists with a negative feedback mechanism at different levels[292,293]. The negative feedback mechanism is the basis of organism self-regulation, which regulates the cellular response to the input signal, according to the fluctuant signal threshold existing in the system, by enhancing, limiting, or terminating it, thus maintaining the relatively stable signal output and the homeostasis[294,295]. Among them, one of the most common types of negative feedback mechanism is the inhibition between a protein and its own gene[296,297], in which the synthesized protein impedes the translation and preceding transcription processes, mediated by its own mRNA and DNA, respectively[298], thus ultimately leading to downregulation of its gene expression[299,300]. Based on this theory, as such, the increased BMP-2 protein concentration caused by exogenous treatment may negatively inhibit the *Bmp-2* gene expression in this experiment[301,302].

On the other hand, the negative feedback loop between Noggin and BMP activity has been discussed by various studies[283,303,304]. For example, Leonard Rifas[290] described that *Bmp-2* gene expression could be induced by exogenous recombinant human Noggin treatment in a human mesenchymal stem cell *in vitro* model. This result was exactly consistent with our data between Noggin protein and *Bmp-2* gene, namely the application of Noggin led to a loss of function of system auto-secreted BMP-2 protein and thus upregulation of *Bmp-2* gene on day 14 and day 30. However, on day 7, the upregulated *Bmp-2* gene expression was not detected in the rNoggin single group but was found in rTGF-β3 + rNoggin group, this may indicate that TGF-β3, as an early antagonist of BMP-2 in this experiment, also participated in this negative feedback regulation loop to support the Noggin-induced *Bmp-2* gene upregulation.

5.5 Complex signaling pathway crosstalk

In addition, there might be a wide range of signaling pathway crosstalk filled with the whole differentiation process. Beyond the signaling interaction between the TGF-β superfamily, TGF-βs can contact modules of pituitary hormone (PTH), fibroblast growth factors (FGF), and Wnt signaling pathways. At the same time, BMPs can create signaling links with Notch, FGF, and Wnt pathways[123]. On the other hand, apart from blocking BMP signaling, Noggin has also been demonstrated to inhibit Activin/Nodal and Wnt signaling[181]. Consequently, to unlock the complex detailed function mechanism, further research is needed for sure.

5.6 Limitations

The effect of the dose gradient of the applied growth factors on the experimental results was not taken into account, which is an obvious limitation of this study. Some studies have reported that the TGF-β superfamily factors served as a double-edged sword in DNA synthesis[305,306]. For example, a low concentration of TGF-β can promote osteogenic differentiation, whereas inhibiting at a high concentration[148,307]. Besides, low doses of active TGF-β have also been shown in chondrocytes to signal preferably through the Smad2/3 pathway, while the Smad1/5 pathway turns into predominant at high doses[119,308]**.** In addition, BMP-2 controls bone formation in a concentration-dependent manner has also been

demonstrated in BTE surveys[309-311]. Thus, an appropriate molecular concentration may play a key role in a differentiation system. Furthermore, in a previous chondrogenic differentiation system, Takashi et al. established that the morphogens treatment order could also lead to different induction effects, as BMP-7 following TGF-β1 resulted in more effective chondrogenesis than TGF-β1 following BMP-7[312]. Accordingly, investigations related to molecular administration sequence and dose should be conducted in the next phase.

On the other hand, although the presence of numerous types of cells gives the muscle tissue the possibility of multiple differentiation, it also increases the uncertainty of its differentiation direction. It is difficult to match various differentiated phenotypes with corresponding cell types in such a complex 3D cellular assembly. As such, a comparison between the muscle tissue explant and cells of a specific type, like myoblasts or satellite cells, may be necessary to be conducted, especially in a 3D pellet culture condition, to confirm the superiority of this muscle tissue induction model. Moreover, compared to the 0-day sample (baseline), the increasing trend of gene expression in the control group might suggest that these induced phenotypes were not absolutely derived from the exogenous molecules. One of the explanations may be that the FBS contained in the normal medium provided some energy for differentiation. The other reason may be attributed to the injury from tissue excision, since the trauma-induced various BMPs expression and followed heterotopic ossification have been verified by many investigators[313,314]. Moreover, to achieve a more realistic *in vitro* physiological simulation system, mechanical and even electrochemical stimulation, as directed by nerves, should also be considered as a complement to biochemical cues in this muscle tissue-based model, because they can also play an important and unique role as temporal biophysical signals to participate in cellular activities[315-317]. Finally, in order to verify whether this specialized muscle tissue differentiation model can be used for future BTE, *in vivo* experiments will be the next step in our plan.

6. Conclusion

The process of tissue morphogenesis is full of interactions and combinations of various cellular signals, and unraveling the relationships among them would be further beneficial to the development of tissue engineering. This experiment developed a new *in vitro* muscle differentiation model and loaded it with three classical growth factors, rBMP-2, rTGF-β3, and rNoggin, singly or with diverse combinations. The final data of this study confirmed the reliability of this muscle tissue model in endochondral bone differentiation, from chondrogenesis to osteogenesis. Both rBMP-2 and rTGF-β3 showed their osteoblastic differentiation potential, respectively, as well as an early antagonism but late synergism interaction. Interestingly, besides antagonizing rBMP-2 effectively in the whole process, rNoggin also inhibited rTGF-β3 activities in the intermediate stage of differentiation. However, rNoggin appeared to surprisingly play a positive role when it combined with rTGF-β3 in the initial and late phases, or when it combined with rTGF-β3/rBMP-2 in the anaphase of differentiation. Nevertheless, the ever-changing complex mechanism of intermolecular interactions may depend on the cellular microenvironment of the moment. Furthermore, the classical bioregulatory negative feedback mechanism was discovered inside this system, both between protein/gene and protein/antagonist. In summary, the multiple growth factors application tissue model provided some critical clues to unlocking the molecular interaction during endochondral bone formation. Although optimization is still needed for this innovative model, it may offer a new strategy for future BTE.

References

1 Cattalini, J. P., Boccaccini, A. R., Lucangioli, S. & Mourino, V. Bisphosphonate-based strategies for bone tissue engineering and orthopedic implants. *Tissue Eng Part B Rev* **18**, 323-340, doi:10.1089/ten.TEB.2011.0737 (2012).

2 Liu, Y., Wu, G. & de Groot, K. Biomimetic coatings for bone tissue engineering of critical-sized defects. *J R Soc Interface* **7 Suppl 5**, S631-647, doi:10.1098/rsif.2010.0115.focus (2010).

3 Boskey, A. L. Mineralization of Bones and Teeth. *Elements* **3**, 385-391, doi:10.2113/gselements.3.6.385 (2007).

4 Novitskaya, E. *et al.* Recent advances on the measurement and calculation of the elastic moduli of cortical and trabecular bone: A review. *Theoretical and Applied Mechanics* **38**, 209-297, doi:10.2298/tam1103209n (2011).

5 Boskey, A. L. Bone composition: relationship to bone fragility and antiosteoporotic drug effects. *Bonekey Rep* **2**, 447, doi:10.1038/bonekey.2013.181 (2013).

6 Olszta, M. J. *et al.* Bone structure and formation: A new perspective. *Materials Science and Engineering: R: Reports* **58**, 77-116, doi:10.1016/j.mser.2007.05.001 (2007).

7 Katsimbri, P. The biology of normal bone remodelling. *Eur J Cancer Care (Engl)* **26**, doi:10.1111/ecc.12740 (2017).

8 Rickard, D. J. *et al.* Isolation and characterization of osteoblast precursor cells from human bone marrow. *J Bone Miner Res* **11**, 312-324, doi:10.1002/jbmr.5650110305 (1996).

9 Friedenstein, A. J. Precursor cells of mechanocytes. *Int Rev Cytol* **47**, 327-359, doi:10.1016/s0074-7696(08)60092-3 (1976).

10 Caetano-Lopes, J., Canhao, H. & Fonseca, J. E. Osteoblasts and bone formation. *Acta Reumatol Port* **32**, 103-110 (2007).

11 Buenzli, P. R. & Sims, N. A. Quantifying the osteocyte network in the human skeleton. *Bone* **75**, 144-150, doi:10.1016/j.bone.2015.02.016 (2015).

12 Schaffler, M. B., Cheung, W. Y., Majeska, R. & Kennedy, O. Osteocytes: master orchestrators of bone. *Calcif Tissue Int* **94**, 5-24, doi:10.1007/s00223-013-9790-y (2014).

13 Bonewald, L. F. Osteocytes as dynamic multifunctional cells. *Ann N Y Acad Sci* **1116**, 281-290, doi:10.1196/annals.1402.018 (2007).

14 Florencio-Silva, R., Sasso, G. R., Sasso-Cerri, E., Simoes, M. J. & Cerri, P. S. Biology of Bone Tissue: Structure, Function, and Factors That Influence Bone Cells. *Biomed Res Int* **2015**, 421746, doi:10.1155/2015/421746 (2015).

15 Everts, V. *et al.* The bone lining cell: its role in cleaning Howship's lacunae and initiating bone formation. *J Bone Miner Res* **17**, 77-90, doi:10.1359/jbmr.2002.17.1.77 (2002).

16 Karsenty, G. & Ferron, M. The contribution of bone to whole-organism physiology. *Nature* **481**, 314-320, doi:10.1038/nature10763 (2012).

17 Boyle, W. J., Simonet, W. S. & Lacey, D. L. Osteoclast differentiation and activation. *Nature* **423**, 337-342, doi:10.1038/nature01658 (2003).

18 Kini, U. & Nandeesh, B. in *Radionuclide and hybrid bone imaging* 29-57 (Springer, 2012).

19 Ralston, S. H. Bone structure and metabolism. *Medicine* **41**, 581-585, doi:10.1016/j.mpmed.2013.07.007 (2013).

20 Choi, S. M., Chaudhry, P., Zo, S. M. & Han, S. S. Advances in Protein-Based Materials: From Origin to Novel Biomaterials. *Adv Exp Med Biol* **1078**, 161-210, doi:10.1007/978-981-13-0950-2_10 (2018).

21 Balasubramanian, P., Prabhakaran, M. P., Sireesha, M. & Ramakrishna, S. in *Polymer Composites–Polyolefin Fractionation–Polymeric Peptidomimetics–Collagens* 173-206 (Springer, 2012).

22 Lian, J. B. & Gundberg, C. M. Osteocalcin. Biochemical considerations and clinical applications. *Clin Orthop Relat Res*, 267-291 (1988).

23 Mosher, D. *Fibronectin*. (Elsevier, 2012).

24 Puleo, D. A. & Bizios, R. Mechanisms of fibronectin-mediated attachment of osteoblasts to substrates in vitro. *Bone Miner* **18**, 215-226, doi:10.1016/0169-6009(92)90808-q (1992).

25 Sui, G. *et al.* Poly-L-lactic acid/hydroxyapatite hybrid membrane for bone tissue regeneration. *J Biomed Mater Res A* **82**, 445-454, doi:10.1002/jbm.a.31166 (2007).

26 Swetha, M. *et al.* Biocomposites containing natural polymers and hydroxyapatite for bone tissue engineering. *Int J Biol Macromol* **47**, 1-4, doi:10.1016/j.ijbiomac.2010.03.015 (2010).

27 Zhou, H. & Lee, J. Nanoscale hydroxyapatite particles for bone tissue engineering. *Acta Biomater* **7**, 2769-2781, doi:10.1016/j.actbio.2011.03.019 (2011).

28 Giffin, J. L., Gaitor, D. & Franz-Odendaal, T. A. The Forgotten Skeletogenic Condensations: A Comparison of Early Skeletal Development Amongst Vertebrates. *J Dev Biol* **7**, 4, doi:10.3390/jdb7010004 (2019).

29 Olsen, B. R., Reginato, A. M. & Wang, W. Bone development. *Annu Rev Cell Dev Biol* **16**, 191-220, doi:10.1146/annurev.cellbio.16.1.191 (2000).

30 Berendsen, A. D. & Olsen, B. R. Bone development. *Bone* **80**, 14-18, doi:10.1016/j.bone.2015.04.035 (2015).

31 Wolff, L. I. & Hartmann, C. A Second Career for Chondrocytes-Transformation into Osteoblasts. *Curr Osteoporos Rep* **17**, 129-137, doi:10.1007/s11914-019-00511-3 (2019).

32 Dishowitz, M. I., Terkhorn, S. P., Bostic, S. A. & Hankenson, K. D. Notch signaling components are upregulated during both endochondral and intramembranous bone regeneration. *J Orthop Res* **30**, 296-303, doi:10.1002/jor.21518 (2012).

33 Wong, S. A. *et al.* Microenvironmental Regulation of Chondrocyte Plasticity in Endochondral Repair-A New Frontier for Developmental Engineering. *Front Bioeng Biotechnol* **6**, 58, doi:10.3389/fbioe.2018.00058 (2018).

34 Stevens, M. M. Biomaterials for bone tissue engineering. *Materials Today* **11**, 18-25, doi:10.1016/s1369-7021(08)70086-5 (2008).

35 Regard, J. B., Zhong, Z., Williams, B. O. & Yang, Y. Wnt signaling in bone development and disease: making stronger bone with Wnts. *Cold Spring Harb Perspect Biol* **4**, doi:10.1101/cshperspect.a007997 (2012).

36 Balmayor, E. R. & van Griensven, M. in *Mesenchymal Stem Cell Therapy* Ch. Chapter 6, 101-116 (2013).

37 Xian, C. J., Zhou, F. H., McCarty, R. C. & Foster, B. K. Intramembranous ossification mechanism for bone bridge formation at the growth plate cartilage injury site. *J Orthop Res* **22**, 417-426, doi:10.1016/j.orthres.2003.08.003 (2004).

38 Franz-Odendaal, T. A. Induction and patterning of intramembranous bone. *Front Biosci (Landmark Ed)* **16**, 2734-2746, doi:10.2741/3882 (2011).

39 Blumer, M. J. F. Bone tissue and histological and molecular events during development of the long bones. *Ann Anat* **235**, 151704, doi:10.1016/j.aanat.2021.151704 (2021).

40 Jing, Y. *et al.* Chondrogenesis and osteogenesis are one continuous developmental and lineage defined biological process. *Sci Rep* **7**, 10020, doi:10.1038/s41598-017-10048-z (2017).

41 Breeland, G., Sinkler, M. A. & Menezes, R. G. J. S. *Embryology, bone ossification*. (2020).

42 Mackie, E. J., Ahmed, Y. A., Tatarczuch, L., Chen, K. S. & Mirams, M. Endochondral ossification: how cartilage is converted into bone in the developing skeleton. *Int J Biochem Cell Biol* **40**, 46-62, doi:10.1016/j.biocel.2007.06.009 (2008).

43 Aghajanian, P. & Mohan, S. The art of building bone: emerging role of chondrocyte-to-osteoblast transdifferentiation in endochondral ossification. *Bone Res* **6**, 19, doi:10.1038/s41413-018-0021-z (2018).

44 Cieslar-Pobuda, A. *et al.* Transdifferentiation and reprogramming: Overview of the processes, their similarities and differences. *Biochimica et biophysica acta. Molecular cell research* **1864**, 1359-1369, doi:10.1016/j.bbamcr.2017.04.017 (2017).

45 Lin, D. P. L., Carnagarin, R., Dharmarajan, A. & Dass, C. R. Transdifferentiation of myoblasts into osteoblasts - possible use for bone therapy. *The Journal of pharmacy and pharmacology* **69**, 1661-1671, doi:10.1111/jphp.12790 (2017).

46 Aghajanian, P., Xing, W., Cheng, S. & Mohan, S. Epiphyseal bone formation occurs via thyroid hormone regulation of chondrocyte to osteoblast transdifferentiation. *Sci Rep* **7**, 10432, doi:10.1038/s41598-017-11050-1 (2017).

47 Yang, L., Tsang, K. Y., Tang, H. C., Chan, D. & Cheah, K. S. Hypertrophic chondrocytes can become osteoblasts and osteocytes in endochondral bone formation. *Proc Natl Acad Sci U S A* **111**, 12097-12102, doi:10.1073/pnas.1302703111 (2014).

48 Galotto, M. *et al.* Hypertrophic chondrocytes undergo further differentiation to osteoblast-like cells and participate in the initial bone formation in developing chick embryo. *J Bone Miner Res* **9**, 1239-1249, doi:10.1002/jbmr.5650090814 (1994).

49 Bianco, P., Cancedda, F. D., Riminucci, M. & Cancedda, R. Bone formation via cartilage models: The “borderline” chondrocyte. *Matrix Biology* **17**, 185-192, doi:10.1016/s0945-053x(98)90057-9 (1998).

50 Zhang, D. *et al.* Targeting local lymphatics to ameliorate heterotopic ossification via FGFR3-BMPR1a pathway. *Nat Commun* **12**, 4391, doi:10.1038/s41467-021-24643-2 (2021).

51 Espandar, R. & Haghpanah, B. Acceptable outcome following resection of bilateral large popliteal space heterotopic ossification masses in a spinal cord injured patient: a case report. *J Orthop Surg Res* **5**, 39, doi:10.1186/1749-799X-5-39 (2010).

52 Wang, X. *et al.* Inhibition of overactive TGF-beta attenuates progression of heterotopic ossification in mice. *Nat Commun* **9**, 551, doi:10.1038/s41467-018-02988-5 (2018).

53 Upadhyay, J. *et al.* The Expansion of Heterotopic Bone in Fibrodysplasia Ossificans Progressiva Is Activin A-Dependent. *J Bone Miner Res* **32**, 2489-2499, doi:10.1002/jbmr.3235 (2017).

54 Shi, F., Gao, J., Zou, J., Ying, Y. & Lin, H. Targeting heterotopic ossification by inhibiting activin receptorlike kinase 2 function (Review). *Mol Med Rep* **20**, 2979-2989, doi:10.3892/mmr.2019.10556 (2019).

55 Lounev, V. Y. *et al.* Identification of progenitor cells that contribute to heterotopic skeletogenesis. *The Journal of bone and joint surgery. American volume* **91**, 652-663, doi:10.2106/JBJS.H.01177 (2009).

56 Carroll, S. F., Buckley, C. T. & Kelly, D. J. Cyclic Tensile Strain Can Play a Role in Directing both Intramembranous and Endochondral Ossification of Mesenchymal Stem Cells. *Front Bioeng Biotechnol* **5**, 73, doi:10.3389/fbioe.2017.00073 (2017).

57 Glaser, D. L. *et al.* In vivo somatic cell gene transfer of an engineered Noggin mutein prevents BMP4-induced heterotopic ossification. *The Journal of bone and joint surgery. American volume* **85**, 2332-2342, doi:10.2106/00004623-200312000-00010 (2003).

58 Gurkan, U. A. *et al.* Immune and inflammatory pathways are involved in inherent bone marrow ossification. *Clin Orthop Relat Res* **470**, 2528-2540, doi:10.1007/s11999-012-2459-4 (2012).

59 Shore, E. M. & Kaplan, F. S. Inherited human diseases of heterotopic bone formation. *Nat Rev Rheumatol* **6**, 518-527, doi:10.1038/nrrheum.2010.122 (2010).

60 Bahney, C. S. *et al.* Stem cell-derived endochondral cartilage stimulates bone healing by tissue transformation. *J Bone Miner Res* **29**, 1269-1282, doi:10.1002/jbmr.2148 (2014).

61 Owston, H. E. *et al.* Induced Periosteum-Mimicking Membrane with Cell Barrier and Multipotential Stromal Cell (MSC) Homing Functionalities. *Int J Mol Sci* **21**, doi:10.3390/ijms21155233 (2020).

62 Pettersson, L. F., Kingham, P. J., Wiberg, M. & Kelk, P. In Vitro Osteogenic Differentiation of Human Mesenchymal Stem Cells from Jawbone Compared with Dental Tissue. *Tissue Eng Regen Med* **14**, 763-774, doi:10.1007/s13770-017-0071-0 (2017).

63 Chen, Y., Chen, S., Kawazoe, N. & Chen, G. Promoted Angiogenesis and Osteogenesis by Dexamethasone-loaded Calcium Phosphate Nanoparticles/Collagen Composite Scaffolds with Microgroove Networks. *Sci Rep* **8**, 14143, doi:10.1038/s41598-018-32495-y (2018).

64 He, X. *et al.* BMP2 genetically engineered MSCs and EPCs promote vascularized bone regeneration in rat critical-sized calvarial bone defects. *PLoS One* **8**, e60473, doi:10.1371/journal.pone.0060473 (2013).

65 Dennis, S. C., Berkland, C. J., Bonewald, L. F. & Detamore, M. S. Endochondral ossification for enhancing bone regeneration: converging native extracellular matrix biomaterials and developmental engineering in vivo. *Tissue Eng Part B Rev* **21**, 247-266, doi:10.1089/ten.TEB.2014.0419 (2015).

66 Amini, A. R., Laurencin, C. T. & Nukavarapu, S. P. Bone tissue engineering: recent advances and challenges. *Crit Rev Biomed Eng* **40**, 363-408, doi:10.1615/critrevbiomedeng.v40.i5.10 (2012).

67 St John, T. A. *et al.* Physical and monetary costs associated with autogenous bone graft harvesting. *American journal of orthopedics (Belle Mead, N.J.)* **32**, 18-23 (2003).

68 Mercado-Pagan, A. E., Stahl, A. M., Shanjani, Y. & Yang, Y. Vascularization in bone tissue engineering constructs. *Ann Biomed Eng* **43**, 718-729, doi:10.1007/s10439-015-1253-3 (2015).

69 Diomede, F. *et al.* Biofunctionalized Scaffold in Bone Tissue Repair. *Int J Mol Sci* **19**, doi:10.3390/ijms19041022 (2018).

70 Mani, M. P., Jaganathan, S. K. & Supriyanto, E. Enriched Mechanical Strength and Bone Mineralisation of Electrospun Biomimetic Scaffold Laden with Ylang Ylang Oil and Zinc Nitrate for Bone Tissue Engineering. *Polymers (Basel)* **11**, doi:10.3390/polym11081323 (2019).

71 Liu, T., Zhang, X., Luo, Y., Huang, Y. & Wu, G. Slowly Delivered Icariin/Allogeneic Bone Marrow-Derived Mesenchymal Stem Cells to Promote the Healing of Calvarial Critical-Size Bone Defects. *Stem Cells Int* **2016**, 1416047, doi:10.1155/2016/1416047 (2016).

72 Tian, B. *et al.* The immunogenic reaction and bone defect repair function of epsilon-poly-L-lysine (EPL)-coated nanoscale PCL/HA scaffold in rabbit calvarial bone defect. *J Mater Sci Mater Med* **32**, 63, doi:10.1007/s10856-021-06533-7 (2021).

73 Abbasi, N., Lee, R. S. B., Ivanovski, S., Love, R. M. & Hamlet, S. In vivo bone regeneration assessment of offset and gradient melt electrowritten (MEW) PCL scaffolds. *Biomater Res* **24**, 17, doi:10.1186/s40824-020-00196-1 (2020).

74 Cassaro, C. V. *et al.* Fibrin biopolymer as scaffold candidate to treat bone defects in rats. *J Venom Anim Toxins Incl Trop Dis* **25**, e20190027, doi:10.1590/1678-9199-JVATITD-2019-0027 (2019).

75 Xiong, F., Hausdorf, J., Niethammer, T. R., Jansson, V. A. & Klar, R. M. Temporal TGF-beta Supergene Family Signalling Cues Modulating Tissue Morphogenesis: Chondrogenesis within a Muscle Tissue Model? *Int J Mol Sci* **21**, doi:10.3390/ijms21144863 (2020).

76 Betz, V. M. *et al.* The effect of BMP-7 gene activated muscle tissue implants on the repair of large segmental bone defects. *Injury* **46**, 2351-2358, doi:10.1016/j.injury.2015.09.016 (2015).

77 Betz, V. M. *et al.* Bone morphogenetic protein-2 is a stronger inducer of osteogenesis within muscle tissue than heterodimeric bone morphogenetic protein-2/6 and -2/7: Implications for expedited gene-enhanced bone repair. *J Gene Med* **20**, e3042, doi:10.1002/jgm.3042 (2018).

78 Ren, B. *et al.* Gene-activated tissue grafts for sustained bone morphogenetic protein-2 delivery and bone engineering: Is muscle with fascia superior to muscle and fat? *J Tissue Eng Regen Med* **12**, 1002-1011, doi:10.1002/term.2575 (2018).

79 Betz, O. B. *et al.* Healing of large segmental bone defects induced by expedited bone morphogenetic protein-2 gene-activated, syngeneic muscle grafts. *Hum Gene Ther* **20**, 1589-1596, doi:10.1089/hum.2009.037 (2009).

80 Bosch, P. *et al.* Osteoprogenitor cells within skeletal muscle. *J Orthop Res* **18**, 933-944, doi:10.1002/jor.1100180613 (2000).

81 Ren, B. *et al.* Osteoinduction within BMP-2 transduced muscle tissue fragments with and without a fascia layer: implications for bone tissue engineering. *Gene Ther* **26**, 16-28, doi:10.1038/s41434-018-0047-2 (2019).

82 Virk, M. S. *et al.* "Same day" ex-vivo regional gene therapy: a novel strategy to enhance bone repair. *Molecular therapy : the journal of the American Society of Gene Therapy* **19**, 960-968, doi:10.1038/mt.2011.2 (2011).

83 Betz, V. M. *et al.* BMP-2 gene activated muscle tissue fragments for osteochondral defect regeneration in the rabbit knee. *J Gene Med* **19**, doi:10.1002/jgm.2972 (2017).

84 Betz, V. M., Betz, O. B., Harris, M. B., Vrahas, M. S. & Evans, C. H. Bone tissue engineering and repair by gene therapy. *Front Biosci* **13**, 833-841, doi:10.2741/2724 (2008).

85 Blair, H. C. *et al.* Osteoblast Differentiation and Bone Matrix Formation In Vivo and In Vitro. *Tissue Eng Part B Rev* **23**, 268-280, doi:10.1089/ten.TEB.2016.0454 (2017).

86 Albert, R. Scale-free networks in cell biology. *J Cell Sci* **118**, 4947-4957, doi:10.1242/jcs.02714 (2005).

87 Brand, M. D. Regulation analysis of energy metabolism. *J Exp Biol* **200**, 193-202, doi:10.1242/jeb.200.2.193 (1997).

88 Betz, O. B. *et al.* Repair of large segmental bone defects: BMP-2 gene activated muscle grafts vs. autologous bone grafting. *BMC Biotechnol* **13**, 65, doi:10.1186/1472-6750-13-65 (2013).

89 Perniconi, B. & Coletti, D. Skeletal muscle tissue engineering: best bet or black beast? *Front Physiol* **5**, 255, doi:10.3389/fphys.2014.00255 (2014).

90 He, T., Hausdorf, J., Chevalier, Y. & Klar, R. M. Trauma induced tissue survival in vitro with a muscle-biomaterial based osteogenic organoid system: a proof of concept study. *BMC Biotechnol* **20**, 8, doi:10.1186/s12896-020-0602-y (2020).

91 Wozney, J. M. *et al.* Novel regulators of bone formation: molecular clones and activities. *Science* **242**, 1528-1534, doi:10.1126/science.3201241 (1988).

92 Lin, L., Shen, Q., Xue, T. & Yu, C. Heterotopic ossification induced by Achilles tenotomy via endochondral bone formation: expression of bone and cartilage related genes. *Bone* **46**, 425-431, doi:10.1016/j.bone.2009.08.057 (2010).

93 Song, K. *et al.* Identification of a key residue mediating bone morphogenetic protein (BMP)-6 resistance to noggin inhibition allows for engineered BMPs with superior agonist activity. *J Biol Chem* **285**, 12169-12180, doi:10.1074/jbc.M109.087197 (2010).

94 Ripamonti, U., Ramoshebi, L. N., Teare, J., Renton, L. & Ferretti, C. The induction of endochondral bone formation by transforming growth factor-?3: Experimental studies in the non-human primate Papio ursinus. *Journal of Cellular and Molecular Medicine* **ja**, doi:10.1111/j.1582-4934.2008.00126.x (2007).

95 Betz, O. B. *et al.* The repair of critical-sized bone defects using expedited, autologous BMP-2 gene-activated fat implants. *Tissue Eng Part A* **16**, 1093-1101, doi:10.1089/ten.TEA.2009.0656 (2010).

96 Klar, R. M., Duarte, R., Dix-Peek, T. & Ripamonti, U. The induction of bone formation by the recombinant human transforming growth factor-beta3. *Biomaterials* **35**, 2773-2788, doi:10.1016/j.biomaterials.2013.12.062 (2014).

97 Derynck, R. & Budi, E. H. Specificity, versatility, and control of TGF-beta family signaling. *Science signaling* **12**, eaav5183, doi:10.1126/scisignal.aav5183 (2019).

98 Tay, C. Y., Irvine, S. A., Boey, F. Y., Tan, L. P. & Venkatraman, S. Micro-/nano-engineered cellular responses for soft tissue engineering and biomedical applications. *Small (Weinheim an der Bergstrasse, Germany)* **7**, 1361-1378, doi:10.1002/smll.201100046 (2011).

99 Breuls, R. G., Jiya, T. U. & Smit, T. H. Scaffold stiffness influences cell behavior: opportunities for skeletal tissue engineering. *Open Orthop J* **2**, 103-109, doi:10.2174/1874325000802010103 (2008).

100 Keller, B. *et al.* Interaction of TGFbeta and BMP signaling pathways during chondrogenesis. *PLoS One* **6**, e16421, doi:10.1371/journal.pone.0016421 (2011).

101 Thielen, N. G. M., van der Kraan, P. M. & van Caam, A. P. M. TGFbeta/BMP Signaling Pathway in Cartilage Homeostasis. *Cells* **8**, doi:10.3390/cells8090969 (2019).

102 Mueller, T. D. & Nickel, J. Promiscuity and specificity in BMP receptor activation. *FEBS Lett* **586**, 1846-1859, doi:10.1016/j.febslet.2012.02.043 (2012).

103 van der Kraan, P. M. The changing role of TGFbeta in healthy, ageing and osteoarthritic joints. *Nat Rev Rheumatol* **13**, 155-163, doi:10.1038/nrrheum.2016.219 (2017).

104 de Caestecker, M. The transforming growth factor-beta superfamily of receptors. *Cytokine Growth Factor Rev* **15**, 1-11, doi:10.1016/j.cytogfr.2003.10.004 (2004).

105 Gordon, K. J. & Blobe, G. C. Role of transforming growth factor-beta superfamily signaling pathways in human disease. *Biochim Biophys Acta* **1782**, 197-228, doi:10.1016/j.bbadis.2008.01.006 (2008).

106 Hinck, A. P. Structural studies of the TGF-betas and their receptors - insights into evolution of the TGF-beta superfamily. *FEBS Lett* **586**, 1860-1870, doi:10.1016/j.febslet.2012.05.028 (2012).

107 van der Kraan, P. M., Goumans, M. J., Blaney Davidson, E. & ten Dijke, P. Age-dependent alteration of TGF-beta signalling in osteoarthritis. *Cell Tissue Res* **347**, 257-265, doi:10.1007/s00441-011-1194-6 (2012).

108 Heldin, C. H., Miyazono, K. & ten Dijke, P. TGF-beta signalling from cell membrane to nucleus through SMAD proteins. *Nature* **390**, 465-471, doi:10.1038/37284 (1997).

109 van der Kraan, P. M., Blaney Davidson, E. N., Blom, A. & van den Berg, W. B. TGF-beta signaling in chondrocyte terminal differentiation and osteoarthritis: modulation and integration of signaling pathways through receptor-Smads. *Osteoarthritis Cartilage* **17**, 1539-1545, doi:10.1016/j.joca.2009.06.008 (2009).

110 Aykul, S. & Martinez-Hackert, E. Transforming Growth Factor-beta Family Ligands Can Function as Antagonists by Competing for Type II Receptor Binding. *J Biol Chem* **291**, 10792-10804, doi:10.1074/jbc.M115.713487 (2016).

111 Sieber, C., Kopf, J., Hiepen, C. & Knaus, P. Recent advances in BMP receptor signaling. *Cytokine Growth Factor Rev* **20**, 343-355, doi:10.1016/j.cytogfr.2009.10.007 (2009).

112 Lavery, K., Swain, P., Falb, D. & Alaoui-Ismaili, M. H. BMP-2/4 and BMP-6/7 differentially utilize cell surface receptors to induce osteoblastic differentiation of human bone marrow-derived mesenchymal stem cells. *J Biol Chem* **283**, 20948-20958, doi:10.1074/jbc.M800850200 (2008).

113 Xiong, F. *Induction of chondrogenic morphogenesis in tissue culture using different combinations of transforming growth factor-beta superfamily proteins in vitro*, lmu, (2020).

114 Weiss, A. & Attisano, L. The TGFbeta superfamily signaling pathway. *Wiley interdisciplinary reviews. Developmental biology* **2**, 47-63, doi:10.1002/wdev.86 (2013).

115 Wu, J., Ren, B., Shi, F., Hua, P. & Lin, H. BMP and mTOR signaling in heterotopic ossification: Does their crosstalk provide therapeutic opportunities? *J Cell Biochem* **120**, 12108-12122, doi:10.1002/jcb.28710 (2019).

116 Vander Ark, A., Cao, J. & Li, X. TGF-beta receptors: In and beyond TGF-beta signaling. *Cell Signal* **52**, 112-120, doi:10.1016/j.cellsig.2018.09.002 (2018).

117 Shi, Y. & Massagué, J. Mechanisms of TGF-β Signaling from Cell Membrane to the Nucleus. *Cell* **113**, 685-700, doi:10.1016/s0092-8674(03)00432-x (2003).

118 Feng, X. H. & Derynck, R. Specificity and versatility in tgf-beta signaling through Smads. *Annu Rev Cell Dev Biol* **21**, 659-693, doi:10.1146/annurev.cellbio.21.022404.142018 (2005).

119 Blaney Davidson, E. N. *et al.* Increase in ALK1/ALK5 ratio as a cause for elevated MMP-13 expression in osteoarthritis in humans and mice. *Journal of immunology (Baltimore, Md. : 1950)* **182**, 7937-7945, doi:10.4049/jimmunol.0803991 (2009).

120 Miyazono, K., Maeda, S. & Imamura, T. BMP receptor signaling: transcriptional targets, regulation of signals, and signaling cross-talk. *Cytokine Growth Factor Rev* **16**, 251-263, doi:10.1016/j.cytogfr.2005.01.009 (2005).

121 Wu, M., Chen, G. & Li, Y. P. TGF-beta and BMP signaling in osteoblast, skeletal development, and bone formation, homeostasis and disease. *Bone Res* **4**, 16009, doi:10.1038/boneres.2016.9 (2016).

122 Song, B., Estrada, K. D. & Lyons, K. M. Smad signaling in skeletal development and regeneration. *Cytokine Growth Factor Rev* **20**, 379-388, doi:10.1016/j.cytogfr.2009.10.010 (2009).

123 Chen, G., Deng, C. & Li, Y. P. TGF-beta and BMP signaling in osteoblast differentiation and bone formation. *Int J Biol Sci* **8**, 272-288, doi:10.7150/ijbs.2929 (2012).

124 Grafe, I. *et al.* TGF-beta Family Signaling in Mesenchymal Differentiation. *Cold Spring Harb Perspect Biol* **10**, a022202, doi:10.1101/cshperspect.a022202 (2018).

125 Mu, Y., Gudey, S. K. & Landstrom, M. Non-Smad signaling pathways. *Cell Tissue Res* **347**, 11-20, doi:10.1007/s00441-011-1201-y (2012).

126 Bandyopadhyay, A., Yadav, P. S. & Prashar, P. BMP signaling in development and diseases: a pharmacological perspective. *Biochem Pharmacol* **85**, 857-864, doi:10.1016/j.bcp.2013.01.004 (2013).

127 Miller, E. S., Esterly, N. B. & Fairley, J. A. Progressive osseous heteroplasia. *Arch Dermatol* **132**, 787-791, doi:doi:10.1001/archderm.1996.03890310073010 (1996).

128 Xie, Z. *et al.* Imbalance Between Bone Morphogenetic Protein 2 and Noggin Induces Abnormal Osteogenic Differentiation of Mesenchymal Stem Cells in Ankylosing Spondylitis. *Arthritis Rheumatol* **68**, 430-440, doi:10.1002/art.39433 (2016).

129 Alliston, T., Piek, E. & Derynck, R. *TGF-beta Family Signaling in Skeletal Development, Maintenance, and Disease*. Vol. 50 (2008).

130 Reddi, A. H. Bone morphogenesis and modeling: soluble signals sculpt osteosomes in the solid state. *Cell* **89**, 159-161, doi:10.1016/s0092-8674(00)80193-2 (1997).

131 Sartori, R., Gregorevic, P. & Sandri, M. TGFbeta and BMP signaling in skeletal muscle: potential significance for muscle-related disease. *Trends in endocrinology and metabolism: TEM* **25**, 464-471, doi:10.1016/j.tem.2014.06.002 (2014).

132 Ripamonti, U. *et al.* The synergistic induction of bone formation by the osteogenic proteins of the TGF-beta supergene family. *Biomaterials* **104**, 279-296, doi:10.1016/j.biomaterials.2016.07.018 (2016).

133 Herpin, A., Lelong, C. & Favrel, P. Transforming growth factor-beta-related proteins: an ancestral and widespread superfamily of cytokines in metazoans. *Dev Comp Immunol* **28**, 461-485, doi:10.1016/j.dci.2003.09.007 (2004).

134 Poniatowski, L. A., Wojdasiewicz, P., Gasik, R. & Szukiewicz, D. Transforming growth factor Beta family: insight into the role of growth factors in regulation of fracture healing biology and potential clinical applications. *Mediators of inflammation* **2015**, 137823, doi:10.1155/2015/137823 (2015).

135 Shah, M., Foreman, D. M. & Ferguson, M. W. Neutralisation of TGF-beta 1 and TGF-beta 2 or exogenous addition of TGF-beta 3 to cutaneous rat wounds reduces scarring. *J Cell Sci* **108 (Pt 3)**, 985-1002, doi:10.1242/jcs.108.3.985 (1995).

136 Sakou, T. *et al.* Localization of Smads, the TGF-beta family intracellular signaling components during endochondral ossification. *J Bone Miner Res* **14**, 1145-1152, doi:10.1359/jbmr.1999.14.7.1145 (1999).

137 Serra, R., Karaplis, A. & Sohn, P. Parathyroid hormone-related peptide (PTHrP)-dependent and -independent effects of transforming growth factor beta (TGF-beta) on endochondral bone formation. *J Cell Biol* **145**, 783-794, doi:10.1083/jcb.145.4.783 (1999).

138 Crane, J. L. & Cao, X. Bone marrow mesenchymal stem cells and TGF-beta signaling in bone remodeling. *J Clin Invest* **124**, 466-472, doi:10.1172/JCI70050 (2014).

139 Kim, I. G., Ko, J., Lee, H. R., Do, S. H. & Park, K. Mesenchymal cells condensation-inducible mesh scaffolds for cartilage tissue engineering. *Biomaterials* **85**, 18-29, doi:10.1016/j.biomaterials.2016.01.048 (2016).

140 Chen, L. *et al.* Growth Factor and Its Polymer Scaffold-Based Delivery System for Cartilage Tissue Engineering. *Int J Nanomedicine* **15**, 6097-6111, doi:10.2147/IJN.S249829 (2020).

141 Leah, E. Osteoarthritis: TGF-beta overload at bones of cartilage degeneration. *Nat Rev Rheumatol* **9**, 382, doi:10.1038/nrrheum.2013.81 (2013).

142 Kato, Y., Iwamoto, M., Koike, T., Suzuki, F. & Takano, Y. Terminal differentiation and calcification in rabbit chondrocyte cultures grown in centrifuge tubes: regulation by transforming growth factor beta and serum factors. *Proc Natl Acad Sci U S A* **85**, 9552-9556, doi:10.1073/pnas.85.24.9552 (1988).

143 Ballock, R. T. *et al.* TGF-beta 1 prevents hypertrophy of epiphyseal chondrocytes: regulation of gene expression for cartilage matrix proteins and metalloproteases. *Dev Biol* **158**, 414-429, doi:10.1006/dbio.1993.1200 (1993).

144 Bush, J. R. & Beier, F. TGF-beta and osteoarthritis--the good and the bad. *Nature medicine* **19**, 667-669, doi:10.1038/nm.3228 (2013).

145 Blaney Davidson, E. N., van der Kraan, P. M. & van den Berg, W. B. TGF-beta and osteoarthritis. *Osteoarthritis Cartilage* **15**, 597-604, doi:10.1016/j.joca.2007.02.005 (2007).

146 van der Kraan, P. M. Age-related alterations in TGF beta signaling as a causal factor of cartilage degeneration in osteoarthritis. *Bio-medical materials and engineering* **24**, 75-80, doi:10.3233/BME-140976 (2014).

147 Tang, Y. *et al.* TGF-beta1-induced migration of bone mesenchymal stem cells couples bone resorption with formation. *Nature medicine* **15**, 757-765, doi:10.1038/nm.1979 (2009).

148 Crane, J. L., Xian, L. & Cao, X. in *TGF-β Signaling* 287-300 (Springer, 2016).

149 van den Bosch, M. H. *et al.* Canonical Wnt signaling skews TGF-beta signaling in chondrocytes towards signaling via ALK1 and Smad 1/5/8. *Cell Signal* **26**, 951-958, doi:10.1016/j.cellsig.2014.01.021 (2014).

150 Tang, Y. *et al.* TGF-β1–induced migration of bone mesenchymal stem cells couples bone resorption with formation. **15**, 757-765 (2009).

151 Sanford, L. P. *et al.* TGFbeta2 knockout mice have multiple developmental defects that are non-overlapping with other TGFbeta knockout phenotypes. *Development* **124**, 2659-2670, doi:10.1242/dev.124.13.2659 (1997).

152 Ripamonti, U., Dix-Peek, T., Parak, R., Milner, B. & Duarte, R. Profiling bone morphogenetic proteins and transforming growth factor-betas by hTGF-beta3 pre-treated coral-derived macroporous bioreactors: the power of one. *Biomaterials* **49**, 90-102, doi:10.1016/j.biomaterials.2015.01.058 (2015).

153 Reddi, A. H., Reddi, A. J. C. & reviews, g. f. Vol. 20 341-342 (2009).

154 Bleuming, S. A. *et al.* Bone morphogenetic protein signaling suppresses tumorigenesis at gastric epithelial transition zones in mice. *Cancer Res* **67**, 8149-8155, doi:10.1158/0008-5472.CAN-06-4659 (2007).

155 Canalis, E., Brunet, L. J., Parker, K. & Zanotti, S. Conditional inactivation of noggin in the postnatal skeleton causes osteopenia. *Endocrinology* **153**, 1616-1626, doi:10.1210/en.2011-1604 (2012).

156 Gazzerro, E. & Canalis, E. Bone morphogenetic proteins and their antagonists. *Rev Endocr Metab Disord* **7**, 51-65, doi:10.1007/s11154-006-9000-6 (2006).

157 Ripamonti, U. Soluble osteogenic molecular signals and the induction of bone formation. *Biomaterials* **27**, 807-822, doi:10.1016/j.biomaterials.2005.09.021 (2006).

158 Sanchez-Duffhues, G., Hiepen, C., Knaus, P. & Ten Dijke, P. Bone morphogenetic protein signaling in bone homeostasis. *Bone* **80**, 43-59, doi:10.1016/j.bone.2015.05.025 (2015).

159 Kuo, P. L., Huang, Y. T., Chang, C. H. & Chang, J. K. Bone morphogenetic protein-2 and -4 (BMP-2 and -4) mediates fraxetin-induced maturation and differentiation in human osteoblast-like cell lines. *Biol Pharm Bull* **29**, 119-124, doi:10.1248/bpb.29.119 (2006).

160 Even, J., Eskander, M. & Kang, J. Bone morphogenetic protein in spine surgery: current and future uses. *J Am Acad Orthop Surg* **20**, 547-552, doi:10.5435/JAAOS-20-09-547 (2012).

161 Carreira, A. C. *et al.* Bone Morphogenetic Proteins: Promising Molecules for Bone Healing, Bioengineering, and Regenerative Medicine. *Vitam Horm* **99**, 293-322, doi:10.1016/bs.vh.2015.06.002 (2015).

162 Rodan, G. A., Raisz, L. G. & Bilezikian, J. P. *Principles of bone biology*. (Academic press, 1996).

163 Luu, H. H. *et al.* Distinct roles of bone morphogenetic proteins in osteogenic differentiation of mesenchymal stem cells. *J Orthop Res* **25**, 665-677, doi:10.1002/jor.20359 (2007).

164 Abula, K. *et al.* Elimination of BMP7 from the developing limb mesenchyme leads to articular cartilage degeneration and synovial inflammation with increased age. *FEBS Lett* **589**, 1240-1248, doi:10.1016/j.febslet.2015.04.004 (2015).

165 Huang, Z., Ren, P. G., Ma, T., Smith, R. L. & Goodman, S. B. Modulating osteogenesis of mesenchymal stem cells by modifying growth factor availability. *Cytokine* **51**, 305-310, doi:10.1016/j.cyto.2010.06.002 (2010).

166 Noel, D. *et al.* Short-term BMP-2 expression is sufficient for in vivo osteochondral differentiation of mesenchymal stem cells. *Stem Cells* **22**, 74-85, doi:10.1634/stemcells.22-1-74 (2004).

167 Tsuji, K. *et al.* BMP2 activity, although dispensable for bone formation, is required for the initiation of fracture healing. *Nat Genet* **38**, 1424-1429, doi:10.1038/ng1916 (2006).

168 Luo, G. *et al.* BMP-7 is an inducer of nephrogenesis, and is also required for eye development and skeletal patterning. *Genes Dev* **9**, 2808-2820, doi:10.1101/gad.9.22.2808 (1995).

169 Urist, M. R. Bone: formation by autoinduction. *Science* **150**, 893-899, doi:10.1126/science.150.3698.893 (1965).

170 Mimura, T. *et al.* Spatiotemporal control of proliferation and differentiation of bone marrow-derived mesenchymal stem cells recruited using collagen hydrogel for repair of articular cartilage defects. *J Biomed Mater Res B Appl Biomater* **98**, 360-368, doi:10.1002/jbm.b.31859 (2011).

171 Gelse, K. *et al.* Cell-based resurfacing of large cartilage defects: long-term evaluation of grafts from autologous transgene-activated periosteal cells in a porcine model of osteoarthritis. *Arthritis Rheum* **58**, 475-488, doi:10.1002/art.23124 (2008).

172 Aikawa, T. *et al.* Establishment of bone morphogenetic protein 2 responsive chondrogenic cell line. *J Bone Miner Res* **11**, 544-553, doi:10.1002/jbmr.5650110416 (1996).

173 Pathi, S., Rutenberg, J. B., Johnson, R. L. & Vortkamp, A. Interaction of Ihh and BMP/Noggin signaling during cartilage differentiation. *Dev Biol* **209**, 239-253, doi:10.1006/dbio.1998.9181 (1999).

174 Reshef, R., Maroto, M. & Lassar, A. B. Regulation of dorsal somitic cell fates: BMPs and Noggin control the timing and pattern of myogenic regulator expression. *Genes Dev* **12**, 290-303, doi:10.1101/gad.12.3.290 (1998).

175 Klar, R. M. The Induction of Bone Formation: The Translation Enigma. *Front Bioeng Biotechnol* **6**, 74, doi:10.3389/fbioe.2018.00074 (2018).

176 Rosen, V. BMP and BMP inhibitors in bone. *Ann N Y Acad Sci* **1068**, 19-25, doi:10.1196/annals.1346.005 (2006).

177 Benchabane, H. *Regulation of Smad7-dependent inhibition of TGF [beta] superfamily signalling*. (National Library of Canada= Bibliothèque nationale du Canada, Ottawa, 2005).

178 Smith, W. C. & Harland, R. M. Expression cloning of noggin, a new dorsalizing factor localized to the Spemann organizer in Xenopus embryos. *Cell* **70**, 829-840, doi:10.1016/0092-8674(92)90316-5 (1992).

179 Zimmerman, L. B., De Jesus-Escobar, J. M. & Harland, R. M. The Spemann organizer signal noggin binds and inactivates bone morphogenetic protein 4. *Cell* **86**, 599-606, doi:10.1016/s0092-8674(00)80133-6 (1996).

180 Krause, C., Guzman, A. & Knaus, P. Noggin. *Int J Biochem Cell Biol* **43**, 478-481, doi:10.1016/j.biocel.2011.01.007 (2011).

181 Bayramov, A. V. *et al.* Novel functions of Noggin proteins: inhibition of Activin/Nodal and Wnt signaling. *Development* **138**, 5345-5356, doi:10.1242/dev.068908 (2011).

182 Wu, X. B. *et al.* Impaired osteoblastic differentiation, reduced bone formation, and severe osteoporosis in noggin-overexpressing mice. *J Clin Invest* **112**, 924-934, doi:10.1172/JCI15543 (2003).

183 Devlin, R. D. *et al.* Skeletal overexpression of noggin results in osteopenia and reduced bone formation. *Endocrinology* **144**, 1972-1978, doi:10.1210/en.2002-220918 (2003).

184 Tylzanowski, P., Mebis, L. & Luyten, F. P. The Noggin null mouse phenotype is strain dependent and haploinsufficiency leads to skeletal defects. *Dev Dyn* **235**, 1599-1607, doi:10.1002/dvdy.20782 (2006).

185 Gazzerro, E. *et al.* Noggin arrests stromal cell differentiation in vitro. *Bone* **32**, 111-119, doi:10.1016/s8756-3282(02)00948-1 (2003).

186 Wan, D. C. *et al.* Noggin suppression enhances in vitro osteogenesis and accelerates in vivo bone formation. *J Biol Chem* **282**, 26450-26459, doi:10.1074/jbc.M703282200 (2007).

187 Walsh, D. W., Godson, C., Brazil, D. P. & Martin, F. Extracellular BMP-antagonist regulation in development and disease: tied up in knots. *Trends Cell Biol* **20**, 244-256, doi:10.1016/j.tcb.2010.01.008 (2010).

188 Brunet, L. J., McMahon, J. A., McMahon, A. P. & Harland, R. M. Noggin, cartilage morphogenesis, and joint formation in the mammalian skeleton. *Science* **280**, 1455-1457, doi:10.1126/science.280.5368.1455 (1998).

189 Gong, Y. *et al.* Heterozygous mutations in the gene encoding noggin affect human joint morphogenesis. *Nat Genet* **21**, 302-304, doi:10.1038/6821 (1999).

190 Huang, Y. *et al.* Induction of Articular Chondrogenesis by Chitosan/Hyaluronic-Acid-Based Biomimetic Matrices Using Human Adipose-Derived Stem Cells. *Int J Mol Sci* **20**, doi:10.3390/ijms20184487 (2019).

191 Cicione, C. *et al.* Alternative protocols to induce chondrogenic differentiation: transforming growth factor-beta superfamily. *Cell Tissue Bank* **16**, 195-207, doi:10.1007/s10561-014-9472-7 (2015).

192 He, W. *et al.* Synergistic effects of recombinant Lentiviral-mediated BMP2 and TGF-beta3 on the osteogenic differentiation of rat bone marrow mesenchymal stem cells in vitro. *Cytokine* **120**, 1-8, doi:10.1016/j.cyto.2019.03.020 (2019).

193 Wang, Y. *et al.* Synergistic effects of overexpression of BMP2 and TGFbeta3 on osteogenic differentiation of bone marrow mesenchymal stem cells. *Mol Med Rep* **14**, 5514-5520, doi:10.3892/mmr.2016.5961 (2016).

194 Haschtmann, D., Ferguson, S. J. & Stoyanov, J. V. BMP-2 and TGF-beta3 do not prevent spontaneous degeneration in rabbit disc explants but induce ossification of the annulus fibrosus. *Eur Spine J* **21**, 1724-1733, doi:10.1007/s00586-012-2371-3 (2012).

195 Mehlhorn, A. T. *et al.* Differential effects of BMP-2 and TGF-beta1 on chondrogenic differentiation of adipose derived stem cells. *Cell Prolif* **40**, 809-823, doi:10.1111/j.1365-2184.2007.00473.x (2007).

196 Wakefield, L. M. & Hill, C. S. Beyond TGFbeta: roles of other TGFbeta superfamily members in cancer. *Nat Rev Cancer* **13**, 328-341, doi:10.1038/nrc3500 (2013).

197 Re'em-Kalma, Y., Lamb, T. & Frank, D. Competition between noggin and bone morphogenetic protein 4 activities may regulate dorsalization during Xenopus development. *Proc Natl Acad Sci U S A* **92**, 12141-12145, doi:10.1073/pnas.92.26.12141 (1995).

198 Zakin, L. & De Robertis, E. M. Extracellular regulation of BMP signaling. *Curr Biol* **20**, R89-92, doi:10.1016/j.cub.2009.11.021 (2010).

199 Wang, Y. *et al.* Noggin resistance contributes to the potent osteogenic capability of BMP9 in mesenchymal stem cells. *J Orthop Res* **31**, 1796-1803, doi:10.1002/jor.22427 (2013).

200 Bustin, S. A. & Wittwer, C. T. MIQE: A Step Toward More Robust and Reproducible Quantitative PCR. *Clin Chem* **63**, 1537-1538, doi:10.1373/clinchem.2016.268953 (2017).

201 Bustin, S. A. *et al.* (Oxford University Press, 2009).

202 d, M. G. & Huggett, J. F. The Digital MIQE Guidelines Update: Minimum Information for Publication of Quantitative Digital PCR Experiments for 2020. *Clin Chem* **66**, 1012-1029, doi:10.1093/clinchem/hvaa125 (2020).

203 Vandesompele, J. *et al.* Accurate normalization of real-time quantitative RT-PCR data by geometric averaging of multiple internal control genes. *Genome Biol* **3**, RESEARCH0034, doi:10.1186/gb-2002-3-7-research0034 (2002).

204 Rider, C. C. & Mulloy, B. Bone morphogenetic protein and growth differentiation factor cytokine families and their protein antagonists. *Biochem J* **429**, 1-12, doi:10.1042/BJ20100305 (2010).

205 Izadpanahi, M. *et al.* Nanotopographical cues of electrospun PLLA efficiently modulate non-coding RNA network to osteogenic differentiation of mesenchymal stem cells during BMP signaling pathway. *Mater Sci Eng C Mater Biol Appl* **93**, 686-703, doi:10.1016/j.msec.2018.08.023 (2018).

206 Bami, M. *et al.* Bone morphogenetic protein signaling in musculoskeletal cancer. *J Cancer Res Clin Oncol* **142**, 2061-2072, doi:10.1007/s00432-016-2149-9 (2016).

207 Zhou, S., Yates, K. E., Eid, K. & Glowacki, J. Demineralized bone promotes chondrocyte or osteoblast differentiation of human marrow stromal cells cultured in collagen sponges. *Cell Tissue Bank* **6**, 33-44, doi:10.1007/s10561-005-4253-y (2005).

208 Lowery, J. W. *et al.* The role of BMP2 signaling in the skeleton. *Crit Rev Eukaryot Gene Expr* **21**, 177-185, doi:10.1615/critreveukargeneexpr.v21.i2.60 (2011).

209 Endo, T. Molecular mechanisms of skeletal muscle development, regeneration, and osteogenic conversion. *Bone* **80**, 2-13, doi:10.1016/j.bone.2015.02.028 (2015).

210 DiGirolamo, D. J., Kiel, D. P. & Esser, K. A. Bone and skeletal muscle: neighbors with close ties. *J Bone Miner Res* **28**, 1509-1518, doi:10.1002/jbmr.1969 (2013).

211 Braun, T. & Gautel, M. Transcriptional mechanisms regulating skeletal muscle differentiation, growth and homeostasis. *Nat Rev Mol Cell Biol* **12**, 349-361, doi:10.1038/nrm3118 (2011).

212 Dayanidhi, S. & Lieber, R. L. Skeletal muscle satellite cells: mediators of muscle growth during development and implications for developmental disorders. *Muscle Nerve* **50**, 723-732, doi:10.1002/mus.24441 (2014).

213 Relaix, F. & Zammit, P. S. Satellite cells are essential for skeletal muscle regeneration: the cell on the edge returns centre stage. *Development* **139**, 2845-2856, doi:10.1242/dev.069088 (2012).

214 Yin, H., Price, F. & Rudnicki, M. A. Satellite cells and the muscle stem cell niche. *Physiol Rev* **93**, 23-67, doi:10.1152/physrev.00043.2011 (2013).

215 Oishi, T. *et al.* Osteogenic differentiation capacity of human skeletal muscle-derived progenitor cells. *PLoS One* **8**, e56641, doi:10.1371/journal.pone.0056641 (2013).

216 Schultz, E. & McCormick, K. M. Skeletal muscle satellite cells. *Rev Physiol Biochem Pharmacol* **123**, 213-257, doi:10.1007/BFb0030904 (1994).

217 Asakura, A., Komaki, M. & Rudnicki, M. Muscle satellite cells are multipotential stem cells that exhibit myogenic, osteogenic, and adipogenic differentiation. *Differentiation* **68**, 245-253, doi:10.1046/j.1432-0436.2001.680412.x (2001).

218 Shefer, G., Wleklinski-Lee, M. & Yablonka-Reuveni, Z. Skeletal muscle satellite cells can spontaneously enter an alternative mesenchymal pathway. *J Cell Sci* **117**, 5393-5404, doi:10.1242/jcs.01419 (2004).

219 Peng, H. & Huard, J. Muscle-derived stem cells for musculoskeletal tissue regeneration and repair. *Transpl Immunol* **12**, 311-319, doi:10.1016/j.trim.2003.12.009 (2004).

220 Mastrogiacomo, M., Derubeis, A. R. & Cancedda, R. Bone and cartilage formation by skeletal muscle derived cells. *J Cell Physiol* **204**, 594-603, doi:10.1002/jcp.20325 (2005).

221 Gao, X. *et al.* BMP2 is superior to BMP4 for promoting human muscle-derived stem cell-mediated bone regeneration in a critical-sized calvarial defect model. *Cell transplantation* **22**, 2393-2408, doi:10.3727/096368912X658854 (2013).

222 Wright, V. *et al.* BMP4-expressing muscle-derived stem cells differentiate into osteogenic lineage and improve bone healing in immunocompetent mice. *Molecular therapy : the journal of the American Society of Gene Therapy* **6**, 169-178, doi:10.1006/mthe.2002.0654 (2002).

223 Tajbakhsh, S., Rocancourt, D. & Buckingham, M. Muscle progenitor cells failing to respond to positional cues adopt non-myogenic fates in myf-5 null mice. *Nature* **384**, 266-270, doi:10.1038/384266a0 (1996).

224 De Coppi, P. *et al.* Rosiglitazone modifies the adipogenic potential of human muscle satellite cells. *Diabetologia* **49**, 1962-1973, doi:10.1007/s00125-006-0304-6 (2006).

225 Lee, J. Y. *et al.* Enhancement of bone healing based on ex vivo gene therapy using human muscle-derived cells expressing bone morphogenetic protein 2. *Hum Gene Ther* **13**, 1201-1211, doi:10.1089/104303402320138989 (2002).

226 Cairns, D. M. *et al.* Interplay of Nkx3.2, Sox9 and Pax3 regulates chondrogenic differentiation of muscle progenitor cells. *PLoS One* **7**, e39642, doi:10.1371/journal.pone.0039642 (2012).

227 Ripamonti, U., Duarte, R. & Ferretti, C. Re-evaluating the induction of bone formation in primates. *Biomaterials* **35**, 9407-9422, doi:10.1016/j.biomaterials.2014.07.053 (2014).

228 Allas, L., Boumediene, K. & Bauge, C. Epigenetic dynamic during endochondral ossification and articular cartilage development. *Bone* **120**, 523-532, doi:10.1016/j.bone.2018.10.004 (2019).

229 Liao, J. *et al.* Sox9 potentiates BMP2-induced chondrogenic differentiation and inhibits BMP2-induced osteogenic differentiation. *PLoS One* **9**, e89025, doi:10.1371/journal.pone.0089025 (2014).

230 Chung, U. I., Schipani, E., McMahon, A. P. & Kronenberg, H. M. Indian hedgehog couples chondrogenesis to osteogenesis in endochondral bone development. *J Clin Invest* **107**, 295-304, doi:10.1172/JCI11706 (2001).

231 Athanasiou, K. A., Darling, E. M., DuRaine, G. D., Hu, J. C. & Reddi, A. H. *Articular cartilage*. (CRC Press, 2017).

232 Kheir, E. & Shaw, D. Hyaline articular cartilage. *Orthopaedics and Trauma* **23**, 450-455, doi:10.1016/j.mporth.2009.01.003 (2009).

233 Sophia Fox, A. J., Bedi, A. & Rodeo, S. A. The basic science of articular cartilage: structure, composition, and function. *Sports Health* **1**, 461-468, doi:10.1177/1941738109350438 (2009).

234 Kwon, H., Paschos, N. K., Hu, J. C. & Athanasiou, K. Articular cartilage tissue engineering: the role of signaling molecules. *Cell Mol Life Sci* **73**, 1173-1194, doi:10.1007/s00018-015-2115-8 (2016).

235 Armiento, A. R., Stoddart, M. J., Alini, M. & Eglin, D. Biomaterials for articular cartilage tissue engineering: Learning from biology. *Acta Biomater* **65**, 1-20, doi:10.1016/j.actbio.2017.11.021 (2018).

236 Heinegard, D. Fell-Muir Lecture: Proteoglycans and more--from molecules to biology. *Int J Exp Pathol* **90**, 575-586, doi:10.1111/j.1365-2613.2009.00695.x (2009).

237 McLeod, M. J. Differential staining of cartilage and bone in whole mouse fetuses by alcian blue and alizarin red S. *Teratology* **22**, 299-301, doi:10.1002/tera.1420220306 (1980).

238 Aspberg, A. The different roles of aggrecan interaction domains. *J Histochem Cytochem* **60**, 987-996, doi:10.1369/0022155412464376 (2012).

239 Shi, S., Wang, C., Acton, A. J., Eckert, G. J. & Trippel, S. B. Role of sox9 in growth factor regulation of articular chondrocytes. *J Cell Biochem* **116**, 1391-1400, doi:10.1002/jcb.25099 (2015).

240 Zuo, C. *et al.* SHP2 regulates skeletal cell fate by modifying SOX9 expression and transcriptional activity. *Bone Res* **6**, 12, doi:10.1038/s41413-018-0013-z (2018).

241 Blumer, M. J. *et al.* The role of cartilage canals in endochondral and perichondral bone formation: are there similarities between these two processes? *J Anat* **206**, 359-372, doi:10.1111/j.1469-7580.2005.00404.x (2005).

242 Grässel, S. & Aszódi, A. *Cartilage*. (Springer, 2016).

243 Miron, R. J. *et al.* Osteogain improves osteoblast adhesion, proliferation and differentiation on a bovine-derived natural bone mineral. *Clinical oral implants research* **28**, 327-333, doi:10.1111/clr.12802 (2017).

244 Ding, Y. *et al.* Sweroside-mediated mTORC1 hyperactivation in bone marrow mesenchymal stem cells promotes osteogenic differentiation. *J Cell Biochem* **120**, 16025-16036, doi:10.1002/jcb.28882 (2019).

245 Scott, M. A. *et al.* Brief review of models of ectopic bone formation. *Stem Cells Dev* **21**, 655-667, doi:10.1089/scd.2011.0517 (2012).

246 Karsenty, G., Kronenberg, H. M. & Settembre, C. Genetic control of bone formation. *Annu Rev Cell Dev Biol* **25**, 629-648, doi:10.1146/annurev.cellbio.042308.113308 (2009).

247 Gonzalez-Fernandez, T., Tierney, E. G., Cunniffe, G. M., O'Brien, F. J. & Kelly, D. J. Gene Delivery of TGF-beta3 and BMP2 in an MSC-Laden Alginate Hydrogel for Articular Cartilage and Endochondral Bone Tissue Engineering. *Tissue Eng Part A* **22**, 776-787, doi:10.1089/ten.TEA.2015.0576 (2016).

248 He, A. *et al.* Repair of osteochondral defects with in vitro engineered cartilage based on autologous bone marrow stromal cells in a swine model. *Sci Rep* **7**, 40489, doi:10.1038/srep40489 (2017).

249 Pelttari, K. *et al.* Premature induction of hypertrophy during in vitro chondrogenesis of human mesenchymal stem cells correlates with calcification and vascular invasion after ectopic transplantation in SCID mice. *Arthritis Rheum* **54**, 3254-3266, doi:10.1002/art.22136 (2006).

250 De Bari, C., Dell'Accio, F. & Luyten, F. P. Failure of in vitro-differentiated mesenchymal stem cells from the synovial membrane to form ectopic stable cartilage in vivo. *Arthritis Rheum* **50**, 142-150, doi:10.1002/art.11450 (2004).

251 Kwon, S. H. *et al.* Modulation of BMP-2-induced chondrogenic versus osteogenic differentiation of human mesenchymal stem cells by cell-specific extracellular matrices. *Tissue Eng Part A* **19**, 49-58, doi:10.1089/ten.TEA.2012.0245 (2013).

252 Vasara, A. I., Konttinen, Y. T., Peterson, L., Lindahl, A. & Kiviranta, I. Persisting high levels of synovial fluid markers after cartilage repair: a pilot study. *Clin Orthop Relat Res* **467**, 267-272, doi:10.1007/s11999-008-0434-x (2009).

253 Schmal, H. *et al.* In vivo quantification of intraarticular cytokines in knees during natural and surgically induced cartilage repair. *Cytotherapy* **11**, 1065-1075, doi:10.3109/14653240903219130 (2009).

254 Fortier, L. A., Mohammed, H. O., Lust, G. & Nixon, A. J. Insulin-like growth factor-I enhances cell-based repair of articular cartilage. *J Bone Joint Surg Br* **84**, 276-288, doi:10.1302/0301-620x.84b2.11167 (2002).

255 Scotti, C. *et al.* Recapitulation of endochondral bone formation using human adult mesenchymal stem cells as a paradigm for developmental engineering. *Proc Natl Acad Sci U S A* **107**, 7251-7256, doi:10.1073/pnas.1000302107 (2010).

256 Dai, J. & Rabie, A. B. VEGF: an essential mediator of both angiogenesis and endochondral ossification. *J Dent Res* **86**, 937-950, doi:10.1177/154405910708601006 (2007).

257 Eames, B. F., Sharpe, P. T. & Helms, J. A. Hierarchy revealed in the specification of three skeletal fates by Sox9 and Runx2. *Dev Biol* **274**, 188-200, doi:10.1016/j.ydbio.2004.07.006 (2004).

258 Zhang, H., Zhao, X., Zhang, Z., Chen, W. & Zhang, X. An immunohistochemistry study of Sox9, Runx2, and Osterix expression in the mandibular cartilages of newborn mouse. *Biomed Res Int* **2013**, 265380, doi:10.1155/2013/265380 (2013).

259 Cheng, A. & Genever, P. G. SOX9 determines RUNX2 transactivity by directing intracellular degradation. *J Bone Miner Res* **25**, 2680-2689, doi:10.1002/jbmr.174 (2010).

260 Yamashita, S. *et al.* Sox9 directly promotes Bapx1 gene expression to repress Runx2 in chondrocytes. *Exp Cell Res* **315**, 2231-2240, doi:10.1016/j.yexcr.2009.03.008 (2009).

261 Zhou, G. *et al.* Dominance of SOX9 function over RUNX2 during skeletogenesis. *Proc Natl Acad Sci U S A* **103**, 19004-19009, doi:10.1073/pnas.0605170103 (2006).

262 Fang, S., Li, Y. & Chen, P. Osteogenic effect of bone marrow mesenchymal stem cell-derived exosomes on steroid-induced osteonecrosis of the femoral head. *Drug Des Devel Ther* **13**, 45-55, doi:10.2147/DDDT.S178698 (2019).

263 Zhao, L. *The role of Sox9 in osteogenesis*, Queen's University Belfast, (2008).

264 Daly, A. C., Randall, R. A. & Hill, C. S. Transforming growth factor beta-induced Smad1/5 phosphorylation in epithelial cells is mediated by novel receptor complexes and is essential for anchorage-independent growth. *Mol Cell Biol* **28**, 6889-6902, doi:10.1128/MCB.01192-08 (2008).

265 Goumans, M.-J., Lebrin, F. & Valdimarsdottir, G. Controlling the Angiogenic SwitchA Balance between Two Distinct TGF-b Receptor Signaling Pathways. *Trends in Cardiovascular Medicine* **13**, 301-307, doi:10.1016/s1050-1738(03)00142-7 (2003).

266 Faucheux, C., Ulysse, F., Bareille, R., Reddi, A. H. & Amedee, J. Opposing actions of BMP3 and TGF beta 1 in human bone marrow stromal cell growth and differentiation. *Biochem Biophys Res Commun* **241**, 787-793, doi:10.1006/bbrc.1997.7792 (1997).

267 Izumi, N. *et al.* BMP-7 opposes TGF-beta1-mediated collagen induction in mouse pulmonary myofibroblasts through Id2. *Am J Physiol Lung Cell Mol Physiol* **290**, L120-126, doi:10.1152/ajplung.00171.2005 (2006).

268 Ehnert, S. *et al.* TGF-beta1 as possible link between loss of bone mineral density and chronic inflammation. *PLoS One* **5**, e14073, doi:10.1371/journal.pone.0014073 (2010).

269 Ehnert, S. *et al.* Transforming growth factor beta1 inhibits bone morphogenic protein (BMP)-2 and BMP-7 signaling via upregulation of Ski-related novel protein N (SnoN): possible mechanism for the failure of BMP therapy? *BMC medicine* **10**, 101, doi:10.1186/1741-7015-10-101 (2012).

270 Lee, M. H. *et al.* BMP-2-induced Runx2 expression is mediated by Dlx5, and TGF-beta 1 opposes the BMP-2-induced osteoblast differentiation by suppression of Dlx5 expression. *J Biol Chem* **278**, 34387-34394, doi:10.1074/jbc.M211386200 (2003).

271 Wrighton, K. H., Lin, X., Yu, P. B. & Feng, X. H. Transforming Growth Factor {beta} Can Stimulate Smad1 Phosphorylation Independently of Bone Morphogenic Protein Receptors. *J Biol Chem* **284**, 9755-9763, doi:10.1074/jbc.M809223200 (2009).

272 Singhatanadgit, W., Salih, V. & Olsen, I. Up-regulation of bone morphogenetic protein receptor IB by growth factors enhances BMP-2-induced human bone cell functions. *J Cell Physiol* **209**, 912-922, doi:10.1002/jcp.20799 (2006).

273 Lin, C. Y. *et al.* The use of ASCs engineered to express BMP2 or TGF-beta3 within scaffold constructs to promote calvarial bone repair. *Biomaterials* **34**, 9401-9412, doi:10.1016/j.biomaterials.2013.08.051 (2013).

274 Shintani, N., Siebenrock, K. A. & Hunziker, E. B. TGF-ss1 enhances the BMP-2-induced chondrogenesis of bovine synovial explants and arrests downstream differentiation at an early stage of hypertrophy. *PLoS One* **8**, e53086, doi:10.1371/journal.pone.0053086 (2013).

275 Kim, H. J. & Im, G. I. Combination of transforming growth factor-beta2 and bone morphogenetic protein 7 enhances chondrogenesis from adipose tissue-derived mesenchymal stem cells. *Tissue Eng Part A* **15**, 1543-1551, doi:10.1089/ten.tea.2008.0368 (2009).

276 Weinberg, R. A. Coming full circle-from endless complexity to simplicity and back again. *Cell* **157**, 267-271, doi:10.1016/j.cell.2014.03.004 (2014).

277 Tachi, K. *et al.* Enhancement of bone morphogenetic protein-2-induced ectopic bone formation by transforming growth factor-beta1. *Tissue Eng Part A* **17**, 597-606, doi:10.1089/ten.TEA.2010.0094 (2011).

278 Shen, B., Wei, A., Tao, H., Diwan, A. D. & Ma, D. D. BMP-2 enhances TGF-beta3-mediated chondrogenic differentiation of human bone marrow multipotent mesenchymal stromal cells in alginate bead culture. *Tissue Eng Part A* **15**, 1311-1320, doi:10.1089/ten.tea.2008.0132 (2009).

279 van Beuningen, H. M., Glansbeek, H. L., van der Kraan, P. M. & van den Berg, W. B. Differential effects of local application of BMP-2 or TGF-beta 1 on both articular cartilage composition and osteophyte formation. *Osteoarthritis Cartilage* **6**, 306-317, doi:10.1053/joca.1998.0129 (1998).

280 Xiong, F., Cheng, X., Zhang, C., Klar, R. M. & He, T. Optimizations for identifying reference genes in bone and cartilage bioengineering. *BMC Biotechnol* **21**, 25, doi:10.1186/s12896-021-00685-8 (2021).

281 Kronenberg, H. M. Developmental regulation of the growth plate. *Nature* **423**, 332-336, doi:10.1038/nature01657 (2003).

282 Janssens, K., ten Dijke, P., Janssens, S. & Van Hul, W. Transforming growth factor-beta1 to the bone. *Endocr Rev* **26**, 743-774, doi:10.1210/er.2004-0001 (2005).

283 Gazzerro, E., Gangji, V. & Canalis, E. Bone morphogenetic proteins induce the expression of noggin, which limits their activity in cultured rat osteoblasts. *J Clin Invest* **102**, 2106-2114, doi:10.1172/JCI3459 (1998).

284 Groppe, J. *et al.* Structural basis of BMP signalling inhibition by the cystine knot protein Noggin. *Nature* **420**, 636-642, doi:10.1038/nature01245 (2002).

285 Ahmed, S., Metpally, R. P. R., Sangadala, S. & Reddy, B. V. B. Virtual screening and selection of drug-like compounds to block noggin interaction with bone morphogenetic proteins. *Journal of Molecular Graphics and Modelling* **28**, 670-682, doi:10.1016/j.jmgm.2010.01.006 (2010).

286 Albers, C. E. *et al.* L51P - A BMP2 variant with osteoinductive activity via inhibition of Noggin. *Bone* **51**, 401-406, doi:10.1016/j.bone.2012.06.020 (2012).

287 Cooper, G. M. *et al.* Ex vivo Noggin gene therapy inhibits bone formation in a mouse model of postoperative resynostosis. *Plast Reconstr Surg* **123**, 94S-103S, doi:10.1097/PRS.0b013e318191c05b (2009).

288 Nakayama, N., Duryea, D., Manoukian, R., Chow, G. & Han, C. Y. Macroscopic cartilage formation with embryonic stem-cell-derived mesodermal progenitor cells. *J Cell Sci* **116**, 2015-2028, doi:10.1242/jcs.00417 (2003).

289 Chen, C., Uludag, H., Wang, Z. & Jiang, H. Noggin suppression decreases BMP-2-induced osteogenesis of human bone marrow-derived mesenchymal stem cells in vitro. *J Cell Biochem* **113**, 3672-3680, doi:10.1002/jcb.24240 (2012).

290 Rifas, L. The role of noggin in human mesenchymal stem cell differentiation. *J Cell Biochem* **100**, 824-834, doi:10.1002/jcb.21132 (2007).

291 Hashimi, S. M. Exogenous noggin binds the BMP-2 receptor and induces alkaline phosphatase activity in osteoblasts. *J Cell Biochem* **120**, 13237-13242, doi:10.1002/jcb.28597 (2019).

292 Shi, W. *et al.* Endofin acts as a Smad anchor for receptor activation in BMP signaling. *J Cell Sci* **120**, 1216-1224, doi:10.1242/jcs.03400 (2007).

293 Christiaen, L., Stolfi, A. & Levine, M. BMP signaling coordinates gene expression and cell migration during precardiac mesoderm development. *Dev Biol* **340**, 179-187, doi:10.1016/j.ydbio.2009.11.006 (2010).

294 Perrimon, N. & McMahon, A. P. Negative Feedback Mechanisms and Their Roles during Pattern Formation. *Cell* **97**, 13-16, doi:10.1016/s0092-8674(00)80710-2 (1999).

295 Sun, Q. *et al.* Role of miR-17 family in the negative feedback loop of bone morphogenetic protein signaling in neuron. *PLoS One* **8**, e83067, doi:10.1371/journal.pone.0083067 (2013).

296 Alon, U. Network motifs: theory and experimental approaches. *Nature reviews. Genetics* **8**, 450-461, doi:10.1038/nrg2102 (2007).

297 Balázsi, G., Heath, A. P., Shi, L. & Gennaro, M. L. The temporal response of the Mycobacterium tuberculosis gene regulatory network during growth arrest. *Molecular systems biology* **4**, 225, doi:10.1038/msb.2008.63 (2008).

298 Zhang, M. X. *et al.* Biogenesis of short intronic repeat 27-nucleotide small RNA from endothelial nitric-oxide synthase gene. *J Biol Chem* **283**, 14685-14693, doi:10.1074/jbc.M801933200 (2008).

299 Singh, A. Negative feedback through mRNA provides the best control of gene-expression noise. *IEEE Trans Nanobioscience* **10**, 194-200, doi:10.1109/TNB.2011.2168826 (2011).

300 Brutinel, E. D. & Yahr, T. L. Control of gene expression by type III secretory activity. *Curr Opin Microbiol* **11**, 128-133, doi:10.1016/j.mib.2008.02.010 (2008).

301 Becskei, A. & Serrano, L. Engineering stability in gene networks by autoregulation. *Nature* **405**, 590-593, doi:10.1038/35014651 (2000).

302 Singh, A. & Hespanha, J. P. Optimal feedback strength for noise suppression in autoregulatory gene networks. *Biophysical journal* **96**, 4013-4023, doi:10.1016/j.bpj.2009.02.064 (2009).

303 Zhu, W. *et al.* Noggin regulation of bone morphogenetic protein (BMP) 2/7 heterodimer activity in vitro. *Bone* **39**, 61-71, doi:10.1016/j.bone.2005.12.018 (2006).

304 Winkler, D. G. *et al.* Noggin and sclerostin bone morphogenetic protein antagonists form a mutually inhibitory complex. *J Biol Chem* **279**, 36293-36298, doi:10.1074/jbc.M400521200 (2004).

305 Harris, S. E. *et al.* Effects of transforming growth factor beta on bone nodule formation and expression of bone morphogenetic protein 2, osteocalcin, osteopontin, alkaline phosphatase, and type I collagen mRNA in long-term cultures of fetal rat calvarial osteoblasts. *J Bone Miner Res* **9**, 855-863, doi:10.1002/jbmr.5650090611 (1994).

306 Chen, T. L., Bates, R. L., Dudley, A., Hammonds, R. G., Jr. & Amento, E. P. Bone morphogenetic protein-2b stimulation of growth and osteogenic phenotypes in rat osteoblast-like cells: comparison with TGF-beta 1. *J Bone Miner Res* **6**, 1387-1393, doi:10.1002/jbmr.5650061216 (1991).

307 Karst, M., Gorny, G., Galvin, R. J. & Oursler, M. J. Roles of stromal cell RANKL, OPG, and M-CSF expression in biphasic TGF-beta regulation of osteoclast differentiation. *J Cell Physiol* **200**, 99-106, doi:10.1002/jcp.20036 (2004).

308 Finnson, K. W., Parker, W. L., ten Dijke, P., Thorikay, M. & Philip, A. ALK1 opposes ALK5/Smad3 signaling and expression of extracellular matrix components in human chondrocytes. *J Bone Miner Res* **23**, 896-906, doi:10.1359/jbmr.080209 (2008).

309 Dang, P. N. *et al.* Guiding Chondrogenesis and Osteogenesis with Mineral-Coated Hydroxyapatite and BMP-2 Incorporated within High-Density hMSC Aggregates for Bone Regeneration. *ACS Biomater Sci Eng* **2**, 30-42, doi:10.1021/acsbiomaterials.5b00277 (2016).

310 Shi, Q. *et al.* The osteogenesis of bacterial cellulose scaffold loaded with bone morphogenetic protein-2. *Biomaterials* **33**, 6644-6649, doi:10.1016/j.biomaterials.2012.05.071 (2012).

311 Meinel, L. *et al.* Osteogenesis by human mesenchymal stem cells cultured on silk biomaterials: comparison of adenovirus mediated gene transfer and protein delivery of BMP-2. *Biomaterials* **27**, 4993-5002, doi:10.1016/j.biomaterials.2006.05.021 (2006).

312 Iwakura, T., Sakata, R. & Reddi, A. H. Induction of chondrogenesis and expression of superficial zone protein in synovial explants with TGF-beta1 and BMP-7. *Tissue Eng Part A* **19**, 2638-2644, doi:10.1089/ten.TEA.2013.0047 (2013).

313 Li & Tuan, R. S. Mechanism of traumatic heterotopic ossification: In search of injury-induced osteogenic factors. *J Cell Mol Med* **24**, 11046-11055, doi:10.1111/jcmm.15735 (2020).

314 Strong, A. L. *et al.* BMP Ligand Trap ALK3-Fc Attenuates Osteogenesis and Heterotopic Ossification in Blast-Related Lower Extremity Trauma. *Stem Cells Dev* **30**, 91-105, doi:10.1089/scd.2020.0162 (2021).

315 Urdeitx, P. & Doweidar, M. H. Mechanical stimulation of cell microenvironment for cardiac muscle tissue regeneration: a 3D in-silico model. *Computational Mechanics* **66**, 1003-1023, doi:10.1007/s00466-020-01882-6 (2020).

316 Maleiner, B. *et al.* The Importance of Biophysical and Biochemical Stimuli in Dynamic Skeletal Muscle Models. *Front Physiol* **9**, 1130, doi:10.3389/fphys.2018.01130 (2018).

317 Boonen, K. J. *et al.* Effects of a combined mechanical stimulation protocol: Value for skeletal muscle tissue engineering. *J Biomech* **43**, 1514-1521, doi:10.1016/j.jbiomech.2010.01.039 (2010).

Apendixes

Appendix A: Statistical analyses of *Col2a1, Sox9, Acan* and *Six1* at 7, 14, and 30 days.

Groups	Time(days)	Target genes			
		Col2a1	***Sox9***	***Acan***	***Six1***
Control	7	1.27±0.40	0.19±0.38	0.25±0.41	1.03±0.47
	14	1.50±0.152	-0.54±0.25	0.65±0.10	0.69±0.19
	30	1.15±0.15	0.06±0.13	0.46±0.18	0.72±0.12
	7 vs.14 P-value	0.8141	**0.0356**	0.5576	0.7264
	7 vs. 30 P-value	0.9381	0.5378	0.8460	0.7562
	14vs.30 P-value	0.6142	0.2064	0.8739	0.9986
rBMP-2	7	4.12±0.19	1.45±0.20	1.45±0.25	1.57±0.24
	14	3.31±0.19	1.05±0.19	0.85±0.15	0.98±0.09
	30	1.85±0.12	0.53±0.11	1.74±0.20	1.39±0.17
	7 vs. 14 P-value	**0.0149**	0.2483	0.1402	0.0752
	7 vs. 30 P-value	**<0.0001**	**0.0044**	0.5939	0.7674
	14vs. 30 P-value	**<0.0001**	0.1111	**0.0223**	0.2453
rTGF-β3	7	2.46±0.28	0.29±0.19	1.29±0.18	1.35±0.28
	14	4.09±0.21	1.08±0.23	1.61±0.15	2.31±0.17
	30	2.29±0.24	0.89±0.22	1.82±0.26	1.61±0.21
	7 vs. 14 P-value	**0.0008**	0.0553	0.5341	**0.0238**
	7 vs. 30 P-value	0.8856	0.1570	0.1969	0.6971
	14vs. 30 P-value	**0.0003**	0.8299	0.7504	0.1106
rNoggin	7	1.21±0.38	0.23±0.29	0.42±0.22	0.81±0.23
	14	1.59±0.49	0.47±0.16	0.13±0.29	0.87±0.26
	30	2.03±0.18	0.36±0.18	0.59±0.11	1.13±0.19
	7 vs. 14 P-value	0.7547	0.7184	0.7352	0.9775
	7 vs. 30 P-value	0.3025	0.9075	0.8936	0.5996
	14vs. 30 P-value	0.6996	0.9305	0.3925	0.7220

rTGF-β3 + rBMP-2	7	2.34±0.15	1.25±0.13	1.48±0.14	0.58±0.18
	14	4.11±0.20	1.61±0.15	1.69±0.24	2.68±0.20
	30	2.21±0.18	0.85±0.12	1.94±0.23	1.83±0.11
	7 vs. 14 P-value	**<0.0001**	0.1894	0.7720	**<0.0001**
	7 vs. 30 P-value	0.8838	0.1368	0.3119	**0.0004**
	14vs. 30 P-value	**<0.0001**	**0.0039**	0.6943	**0.0095**
rTGF-β3 + rNoggin	7	2.2±0.15	0.37±0.09	1.63±0.19	1.81±0.19
	14	1.258±0.39	0.89±0.39	0.99±0.32	0.72±0.33
	30	2.04±0.35	1.13±0.14	1.69±0.19	1.6±0.16
	7 vs. 14 P-value	0.1262	0.3179	0.1830	**0.0174**
	7 vs. 30 P-value	0.9360	0.1075	0.9835	0.8176
	14vs. 30 P-value	0.2233	0.7801	0.1371	**0.0466**
rBMP-2 + rNoggin	7	0.61±0.16	0.34±0.28	0.79±0.19	1.06±0.12
	14	1.35±0.86	0.03±0.37	1.02±0.38	1.13±0.47
	30	1.96±0.19	0.25±0.07	1.01±0.15	1.38±0.16
	7 vs. 14 P-value	0.1198	0.7130	0.8109	0.9820
	7 vs. 30 P-value	**0.0042**	0.9742	0.8345	0.7339
	14vs. 30 P-value	0.2252	0.8353	0.9989	0.8348
rTGF-β3 + rBMP-2 + rNoggin	7	2.62±0.33	0.48±0.18	1.03±0.14	0.44±0.21
	14	2.21±0.28	0.52±0.22	1.19±0.34	1.29±0.27
	30	2.95±0.19	1.42±0.15	1.69±0.12	1.76±0.08
	7 vs. 14 P-value	0.5599	0.9891	0.8703	**0.0291**
	7 vs. 30 P-value	0.6841	**0.0094**	0.1409	**0.0012**
	14vs. 30 P-value	0.1763	**0.0125**	0.3107	0.2803

The data were expressed as mean ± standard error of the mean (SEM). $p<0.05$ was considered statistically significant, which was bolded in the table. *Acan = Aggrecan, Sox9 = Sry-box transcription factor 9, Col2a1 = Collagen type II alpha 1 chain, Six1= Six homeobox 1.*

Appendix B: Statistical analyses of *Abi3bp, Alp, Runx2* and *Bmp-2* at 7, 14, and 30 days.

Groups	Time(days)	Target genes			
		Abi3bp	***Alp***	***Runx2***	***Bmp-2***
Control	7	0.94±0.37	-0.45±0.40	1.85±0.39	0.95±0.45
	14	0.31±0.32	0.39±0.28	1.32±0.19	0.55±0.33
	30	0.74±0.17	0.74±0.09	1.76±0.08	0.58±0.11
	7 vs.14 P-value	0.3215	0.1284	0.3393	0.6796
	7 vs. 30 P-value	0.8776	**0.0265**	0.9664	0.7175
	14vs.30 P-value	0.5850	0.6790	0.4680	0.9978
rBMP-2	7	1.75±0.15	0.92±0.21	2.65±0.25	1.07±0.18
	14	1.62±0.16	-0.09±0.15	2.42±0.18	1.47±0.35
	30	2.13±0.30	1.28±0.17	2.81±0.27	1.26±0.10
	7 vs. 14 P-value	0.9158	**0.0029**	0.7674	0.4824
	7 vs. 30 P-value	0.4581	0.3524	0.8804	0.8427
	14vs. 30 P-value	0.2663	**0.0002**	0.4812	0.8118
rTGF-β3	7	1.18±0.22	0.61±0.15	2.28±0.16	1.36±0.22
	14	1.83±0.23	1.41±0.10	3.22±0.10	2.41±0.07
	30	1.75±0.20	1.51±0.201	3.10±0.18	1.67±0.21
	7 vs. 14 P-value	0.1272	**0.0066**	**0.0015**	**0.0028**
	7 vs. 30 P-value	0.1901	**0.006**	**0.0045**	0.4509
	14vs. 30 P-value	0.9686	0.8910	0.8498	**0.0330**
rNoggin	7	1.08±0.36	-0.02±0.36	2.10±0.24	1.24±0.26
	14	0.75±0.29	0.41±0.32	1.74±0.36	1.82±0.13
	30	1.13±0.19	0.39±0.23	1.93±0.20	1.58±0.28
	7 vs. 14 P-value	0.7038	0.5886	0.6350	0.2284
	7 vs. 30 P-value	0.9930	0.6256	0.9022	0.5880
	14vs. 30 P-value	0.6356	0.9979	0.8777	0.7527

rTGF-β3 + rBMP-2	7	1.82±0.27	-0.08±0.21	2.58±0.23	1.89±0.27
	14	1.81±0.09	1.14±0.12	3.63±0.21	2.1±0.21
	30	2.42±0.16	0.82±0.19	2.18±0.29	1.94±0.19
	7 vs. 14 P-value	0.9990	**0.0005**	**0.0234**	0.7835
	7 vs. 30 P-value	0.1057	**0.0069**	0.5112	0.9819
	14vs. 30 P-value	0.0979	0.4060	**0.0025**	0.8776
rTGF-β3 + rNoggin	7	1.58±0.26	0.51±0.14	2.83±0.17	2.02±0.11
	14	0.51±0.20	-0.05±0.26	2.20±0.31	1.57±0.18
	30	1.77±0.13	0.45±0.30	2.28±0.21	1.62±0.19
	7 vs. 14 P-value	**0.0065**	0.2717	0.1896	0.1741
	7 vs. 30 P-value	0.8124	0.9882	0.2492	0.2518
	14vs. 30 P-value	**0.0019**	0.3353	0.9833	0.9702
rBMP-2 + rNoggin	7	0.61±0.21	-0.24±0.14	2.12±0.15	0.90±0.19
	14	0.39±0.31	0.14±0.39	2.04±0.36	1.33±0.38
	30	0.94±0.23	0.78±0.23	1.91±0.13	1.27±0.18
	7 vs. 14 P-value	0.7929	0.5914	0.9646	0.5185
	7 vs. 30 P-value	0.6475	**0.0453**	0.8004	0.6039
	14vs. 30 P-value	0.2944	0.2545	0.9222	0.9859
rTGF-β3 + rBMP-2 + rNoggin	7	1.33±0.25	0.001±0.17	2.58±0.15	1.07±0.22
	14	1.30±0.29	0.09±0.20	1.79±0.26	1.39±0.21
	30	1.96±0.18	1.79±0.26	3.27±0.10	2.02±0.22
	7 vs. 14 P-value	0.9969	0.9513	**0.0181**	0.5459
	7 vs. 30 P-value	0.2085	**0.0001**	**0.0390**	**0.0189**
	14vs. 30 P-value	0.1849	**0.0002**	<**0.0001**	0.1397

The data were expressed as mean ± standard error of the mean (SEM). p<0.05 was considered statistically significant, which was bolded in the table. *Alp= Alkaline phosphatase, Abi3bp = Abi family member-3 binding protein, Bmp-2 = Bone morphogenetic protein-2, Runx2 = Runx family transcription factor 2.*

Appendix C: Statistical analyses of *Ocn, Col1a1, Vegfa* and *Col4a1* at 7, 14 and 30 days.

Groups	Time(days)	Target genes			
		Ocn	***Col1a1***	***Vegfa***	***Col4a1***
Control	7	0.6±0.44	-0.69±0.42	-0.03±0.47	1.12±0.45
	14	0.133±0.15	-1.45±0.12	-0.46±0.29	0.61±0.32
	30	2.56±0.11	0.69±0.17	-0.23±0.10	0.14±0.11
	7 vs.14 P-value	0.4734	0.1467	0.6362	0.5186
	7 vs. 30 P-value	**0.0004**	**0.0070**	0.8977	0.1181
	14vs.30 P-value	<**0.0001**	**0.0001**	0.8834	0.5831
rBMP-2	7	1.92±0.26	-0.49±0.37	1.25±0.28	2.39±0.25
	14	2.3±0.14	-1.05±0.13	0.83±0.29	0.97±0.13
	30	4.0±0.13	0.72±0.18	0.57±0.19	0.93±0.37
	7 vs. 14 P-value	0.3387	0.2887	0.4957	**0.0053**
	7 vs. 30 P-value	<**0.0001**	**0.0097**	0.1746	**0.0043**
	14vs. 30 P-value	<**0.0001**	**0.0004**	0.7456	0.9939
rTGF-β3	7	1.84±0.2	-0.84±0.13	0.54±0.09	1.89±0.29
	14	3.61±0.09	-0.08±0.04	1.21±0.18	1.69±0.20
	30	3.89±0.29	1.64±0.18	1.04±0.15	1.37±0.08
	7 vs. 14 P-value	<**0.0001**	**0.0028**	**0.0163**	0.7741
	7 vs. 30 P-value	<**0.0001**	<**0.0001**	0.0803	0.2276
	14vs. 30 P-value	0.6276	<**0.0001**	0.6903	0.5642
rNoggin	7	0.89±0.29	-0.46±0.32	0.09±0.28	1.31±0.40
	14	0.95±0.28	-0.75±0.21	0.49±0.14	-0.05±0.26
	30	1.87±0.28	0.99±0.47	0.24±0.21	0.59±0.15
	7 vs. 14 P-value	0.9867	0.8331	0.4344	**0.0125**
	7 vs. 30 P-value	0.0698	**0.0280**	0.8717	0.2232
	14vs. 30 P-value	0.0927	**0.0089**	0.7292	0.2887

rTGF-β3 + rBMP-2	7	2.52±0.22	-1.47±0.19	0.96±0.19	1.88±0.18
	14	2.94±0.35	0.16±0.09	1.49±0.12	2.24±0.28
	30	4.23±0.18	0.70±0.10	0.33±0.24	1.77±0.07
	7 vs. 14 P-value	0.5150	**<0.0001**	0.1486	0.4156
	7 vs. 30 P-value	**0.0010**	**<0.0001**	0.0816	0.9221
	14vs. 30 P-value	**0.0096**	**0.0398**	**0.0016**	0.2423
rTGF-β3 + rNoggin	7	2.06±0.21	0.15±0.08	0.81±0.075	1.51±0.15
	14	0.99±0.35	-1.83±0.21	0.62±0.11	1.12±0.35
	30	4.07±0.40	0.51±0.22	0.74±0.23	1.08±0.25
	7 vs. 14 P-value	0.0952	**<0.0001**	0.6761	0.2577
	7 vs. 30 P-value	**0.0018**	0.3506	0.9493	0.2397
	14vs. 30 P-value	**<0.0001**	**<0.0001**	0.8498	0.9987
rBMP-2 + rNoggin	7	1.28±0.20	-1.08±0.22	0.58±0.29	1.03±0.12
	14	0.67±0.34	-1.65±0.32	1.02±0.20	1.03±0.50
	30	2.87±0.27	1.62±0.24	-0.28±0.18	0.54±0.19
	7 vs. 14 P-value	0.2930	0.3093	0.3960	0.8999
	7 vs. 30 P-value	**0.0027**	**<0.0001**	**0.0436**	0.5391
	14vs. 30 P-value	**0.0001**	**<0.0001**	**0.0031**	0.5369
rTGF-β3 + rBMP-2 + rNoggin	7	1.64±0.14	-0.79±0.22	0.52±0.12	1.53±0.26
	14	1.44±0.21	-1.39±0.20	0.86±0.24	0.73±0.23
	30	4.93±0.15	1.42±0.19	0.86±0.15	1.01±0.15
	7 vs. 14 P-value	0.6957	0.1391	0.3942	**0.0487**
	7 vs. 30 P-value	**<0.0001**	**<0.0001**	0.3875	0.2383
	14vs. 30 P-value	**<0.0001**	**<0.0001**	0.9899	0.6400

The data were expressed as mean ± standard error of the mean (SEM). p<0.05 was considered statistically significant, which was bolded in the table*. Ocn = Osteocalcin, Col4a1 = Collagen type IV alpha 1 chain, Vegfa = Vascular endothelial growth factor A, Col1a1 = Collagen type I alpha 1 chain.*

Appendix D: Statistical analyses of histomorphometrical results at 7, 14 and 30 days.

Groups	Time(days)	Staining Medhods			
		Alcian Blue	**Alizarin-Red S**	**IHC-ACAN**	**IHC-OCN**
Control	7	0.35±0.08	1.94±0.17	4.87±0.62	2.07±0.19
	14	1.87±0.17	1.56±0.16	3.79±0.38	1.71±0.15
	30	0.82±0.05	1.77±0.42	3.93±0.37	1.62±0.27
	7 vs.14 P-value	**<0.0001**	0.6050	0.2680	0.4519
	7 vs. 30 P-value	0.0263	0.9065	0.3593	0.3096
	14vs.30 P-value	**<0.0001**	0.8488	0.9768	0.9561
rBMP-2	7	1.15±0.20	3.67±0.22	7.56±0.37	3.35±0.13
	14	4.3±0.35	3.48±0.32	8.79±0.51	2.80±0.52
	30	1.55±0.33	2.89±0.33	6.92±0.67	2.93±0.30
	7 vs. 14 P-value	**<0.0001**	0.8836	0.2609	0.5356
	7 vs. 30 P-value	0.6344	0.1783	0.6827	0.6898
	14vs. 30 P-value	**<0.0001**	0.3632	0.0622	0.9645
rTGF-β3	7	0.97±0.10	1.95±0.23	6.60±0.22	2.68±0.26
	14	4.11±0.30	3.31±0.16	7.60±0.57	2.86±0.26
	30	1.31±0.09	3.13±0.30	6.65±0.24	2.76±0.29
	7 vs. 14 P-value	**<0.0001**	**0.0033**	0.1917	0.8825
	7 vs. 30 P-value	0.4214	**0.0092**	0.9955	0.9795
	14vs. 30 P-value	**<0.0001**	0.8648	0.2214	0.9565
rNoggin	7	0.52±0.06	2.48±0.24	4.15±0.32	2.30±0.36
	14	2.24±0.15	2.20±0.78	5.87±0.72	2.11±0.16
	30	0.8±0.11	2.56±0.35	4.45±0.77	2.35±0.26
	7 vs. 14 P-value	**<0.0001**	0.9232	0.1689	0.8688
	7 vs. 30 P-value	0.2277	0.9929	0.9363	0.9921
	14vs. 30 P-value	**<0.0001**	0.8746	0.2893	0.8076

rTGF-β3 + rBMP-2	7	1.09±0.17	3.43±0.26	7.20±0.29	2.70±0.21
	14	3.74±0.54	2.98±0.20	7.66±0.59	2.80±0.27
	30	1.84±0.15	4.58±0.33	10.9±0.82	3.24±0.28
	7 vs. 14 P-value	**0.0002**	0.4939	0.8499	0.9592
	7 vs. 30 P-value	0.2873	**0.0222**	**0.0016**	0.3212
	14vs. 30 P-value	**0.0034**	**0.0022**	**0.0048**	0.4604
rTGF-β3 + rNoggin	7	0.70±0.08	3.14±0.64	5.66±0.30	2.98±0.36
	14	2.57±0.14	1.22±0.28	6.40±0.19	2.81±0.19
	30	1.30±0.15	1.56±0.29	6.60±0.56	2.37±0.11
	7 vs. 14 P-value	<**0.0001**	**0.0198**	0.3779	0.8647
	7 vs. 30 P-value	**0.0145**	0.0578	0.2226	0.2058
	14vs. 30 P-value	<**0.0001**	0.8446	0.9290	0.4296
rBMP-2 + rNoggin	7	0.66±0.11	2.24±0.48	3.94±0.95	2.52±0.40
	14	2.21±0.08	1.67±0.11	3.11±0.32	1.81±0.15
	30	0.91±0.12	2.04±0.64	4.88±0.60	2.35±0.16
	7 vs. 14 P-value	<**0.0001**	0.6679	0.6681	0.1601
	7 vs. 30 P-value	0.2385	0.9537	0.5954	0.8873
	14vs. 30 P-value	<**0.0001**	0.8358	0.1859	0.3283
rTGF-β3 + rBMP-2 + rNoggin	7	0.96±0.07	1.56±0.41	5.72±0.45	2.49±0.16
	14	3.63±0.31	3.22±0.21	7.55±0.52	3.15±0.15
	30	1.06±0.16	4.02±0.11	7.04±0.43	2.96±0.17
	7 vs. 14 P-value	<**0.0001**	**0.0020**	**0.0374**	**0.0294**
	7 vs. 30 P-value	0.9442	<**0.0001**	0.1525	0.1373
	14vs. 30 P-value	<**0.0001**	0.1401	0.7244	0.6873

The data were expressed as mean ± standard error of the mean (SEM). $p<0.05$ was considered statistically significant, which was bolded in the table. IHC = Immunohistochemistry, ACAN = Aggrecan, OCN = Osteocalcin.

Acknowledgements

The journey to achieve my Doctoral Degree in Human Medicine (Dr. med.) was difficult, and the Cov-19 pandemic made it even more challenging. However, what does not kill one makes one stronger; this journey of study will be the treasure of my life. Here, I would like to express my deepest gratitude to the people who have helped me on this journey:

To Prof. Dipl.-Ing. Dr. med. Volkmar Jansson and Prof. Dr. med. Boris Holzapfel, the former and present director of the Department of Orthopaedics, Physical Medicine & Rehabilitation, University Hospital of LMU, Germany. Thank you for having accepted and allowed me to complete, respectively, my research study and education in the Laboratory of Musculoskeletal Research Center of Munich.

To Prof. Dr. med. Peter E. Müller, my supervisor, for guiding and mentoring me during my doctoral study at LMU. Thank you for a great amount of support during my research investigation.

To Dr. Roland M. Klar and Dr. tech. Yan Chevalier, my Project Leaders/Coordinators/co-supervisors. Thank you for your systematic and scientific training for me, which brought me into the field of regenerative and biomechanical medicine that has allowed me to build my scientific research framework. Your guidance, mentorship and advice helped solve many challenging issues during my time at the laboratory.

To PD. Dr. Attila Aszódi and PD. Dr. med. Thomas Richard Niethammer, my Target Agreement Co-ordinators. Thank you for your guidance and helping me complete the interim and final evaluations. Especially PD. Dr. Attila Aszódi, thank you for your professional suggestion on my project and for organizing routine student seminars that broadened my research horizons.

To Ms. Bärbel Schmitt, Ms. Zsuzsanna Farkas, the medical technicians of the laboratory, for your reliable technical support. Ms. Bärbel Schmitt, your humor has brought much happiness to our tedious research life, thanks.

Acknowledgements

To Prof. Dr. med. Susanne Mayer, Dr. rer. nat. Maximilian Saller, Dr. Dipl.-Ing. (FH) Matthias Woiczinski, Mrs. Inês Santos, Ms. Ute Brooks, Ms. Heidrun Grondinger, Dipl.-Ing. Michael Kraxenberger and all the other laboratory members, for your generous assistance during my stay at the laboratory.

To Fanxiao Liu, Xiangyun Cheng, Fei Xiong, Ping Li, Xujia Wang and Rui Tang, my Chinese friends in the laboratory, for your encouragement and companionship. Especially Xiangyun Cheng, you really helped me a lot, both at work and in daily life; I will always remember this friendship.

To Nikolay Atanasov and Renata Guimaraees, two friends in the same group, for your companionship and helping in my difficult times. Hope to see you again in the near future.

To the China Scholarship Council (CSC), for your financial support, which permitted me to finish my doctoral study abroad. Furthermore, thanks to Dr. Dongmei Zhang, for assistance with the LMU-CSC program scholarship application. Moreover, thanks to friends in the LMU-CSC program, for making me feel the warmth of family in a foreign country.

Finally, to my family. Jimei Li, my dear wife, it is your love and company that makes me not feel alone. And my parents, thanks for your understanding and support throughout my doctoral study.

Affidavit

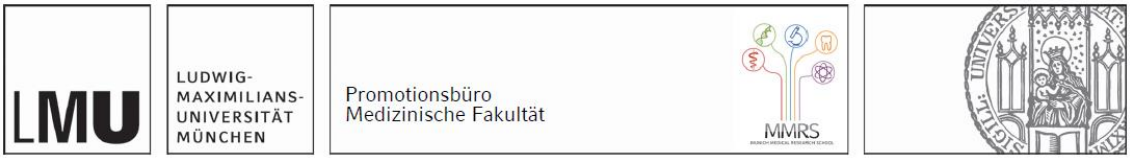

Affidavit

Liu, Heng
Surname, first name

I hereby declare, that the submitted thesis entitled:

Regulatory effect of TGF-β3, BMP-2 and Noggin during the induction of endochondral bone formation: an *in vitro* study using rectus abdominis muscle from rat

……

is my own work. I have only used the sources indicated and have not made unauthorised use of services of a third party. Where the work of others has been quoted or reproduced, the source is always given.

I further declare that the submitted thesis or parts thereof have not been presented as part of an examination degree to any other university.

Planegg, 21.09.2022
place, date

Heng Liu
Signature doctoral candidate